

**FACULDADE DE ENGENHARIA DA UNIVERSIDADE DO PORTO**



# **Control of underwater vehicles on autonomous docking maneuvers**

**José Miguel Almeida Braga**

Mestrado Integrado em Engenharia Electrotécnica e de Computadores

Supervisor: João Borges de Sousa (Eng.)

June 2010

© José Braga, 2010

# **Control of underwater vehicles on autonomous docking maneuvers**

**José Miguel Almeida Braga**

Mestrado Integrado em Engenharia Electrotécnica e de Computadores

Aprovado em provas públicas pelo Júri:

Presidente: Mário Jorge Rodrigues de Sousa (Prof.)

---

Arguente: Luís Miguel Barros Lopes (Prof.)

---

Vogal: João Borges de Sousa (Eng.)

---

July 9, 2010



# Abstract

This work concerns the development of a control strategy for an Autonomous Underwater Vehicle (AUV) to dock into a docking station mounted on a Remotely Operated Vehicle (ROV). The docking station allows for the transfer of data and power.

An hierarchical architecture of control is introduced to allow high level supervision and execution of basic maneuvers using state references for the low level controllers.

Hybrid systems theory is applied to enable interaction between discrete events and nonlinear ordinary differential equations which model the behavior of underwater vehicles. The high level control is achieved with hybrid automata.

Backward reach sets under adversarial behavior are computed using only known bounds of the external disturbances. This allows to derive safe maneuvers that guarantee docking even in the presence of those disturbances.

Medium level controllers to execute waypoint following, follow track and roundabout maneuvers were developed and implemented.

Low level nonlinear controllers are implemented using sliding mode theory to provide robustness in the presence of parametric uncertainties and external disturbances.

Potential fields are applied to the obstacle avoidance system.

Models and controllers were implemented in MATLAB to test and study the approach and analyze results.



# Resumo

Este trabalho desenvolve uma estratégia de controlo para guiar um veículo autónomo subaquático (AUV) para “estacionar” dentro de uma estrutura cónica montada num veículo remotamente operado (ROV). A estação permite a transferência de dados e energia.

Uma arquitectura hierarquizada de controlo é aplicada para permitir supervisão e execução de manobras básicas através do cálculo das referências para os controladores de baixo nível.

Teoria de sistemas híbridos é implementada para permitir a interacção de eventos discretos com equações diferenciais ordinárias não lineares que modelam o comportamento de veículos submarinos. O controlo de alto nível é efectuado através de autómatos híbridos.

Computação do *backward reach set* na presença de perturbações externas para possibilitar a criação de um percurso que permita ao veículo compensar o efeito das perturbações.

Desenvolvimento controladores de nível médio para execução de manobras de seguimento de *waypoints*, seguimento de rectas e manobras de *roundabout* em torno de obstáculos.

Estudo de controladores não lineares de baixo nível em modo de deslizamento para garantir robustez na presença de incertezas de modelo e perturbações externas.

Aplicação de teoria de potencial para evitar obstáculos.

Os problemas formulados são implementados no software MATLAB para teste e estudo da solução e análise de resultados.



*“Engineers like to solve problems.  
If there are no problems handily available, they will create their own problems.”*

Scott Adams



# **Thanks to**

First, I would like to thank my supervisor João Borges de Sousa for giving me the opportunity of developing this work with his supervision. I am truly grateful for all your guidance and advices that lead me to accomplish this thesis and also by letting me learn on my own and adopt my work methodologies.

I would like to thank my lab partner Pedro Calado for all the discussions we had that helped me performing a better job. I am very grateful for all the good atmosphere that I have experienced along this semester in the lab.

Also I would like to thank my colleagues Amável Pinheiro, Carlos Oliveira, Luis Rocha, David Lima and Andry Maykol for their help, contributions and advices for this thesis.

I also have to note the tremendous help and support that my girlfriend Sandra Mendo gave me throughout my whole experience in FEUP, the journey would not have been the same without you.

Last but not least, I would like to thank my parents, José and Helena, and my brother João for all your support.

José Braga



# Contents

<b>Abstract</b>	<b>i</b>
<b>Resumo</b>	<b>iii</b>
<b>Thanks to</b>	<b>vii</b>
<b>Acronyms</b>	<b>xix</b>
<b>1 Introduction</b>	<b>1</b>
1.1 Motivation . . . . .	1
1.2 Objectives . . . . .	3
1.3 Outline . . . . .	3
<b>2 Background material</b>	<b>5</b>
2.1 Models of underwater vehicles . . . . .	5
2.1.1 Kinematics . . . . .	5
2.1.2 Rigid-body dynamics . . . . .	8
2.1.3 Hydrodynamic forces and moments . . . . .	8
2.1.4 Modifications to account for ocean current . . . . .	11
2.1.5 Actuator forces . . . . .	11
2.2 Hybrid Systems . . . . .	14
2.3 Reachability results . . . . .	16
2.3.1 Reach Sets . . . . .	16
2.3.2 Dynamic optimization for reach set computation . . . . .	19
2.4 Lyapunov stability . . . . .	26
2.4.1 Nonlinear systems and Equilibrium points . . . . .	26
2.4.2 Stability definitions . . . . .	28
2.4.3 Lyapunov's Direct Method . . . . .	30
2.5 Nonlinear Control techniques . . . . .	34
2.5.1 Sliding Mode Control . . . . .	34
2.5.2 Multiple Sliding Surface . . . . .	42
2.5.3 Dynamic Surface Control . . . . .	43
<b>3 State of the art in autonomous docking systems</b>	<b>47</b>
3.1 Introduction . . . . .	47
3.2 Problem description . . . . .	47
3.3 Overview . . . . .	48

<b>4 Problem statement</b>	<b>59</b>
4.1 Introduction . . . . .	59
4.2 Requirements . . . . .	59
4.2.1 LAUV . . . . .	60
4.2.2 ROV Luso . . . . .	61
4.3 Models of the vehicles . . . . .	62
4.3.1 Model for the LAUV . . . . .	62
4.3.2 Model for the ROV . . . . .	66
4.4 Scenarios . . . . .	68
4.5 Assumptions . . . . .	68
4.6 Problem 1 – Docking without disturbances with the ROV fixed . . . . .	69
4.6.1 Assumptions . . . . .	69
4.6.2 Formal statement . . . . .	70
4.7 Problem 2 – Docking without disturbances with the ROV in motion . . . . .	70
4.7.1 Assumptions . . . . .	70
4.7.2 Formal statement . . . . .	71
4.8 Problem 3 – Docking with disturbances . . . . .	72
4.8.1 Assumptions . . . . .	72
4.8.2 Formal statement . . . . .	72
4.9 Problem 4 – Collision Avoidance in the early stages of the operation . . . . .	73
4.9.1 Assumptions . . . . .	73
4.9.2 Formal statement . . . . .	74
4.10 Problem 5 – Abort sequence . . . . .	75
4.10.1 Assumptions . . . . .	75
4.10.2 Formal statement . . . . .	75
<b>5 Approach</b>	<b>77</b>
5.1 Introduction . . . . .	77
5.2 Basic maneuvers . . . . .	77
5.3 Architecture . . . . .	78
5.4 Backward reach set computation . . . . .	79
5.4.1 Introduction . . . . .	79
5.4.2 Backreach Set under adversarial behavior . . . . .	80
5.4.3 Switch controllers at the boundary of the reach set . . . . .	82
5.5 Motion planning . . . . .	83
5.6 Maneuver 1: Line of Sight guidance . . . . .	86
5.7 Maneuver 2: Follow Track . . . . .	86
5.8 Maneuver 3: Roundabout . . . . .	89
5.8.1 Collision avoidance system using gradient lines by geometrical construction . . . . .	89
5.9 LAUV decoupled control systems . . . . .	92
5.9.1 Forward speed control . . . . .	93
5.9.2 Steering system control . . . . .	93
5.9.3 Diving system control . . . . .	94
5.10 Problem 1 – Docking without disturbances with the ROV fixed . . . . .	96
5.10.1 Hybrid systems approach for high level control . . . . .	96
5.10.2 Stability of the low level controllers . . . . .	98

5.11	Problem 2 – Docking without disturbances with the ROV in motion . . . . .	98
5.11.1	Coordinate transformation . . . . .	99
5.11.2	Solution . . . . .	99
5.12	Problem 3 – Docking with disturbances . . . . .	100
5.12.1	Follow Track maneuver . . . . .	101
5.12.2	Control design using reachability results . . . . .	101
5.12.3	Stability of the solution . . . . .	101
5.13	Problem 4 – Collision Avoidance in the early stages of the operation . . . . .	103
5.13.1	Initial state of the LAUV inside the Backreach Set . . . . .	103
5.13.2	Complete Hybrid Systems . . . . .	104
5.14	Problem 5 – Abort sequence . . . . .	105
5.14.1	Receiving a new mission assignment . . . . .	105
5.14.2	Reaching a position outside of the backward reach set . . . . .	105
<b>6</b>	<b>Simulation Results</b>	<b>107</b>
6.1	Models of the vehicles . . . . .	107
6.1.1	LAUV . . . . .	107
6.1.2	ROV . . . . .	109
6.2	Test Plan . . . . .	111
6.3	Problem 1 – Docking without disturbances with the ROV fixed . . . . .	112
6.3.1	Case 1 . . . . .	112
6.3.2	Case 2 . . . . .	113
6.3.3	Case 3 . . . . .	115
6.4	Problem 2 – Docking without disturbances with the ROV in motion . . . . .	117
6.4.1	Case 1 . . . . .	117
6.4.2	Case 2 . . . . .	118
6.4.3	Case 3 . . . . .	119
6.5	Problem 3 – Docking with disturbances . . . . .	122
6.5.1	Case 1 . . . . .	122
6.5.2	Case 2 . . . . .	123
6.5.3	Case 3 . . . . .	125
6.5.4	Case 4 . . . . .	126
6.6	Problem 4 – Collision Avoidance in the early stages of the operation . . . . .	127
6.6.1	Case 1 . . . . .	127
6.6.2	Case 2 . . . . .	128
6.6.3	Case 3 . . . . .	129
6.6.4	Case 4 . . . . .	130
6.7	Problem 5 – Abort sequence . . . . .	131
6.7.1	Case 1 . . . . .	132
6.7.2	Case 2 . . . . .	132
6.8	Final results . . . . .	133
<b>7</b>	<b>Conclusions</b>	<b>135</b>
7.1	Autonomous docking systems . . . . .	135
7.2	Future work . . . . .	136
<b>References</b>		<b>139</b>



# List of Figures

1.1	A typical Autonomous Underwater Vehicle . . . . .	1
1.2	A typical Remotely Operated Vehicle . . . . .	2
2.1	Body-fixed and earth-fixed reference frames . . . . .	6
2.2	AUV standard fin arrangement . . . . .	12
2.3	Configuration of thrusters in a typical ROV propulsion system. Source: Garus . . . . .	12
2.4	Layout of thrusters in the horizontal subsystem responsible for the horizontal motion. Source: Garus . . . . .	13
2.5	Example of a hybrid automaton . . . . .	15
2.6	Possible collision between an AUV with an obstacle . . . . .	17
2.7	Reach set for a system starting from set $X_0$ . . . . .	17
2.8	Backward reach set for the target set $(t_1, X_1)$ . . . . .	18
2.9	Principle of optimality . . . . .	20
2.10	Antagonistic player in differential games . . . . .	24
2.11	The u-stable bridge . . . . .	25
2.12	A stable equilibrium . . . . .	28
2.13	A asymptotically stable equilibrium . . . . .	29
2.14	Example of a positive definite function $\mathbb{R}^2$ . . . . .	31
2.15	Lyapunov function in $\mathbb{R}^2$ . . . . .	32
2.16	Lyapunov function for $\mathbb{R}^2$ in contour curves . . . . .	32
2.17	The sliding condition . . . . .	36
2.18	The sliding mode for a system with $n=2$ . . . . .	37
2.19	Chattering as a result of imperfect control switchings . . . . .	38
2.20	Boundary Layer . . . . .	39
3.1	REMUS Docking system. Source: Allen et. al. . . . .	49
3.2	An omni-directional docking system. Source: Singh et. al. . . . .	51
3.3	Trajectory planning for the AUV. Source: Jantapremjit and Wilson . . . . .	53
3.4	MBARI docking system for a 54-cm diameter AUV. Source: McEwen et. al. . . . .	55
3.5	Vision guided docking system. Source: Park et. al. . . . .	56
3.6	Method to compensate the effect of cross currents. Source: Park et. al. . . . .	57
4.1	The docking problem . . . . .	60
4.2	The Light Autonomous Underwater Vehicle . . . . .	60
4.3	ROV Luso . . . . .	61
4.4	The docking problem expressed in the ROV body-fixed reference frame . . . . .	69

4.5	The docking problem when the ROV is performing dynamic positioning . . . . .	71
4.6	The docking problem when the ROV in motion . . . . .	72
4.7	The docking problem with ocean currents . . . . .	73
4.8	The collision avoidance problem . . . . .	74
4.9	The abort docking problem . . . . .	75
5.1	Architecture of the control . . . . .	80
5.2	Distance between the vehicles and backward reach set under adversarial behavior without disturbances . . . . .	82
5.3	Distance between the vehicles and backward reach set under adversarial behavior with lateral ocean current $v_c = 0.4$ m/s . . . . .	83
5.4	Switch between controllers using backward reachability . . . . .	84
5.5	Motion plan with the initial set of waypoints . . . . .	84
5.6	Motion planning with reach set information . . . . .	85
5.7	Final motion plan using backreach set under adversarial behavior information . . . . .	85
5.8	Cross Track Error definitions . . . . .	87
5.9	Roundabout maneuver to avoid collision . . . . .	90
5.10	Division of the state space into sectors . . . . .	91
5.11	Problem 1 control block diagram . . . . .	97
5.12	High level controller for Problem 1 . . . . .	97
5.13	Problem 2 control block diagram . . . . .	100
5.14	Possible error when using pure line of sight guidance . . . . .	101
5.15	High level controller for Problem 3 . . . . .	102
5.16	Problem 3 control block diagram . . . . .	102
5.17	Possible trajectories when starting inside the safety zone . . . . .	104
5.18	High level controller for Problem 4 . . . . .	104
5.19	Possible trajectories during the final docking maneuver . . . . .	106
6.1	Problem 1 - case 1: Position of the vehicle in the XY and XZ planes, respectively . . . . .	113
6.2	Problem 1 - case 1: The position of the vehicle along time and the euclidean distance between both vehicles . . . . .	113
6.3	Problem 1 - case 1: The velocity of the vehicle expressed in its body-fixed reference frame and the necessary actuation across time . . . . .	114
6.4	Problem 1 - case 2: Position of the vehicle in the XY and XZ planes, respectively . . . . .	114
6.5	Problem 1 - case 2: The position of the vehicle along time and the euclidean distance between both vehicles . . . . .	115
6.6	Problem 1 - case 2: The velocity of the vehicle expressed in its body-fixed reference frame and the necessary actuation across time . . . . .	115
6.7	Problem 1 - case 3: Position of the vehicle in the XY and XZ planes, respectively . . . . .	116
6.8	Problem 1 - case 3: The position of the vehicle along time and the euclidean distance between both vehicles . . . . .	116
6.9	Problem 1 - case 3: The velocity of the vehicle expressed in its body-fixed reference frame and the necessary actuation across time . . . . .	117

6.10 Problem 2 - case 1: Position of the vehicle expressed in the ROV body frame in the XY and XZ planes, respectively . . . . .	118
6.11 Problem 2 - case 1: Position of the vehicles in the inertial frame . . . . .	118
6.12 Problem 2 - case 1: The position of the vehicle in the ROV body frame along time and the euclidean distance between both vehicles . . . . .	119
6.13 Problem 2 - case 1: The velocity of the vehicle expressed in its body-fixed reference frame and the necessary actuation across time . . . . .	119
6.14 Problem 2 - case 2: Position of the vehicle expressed in the ROV body frame in the XY and XZ planes, respectively . . . . .	120
6.15 Problem 2 - case 2: The position of the vehicle in the ROV body frame along time and the euclidean distance between both vehicles . . . . .	120
6.16 Problem 2 - case 2: The velocity of the vehicle expressed in its body-fixed reference frame and the necessary actuation across time . . . . .	120
6.17 Problem 2 - case 3: Position of the vehicle expressed in the ROV body frame in the XY and XZ planes, respectively . . . . .	121
6.18 Problem 2 - case 3: The position of the vehicle in the ROV body frame along time and the euclidean distance between both vehicles . . . . .	121
6.19 Problem 2 - case 3: The velocity of the vehicle expressed in its body-fixed reference frame and the necessary actuation across time . . . . .	122
6.20 Problem 3 - case 1: Position of the vehicle expressed in the ROV body frame in the XY and XZ planes, respectively . . . . .	123
6.21 Problem 3 - case 1: Final moments of docking in the horizontal plane . .	124
6.22 Problem 3 - case 1: The position of the vehicle in the ROV body frame along time and the euclidean distance between both vehicles . . . . .	124
6.23 Problem 3 - case 1: The velocity of the vehicle expressed in its body-fixed reference frame and the necessary actuation across time . . . . .	124
6.24 Problem 3 - case 2: Position of the vehicle expressed in the ROV body frame in the XY and XZ planes, respectively . . . . .	125
6.25 Problem 3 - case 2: Final moments of docking in the horizontal plane, and the position of the vehicle in the ROV body frame along time . . . . .	125
6.26 Problem 3 - case 3: Position of the vehicle expressed in the ROV body frame in the XY and XZ planes, respectively . . . . .	126
6.27 Problem 3 - case 3: Final moments of docking in the horizontal plane, and the position of the vehicle in the ROV body frame along time . . . . .	126
6.28 Problem 3 - case 4: Position of the vehicle expressed in the ROV body frame in the XY and XZ planes, respectively . . . . .	127
6.29 Problem 3 - case 4: Final moments of docking in the horizontal plane, and the position of the vehicle in the ROV body frame along time . . . . .	127
6.30 Problem 4 - case 1: Position of the vehicle expressed in the ROV body frame in the XY and XZ planes, respectively . . . . .	128
6.31 Problem 4 - case 2: Position of the vehicle expressed in the ROV body frame in the XY and XZ planes, respectively . . . . .	128
6.32 Problem 4 - case 2: Final moments of docking in the horizontal plane, and the distance between vehicles during docking . . . . .	129
6.33 Problem 4 - case 3: Position of the vehicle expressed in the ROV body frame in the XY and XZ planes, respectively . . . . .	129

6.34 Problem 4 - case 3: Final moments of docking in the horizontal plane, and the distance between vehicles during docking . . . . .	130
6.35 Problem 4 - case 4: Position of the vehicle expressed in the ROV body frame in the XY and XZ planes, respectively . . . . .	130
6.36 Problem 4 - case 4: Final moments of docking in the horizontal plane, and the distance between vehicles during docking . . . . .	131
6.37 Problem 4 - case 4: Position of the vehicle expressed in the ROV body frame in the XY and XZ planes, respectively . . . . .	131
6.38 Problem 5 - case 1: Position of the vehicle in the horizontal plane during an abort situation . . . . .	132
6.39 Problem 5 - case 2: Position of the vehicle in the presence of strong ex- ternal disturbances . . . . .	133

# List of Tables

2.1	Notation used for marine vehicles, source: Fossen [1] . . . . .	6
4.1	LAUV technical specifications . . . . .	61
4.2	ROV Luso technical specifications . . . . .	62
6.1	Test Plan for the first three problems . . . . .	111
6.2	Final results for problem 1 . . . . .	133
6.3	Final results for problem 2 . . . . .	133
6.4	Final results for problem 3 . . . . .	134
6.5	Final results for problem 4 . . . . .	134
6.6	Final results for problem 5 . . . . .	134



# Acronyms

2D	2-Dimensions
3D	3-Dimensions
ADS	Autonomous Docking System
AHS	Automated Highway System
ALIVE	Autonomous Light Intervention Vehicle
ASOP	Active Sonar Object Prediction
ASV	Autonomous Surface Vehicle
ATM	Air Traffic Management System
AUV	Autonomous Underwater Vehicle
BRS	Backward Reach Set
CAS	Collision Avoidance System
CB	Center of Buoyancy
CCD	Charge-Coupled Device
CG	Center of Gravity
CTV	Conductivity, Temperature, and Depth
DOF	Degrees of Freedom
DP	Dynamic Positioning
DSC	Dynamic Surface Control
EM	Electromagnetic
EMPEC	Estrutura de Missão Para a Extensão da Plataforma Continental
EOM	Equation of Motion
FRS	Forward Reach Set
FSM	Finite State Machine
GPS	Global Positioning System
GSM	Global System for Mobile Communications
HJB	Hamilton-Jacobi-Bellman
HOSMC	High-Order Sliding Mode Control
HOV	Human Occupied Vehicle
I-AUV	Intervention Autonomous Underwater Vehicles
IMU	Inertial Measurement Unit
INS	Inertial Navigation Systems

LAUV	Light Autonomous Underwater Vehicle
LBL	Long Base Line
LOS	Line-of-Sight
LSTS	Laboratório de Sistemas e Tecnologias Subaquáticas
LTI	Linear Time-Invariant
LTV	Linear Time-Varying
MBARI	The Monterey Bay Aquarium Research Institute
MIMO	Multiple-Input Multiple-Output
MOB	Mobile Offshore Base
MOU	Memorandum of understanding
MSS	Multiple Sliding Surface
ODE	Ordinary Differential Equation
PDE	Partial Differential Equation
PID	Proportional Integral Derivative
SDREM	State-Dependent Riccati Equation Model
SISO	Single-Input Single-Output
SMC	Sliding Mode Control
REMUS	Remote Environmental Monitoring UnitS
ROV	Remotely Operated Vehicle
USBL	Ultra-Short Base Line
USTL	Underwater Systems and Technologies Laboratory
VSC	Variable Structure Control
WHOI	Woods Hole Oceanographic Institution

# Chapter 1

## Introduction

### 1.1 Motivation

The world is hugely influenced by its oceans and seas. They have a drastic impact on global climate and in our ecosystem. This vast watermass possesses a great amount of useful resources, which are of great interest for many fields of science such as marine biology, geology, molecular biology, ocean chemistry, evolutionary biology, etc. The need and desire to explore the vast oceanic environment has contributed with a significant momentum towards the development of advanced oceanographic systems. Some of those oceanographic systems consist of robotic systems such as Autonomous Underwater Vehicles (AUV), Remotely Operated Vehicles (ROV) or Autonomous Surface Vehicles (ASV).

Autonomous Underwater Vehicles are a powerful tool for underwater data gathering. These traditionally torpedo shaped vehicles operate with no physical link with the surface, carrying a set of relevant sensors to perform operations on the oceanic environment.



Figure 1.1: A typical Autonomous Underwater Vehicle

Remotely Operated Vehicles are small submersibles physically connected to the surface by an umbilical cable that provides power and communications. They are able to

perform on many operations such as oceanographic surveys, operations in hazardous environments, underwater structure inspection, and military applications [2].



Figure 1.2: A typical Remotely Operated Vehicle

Ocean exploration requires robust and safe technology and techniques in order to perform ocean surveys more efficiently. AUVs have been a focal point of attention, due to their efficiency on ocean exploration and interventions. However, one major limitation concerns the frequent need for deployment and recover, due to their limited power supply. A docking station capable of transfer power and data to an AUV, allowing it to dock safely, is a much needed resource that will allow an increase of autonomy, therefore reducing the need for support from other vehicles at surface such as ASVs or ships. Hence, an AUV docking system capable of transferring power and data is truly a valuable platform for various types of scientific missions [3].

The Underwater Systems and Technologies Laboratory (USTL) has contributed for a positive evolution of knowledge and technology, with a structured approach for ocean exploration under multiple vehicles in simultaneous operation. Their vision is to implement a networked multi-vehicle system consisting of a number of underwater vehicles, supported by other vehicles at the surface or in the air [4].

Under a memorandum of understanding (MOU) between USTL and the Portuguese Task Group for the Extension of the Continental Shelf (EMEPC) researchers from USTL have been operating the deep-sea ROV Luso in the EMEPC oceanographic surveys.

This works aims the development of a control strategy for autonomous AUV docking inside a dock structure attached to the ROV Luso.

## 1.2 Objectives

This thesis intends to make a positive contribution to the USTL vision, as explained in the previous section. The main objective is to develop an effective control strategy for the docking operation between an AUV and a ROV. The nonlinear dynamics of the underwater vehicles, which operate in six degrees of freedom (DOF), and the uncertainty aspects of the water environment, due to the forces applied by the water particles on the surface of the body, suggest the implementation of a robust control strategy.

A control architecture will be developed to address the several problems at the different levels of autonomy for the mission. Hybrid controllers for docking/homing, either in distributed and non-distributed systems will be developed for maneuver planning. At a lower level of control, the basic maneuvers will be performed by nonlinear control techniques, that provide robust response and stability when facing nonlinearities and uncertainties.

System stability will be studied and the results will be displayed in simulation with the software MATLAB.

## 1.3 Outline

The outline of this report is as follows.

- **Chapter 1** introduces the project motivation and objectives.
- **Chapter 2** seeks to introduce the *background material* required for the development of this project.
- **Chapter 3** presents the current state of the art concerning autonomous docking system for underwater vehicles.
- **Chapter 4** makes the *problem statement* which formally describes some of the problems associated with autonomous docking. Some assumptions are made to help development of the solutions.
- **Chapter 5** presents the *approach* to solve the described problems, *i.e.*, the practical solutions to be implemented.
- **Chapter 6** displays the *simulation results* achieved.
- **Chapter 7** presents my conclusions for this work, including some guidelines for future work regarding autonomous docking systems.



# Chapter 2

## Background material

This chapter introduces the background theory required for the development of this work. Models of underwater vehicles are studied and reviewed. Hybrid systems theory is presented along with reachability theory. Lyapunov stability and nonlinear control techniques are studied.

### 2.1 Models of underwater vehicles

This section emphasizes the mathematical models of the AUV and the ROV. Models of underwater vehicles for simulation purposes were first introduced by Gertler and Hagen [5] in 1967. This section follows closely Fossen [1], Healey [6] who presented the 6 degrees of freedom (DOF) equations of motion (EOM) for underwater vehicles. Silva *et. al.* [7] also derived a model for an AUV for simulation purposes.

#### 2.1.1 Kinematics

In order to determine the position and orientation of a marine vehicle, six independent coordinates are necessary. The first three coordinates with the position (translational motion) of the vehicle along the x-, y- and z-axis, while the last three coordinates treat the attitude and angular rates. In marine vehicles, the six different motion components are defined as: *surge*, *sway*, *heave*, *roll*, *pitch* and *yaw*. See table 2.1.

##### 2.1.1.1 Coordinate Frames

An effective way to analyze the motion of a marine vehicle in 6-DOF is to use two separate coordinate frames as indicated in figure 2.1. There is a moving coordinate frame  $x_b, y_b, z_b$

Table 2.1: Notation used for marine vehicles, source: Fossen [1]

DOF		Forces and Moments	Linear and angular vel.	Position and Euler angles
1	Motion in the x-direction (surge)	$X$	$u$	$x$
2	Motion in the y-direction (sway)	$Y$	$v$	$y$
3	Motion in the z-direction (heave)	$Z$	$w$	$z$
4	Rotation about the x-axis (roll)	$K$	$p$	$\phi$
5	Rotation about the y-axis (pitch)	$M$	$q$	$\theta$
6	Rotation about the z-axis (yaw)	$N$	$r$	$\psi$

fixed to the vehicle called body-fixed reference frame. The origin of this axis is located at the vehicle centerline, moving and rotating with the vehicle, in which the vehicle's center of mass (G) has some position other than the origin of the vehicle fixed frame. The body forces will be computed around this point in later sections. The separation of the center of gravity (CG) from the origin of the body coordinate frame is a key point and necessary here because of the difficulty in computing the hydrodynamic forces in any other frame other than the symmetric center frame chosen while the vehicle's center of gravity can change at any time..

The other coordinate frame is designated as earth-fixed reference frame which can be considered inertial, thanks to neglecting the accelerations of a point on the surface of the Earth. This suggests that the position and orientation of the vehicle should be described relative to the inertial frame, whereas the linear and angular velocities should be expressed in the body-fixed reference frame.

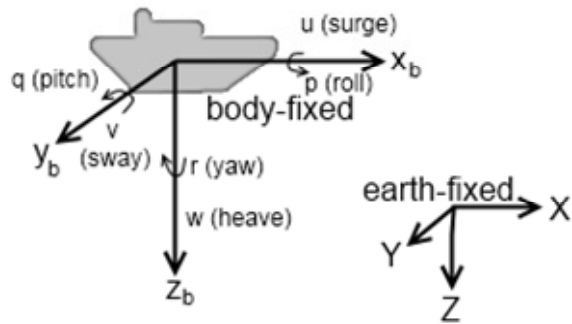


Figure 2.1: Body-fixed and earth-fixed reference frames

### 2.1.1.2 Euler Angles

This section presents the kinematic equations relating the body-fixed reference frame to the earth-fixed reference frame.

If we define:

$$\begin{aligned}\boldsymbol{\eta} &= [\boldsymbol{\eta}_1^T, \boldsymbol{\eta}_2^T]^T && \text{where } \boldsymbol{\eta}_1 = [x, y, z]^T \quad \text{and} \quad \boldsymbol{\eta}_2 = [\phi, \theta, \psi]^T \\ \boldsymbol{v} &= [\boldsymbol{v}_1^T, \boldsymbol{v}_2^T]^T && \text{where } \boldsymbol{v}_1 = [u, v, w]^T \quad \text{and} \quad \boldsymbol{v}_2 = [p, q, r]^T\end{aligned}$$

where  $\boldsymbol{\eta}$  is the position and orientation of the vehicle expressed in the earth-fixed reference frame, and  $\boldsymbol{v}$  is the linear and angular velocities of the vehicle in the body-fixed reference frame. The relation between  $\boldsymbol{\eta}$  and  $\boldsymbol{v}$  is given by:

$$\dot{\boldsymbol{\eta}}_1 = J_1(\boldsymbol{\eta}_2) \boldsymbol{v}_1 \quad (2.1)$$

where  $J_1(\boldsymbol{\eta}_2)$  is a transformation matrix which is related with the Euler angles: roll ( $\phi$ ), pitch ( $\theta$ ) and yaw ( $\psi$ ):

$$J_1(\boldsymbol{\eta}_2) = \begin{bmatrix} c\psi c\theta & -s\psi c\phi + c\psi s\theta s\phi & s\psi s\theta + c\psi c\phi s\theta \\ s\psi c\theta & c\psi c\phi + s\phi s\theta s\psi & -c\psi s\theta + s\theta s\psi c\phi \\ -s\theta & c\theta s\phi & c\theta c\phi \end{bmatrix} \quad (2.2)$$

where  $s(\cdot) = \sin(\cdot)$  and  $c(\cdot) = \cos(\cdot)$ .

The relation between the body-fixed angular velocity vector  $\boldsymbol{v}_2 = [p, q, r]^T$ , and the rate of change of the Euler angles  $[\dot{\phi}, \dot{\theta}, \dot{\psi}]^T$  is given by:

$$\dot{\boldsymbol{\eta}}_2 = J_2(\boldsymbol{\eta}_2) \boldsymbol{v}_2 \quad (2.3)$$

where  $J_2(\boldsymbol{\eta}_2)$  is also a transformation matrix related to the Euler angles, and is expressed by:

$$J_2(\boldsymbol{\eta}_2) = \begin{bmatrix} 1 & s\psi t\theta & c\phi t\theta \\ 0 & c\phi & -s\phi \\ 0 & s\phi/c\theta & c\phi/c\theta \end{bmatrix} \quad (2.4)$$

where  $s(\cdot) = \sin(\cdot)$ ,  $c(\cdot) = \cos(\cdot)$  and  $t(\cdot) = \tan(\cdot)$ . It is important to emphasize that  $J_2(\boldsymbol{\eta}_2)$  has a singularity at  $\theta = \pm 90^\circ$ . However, this does not constitute a problem for our system, because the vehicles never reach this operational point. Nonetheless, to overcome this situation, one could use a quaternion approach [8].

In conclusion we have defined the kinematic equations

$$\dot{\boldsymbol{\eta}} = \begin{bmatrix} J_1(\boldsymbol{\eta}_2) & \mathbf{0} \\ \mathbf{0} & J_2(\boldsymbol{\eta}_2) \end{bmatrix} \boldsymbol{v} \quad (2.5)$$

### 2.1.2 Rigid-body dynamics

In this section the rigid-body equations of motion in 6 degrees of freedom will be derived. Newtonian and lagrangian mechanics will not be discussed. For a comprehensive discussion see Arnold [9]. Likewise, an introduction to translational and rotational equations of motion can be found in Fossen [1] and Healey [6]. The general 6-DOF rigid-body equations of motion for underwater vehicles, in the presence of ocean currents, are presented in 2.6.

$$\begin{aligned}
 m[\dot{u} - vr + wq - x_G(q^2 + r^2) + y_G(pq - \dot{r}) + z_G(pr + \dot{q})] + (W - B)s\theta &= X_f + m(rv_c - qw_c) \\
 m[\dot{v} + ur - wp + x_G(pq + r^2) - y_G(p^2 + r^2) + z_G(qr - \dot{p})] - (W - B)c\theta s\psi &= Y_f + m(pw_c - ru_c) \\
 m[\dot{w} - uq + vp + x_G(pr - \dot{q}) + y_G(qr - \dot{p}) - z_G(p^2 + q^2)] - (W - B)c\theta c\psi &= Z_f + m(qu_c - pv_c) \\
 I_x\dot{p} + (I_z + I_y)qr + I_{xy}(pr - \dot{q}) - I_{yz}(q^2 - r^2) - I_{xz}(pq + \dot{r}) + m[y_G(\dot{w} - uq + vp) \\
 - z_G(\dot{v} + ur - wp)] - (y_GW - y_BB)c\theta c\psi + (z_GW - z_BB)c\theta s\psi &= K_f + my_G(u_cq - v_c p) \\
 I_y\dot{q} + (I_x - I_z)pr - I_{xy}(qr + \dot{p}) + I_{yz}(pq - \dot{r}) + I_{xz}(p^2 - r^2) - m[z_G(\dot{u} - vr + wq) \\
 - z_G(\dot{w} - uq + vp)] - (x_GW - x_BB)c\theta c\psi + (z_GW - z_BB)c\theta s\psi &= M_f + mz_G(v_cr - w_c q) \\
 I_z\dot{r} + (I_y - I_x)pq - I_{xy}(p^2 - q^2) - I_{yz}(pr + \dot{q}) + I_{xz}(qr - \dot{p}) + m[x_G(\dot{v} + ur - wp) \\
 - y_G(\dot{u} - vr + wq)] - (x_GW - x_BB)c\theta s\psi - (y_GW - y_BB)s\theta &= N_f + mx_G(w_c p - u_c r)
 \end{aligned} \tag{2.6}$$

where  $m$  is the vehicle mass,  $I_x$ ,  $I_y$  and  $I_z$  are the moments of inertia about  $x$ -,  $y$ - and  $z$ -axis of the body-frame and  $I_{xy} = I_{yx}$ ,  $I_{xz} = I_{zx}$  and  $I_{yz} = I_{zy}$  are the products of inertia.  $(x_G, y_G, z_G)$  are the coordinates of the vehicle's center of gravity (CG) and  $(x_B, y_B, z_B)$  are the coordinates of the vehicle's center of buoyancy (CB), both expressed in the vehicle body-fixed reference frame.

### 2.1.3 Hydrodynamic forces and moments

Hydrodynamic forces and moments are the result of body/fluid interactions. In general, the hydrodynamic force on a submerged vehicle depends on the relative velocity between the water particles and the vehicle (drag force); the relative acceleration between the water particles and the vehicle (the inertia and added mass terms), and the modifications to the buoyant forces resulting from water particle acceleration. The usual approach to model the hydrodynamic forces and moments is to consider two main components [10]:

1. **Radiation-Induced Forces** — Forces on the body when it is forced to oscillate with the wave excitation frequency and there are no incident waves. They can be divided into three categories:

- *added mass* due to the inertia of the surrounding fluid
- *damping*, caused by skin friction (laminar and turbulent) and vortex shredding
- *restoring forces* due to Archimedes (weight and buoyancy)

2. **Frouard-Kriloff and Diffraction Forces** — Forces on the body when it is restrained from oscillating and there are incident regular waves:

The 6-DOF rigid-body dynamic equations of motion in (2.6) can therefore be expanded with the equation for the forces and moments acting on the vehicle:

$$M\dot{v} + C(v)v + D(v)v + g(\eta) = \tau \quad (2.7)$$

$$\dot{\eta} = J(\eta_2)v \quad (2.8)$$

where  $M$  is the constant inertia and added mass matrix,  $C(v)$  is the Coriolis and centripetal matrix,  $D(v)$  is the damping matrix,  $g(\eta)$  is the vector of restoring forces and moments and  $\tau$  is the vector of body-fixed forces from the actuators. This section explains each one of them.

The *constant inertia and added mass* matrix  $M$  has two different contributions.  $M_{RB}$  which is the rigid-body inertia matrix and  $M_A$  which is the added mass matrix. The added mass matrix  $M_A$  represent the inertial reaction to the fluid particles surrounding the submerged body that are accelerated with it. For a rigid body moving in an ideal fluid, the added mass matrix is symmetrical, i.e.,  $M_A = M_A^T$ . Under the assumption of an ideal fluid, the inertia matrix,  $M$ , will also be symmetrical and thus positive definite, that is

$$M = M^T > 0 \quad (2.9)$$

Therefore,  $M$  takes the form:

$$M = \begin{bmatrix} m - X_{\ddot{u}} & -X_{\dot{v}} & -X_{\dot{w}} & -X_{\dot{p}} & mz_G - X_{\dot{q}} & -my_G - X_{\dot{r}} \\ -X_{\dot{v}} & m - Y_{\dot{v}} & -Y_{\dot{w}} & -mx_G - Y_{\dot{p}} & -Y_{\dot{q}} & mx_G - YY_{\dot{r}} \\ -X_{\dot{w}} & -Y_{\dot{w}} & m - Z_{\dot{w}} & my_G - Z_{\dot{p}} & -mx_G - Z_{\dot{q}} & -Z_{\dot{r}} \\ -X_{\dot{p}} & -mz_G - Y_{\dot{p}} & my_G - Z_{\dot{p}} & I_x - K_{\dot{p}} & -I_{xy} - K_{\dot{q}} & -I_{zx} - K_{\dot{r}} \\ mz_G - X_{\dot{q}} & -Y_{\dot{q}} & -mx_G - Z_{\dot{q}} & -I_{xy} - K_{\dot{q}} & I_y - M_{\dot{q}} & -I_{yz} - M_{\dot{r}} \\ -my_G - X_{\dot{r}} & mx_G - Y_{\dot{r}} & -Z_{\dot{r}} & -I_{zx} - K_{\dot{r}} & -I_{yz} - M_{\dot{r}} & I_z - N_{\dot{r}} \end{bmatrix} \quad (2.10)$$

The notation of SNAME [11] is used in this expression. This notation indicates the degree of freedom on which the hydrodynamic added mass force acts, as well as the cause of

the force. As an example,  $X_{\dot{v}}$  is a force acting along the body fixed  $x$ -axis due to an acceleration  $\dot{v}$  in the  $y$  direction, and can be thought of mathematically as  $X_{\dot{v}} = \frac{\partial X}{\partial \dot{v}}$ .

The *Coriolis and centripetal matrix*  $C(v)$  has also two different components.  $C_{RB}$  matrix which consists of the rigid-body Coriolis and centripetal matrix and  $C_A$  which is the hydrodynamic Coriolis and centripetal matrix, due to the added mass terms.

$$C_A(v) = \begin{bmatrix} 0 & 0 & 0 & 0 & -a_3 & a_2 \\ 0 & 0 & 0 & a_3 & 0 & -a_1 \\ 0 & 0 & 0 & -a_2 & a_1 & 0 \\ 0 & -a_3 & a_2 & 0 & -b_3 & b_2 \\ a_3 & 0 & -a_1 & b_3 & 0 & b_1 \\ -a_2 & a_1 & 0 & -b_2 & b_1 & 0 \end{bmatrix} \quad (2.11)$$

where

$$\begin{aligned} a_1 &= X_{\dot{u}}u + X_{\dot{v}}v + X_{\dot{w}}w + X_{\dot{p}}p + X_{\dot{q}}q + X_{\dot{r}}r \\ a_2 &= X_{\dot{v}}u + Y_{\dot{v}}v + Y_{\dot{w}}w + Y_{\dot{p}}p + Y_{\dot{q}}q + Y_{\dot{r}}r \\ a_3 &= X_{\dot{w}}u + Y_{\dot{w}}v + Z_{\dot{w}}w + Z_{\dot{p}}p + Z_{\dot{q}}q + Z_{\dot{r}}r \\ b_1 &= X_{\dot{p}}u + Y_{\dot{p}}v + Z_{\dot{p}}w + K_{\dot{p}}p + K_{\dot{q}}q + K_{\dot{r}}r \\ b_2 &= X_{\dot{q}}u + Y_{\dot{q}}v + Z_{\dot{q}}w + K_{\dot{q}}p + M_{\dot{q}}q + M_{\dot{r}}r \\ b_3 &= X_{\dot{r}}u + Y_{\dot{r}}v + Z_{\dot{r}}w + K_{\dot{r}}p + M_{\dot{r}}q + N_{\dot{r}}r \end{aligned} \quad (2.12)$$

The *damping matrix*  $D(v)$  represents the hydrodynamic damping in ocean vehicles. The later is mainly caused by the sum of the following components: radiation-induced potential damping due to forced body oscillations; linear skin friction due to laminar boundary layers and quadratic skin friction due to turbulent boundary layers; wave drift damping; and damping due to vortex's shredding (Morison's equation).

The vector of restoring forces and moments  $g(\eta)$  include the gravitational and buoyant forces acting on the body. The gravitational force  $f_G$  will act through the center of gravity (CG) of the body , and similarly, the buoyant force  $f_B$  will act through the center of buoyancy (CB).

$$g(\eta) = \begin{bmatrix} (W - B)s\theta \\ -(W - B)c\theta s\phi \\ -(W - B)c\theta c\phi \\ -(y_G W - y_B B)c\theta c\phi + (z_G W - z_B B)c\theta s\phi \\ (Z_G W - Z_B B)s\theta + (x_G W - x_B B)c\theta c\phi \\ -(x_G W - x_B B)c\theta c\phi - (y_G W - y_B B)s\theta \end{bmatrix} \quad (2.13)$$

### 2.1.4 Modifications to account for ocean current

This section presents a method to include the current-induced forces and moments in the dynamic equations of motions. This method assumes that the equations of motion can be represented in terms of the velocity of the vehicle relative to the ocean currents, expressed in the body-fixed reference frame.

Let

$$\mathbf{v}_r = \mathbf{v} - \mathbf{v}_c \quad (2.14)$$

where  $\mathbf{v}_c = [u_c, v_c, w_c, 0, 0, 0]^T$  is a vector of non-rotational body-fixed current velocities.

From the 6 degrees of freedom equations of motions (2.7), it is possible to define

$$M\dot{\mathbf{v}}_r + C(\mathbf{v}_r)\mathbf{v}_r + D(\mathbf{v}_r)\mathbf{v}_r + g(\eta) = \tau \quad (2.15)$$

$$\dot{\eta} = J(\eta)\mathbf{v} = J(\eta)(\mathbf{v}_r + \mathbf{v}_c) \quad (2.16)$$

It is possible to compute the earth-fixed current velocity vector ( $\mathbf{v}_c^e$ ) as follows

$$\mathbf{v}_c^e = J(\eta)\mathbf{v}_c \quad (2.17)$$

where  $\mathbf{v}_c^e = [u_c^e, v_c^e, w_c^e, 0, 0, 0]^T$ .

Next, the kinematic equations (2.5) can be modified to include the new state variable  $\mathbf{v}_r$ , and a vector  $\mathbf{v}_c^e$  describing the earth-fixed current velocity

$$\dot{\eta} = J(\eta)\mathbf{v}_r + \mathbf{v}_c^e \quad (2.18)$$

### 2.1.5 Actuator forces

#### 2.1.5.1 AUV actuator forces

The control of a small AUV at anything other than slow speed operations, must be accomplished by using *control surfaces* since the effect of thrusters decreases as the forward speed of the vehicle increases. These control surfaces are comprised of fins/planes and rudders. The forces and moments originated by these actuators are derived from airfoil theory and consist of drag and lift components. With the exception of the longitudinal direction (x-axis), the forces and moments applied to the vehicle are directly proportional to the amount of angular deflection of the control surfaces. The vector of forces and moments caused by these surfaces for a standard fin arrangement<sup>1</sup> is presented in equation (2.19). In general, AUVs have a thruster for speed control. Therefore, the thruster

---

<sup>1</sup>A standard fin arrangement has two pairs of control surfaces. Each pair of control surfaces, stern planes, bow planes or rudders, move together and are not independently controlled

force has to be considered. Also, one must consider the moment generated by the thruster, about the longitudinal axis. Hence,

$$f_\delta = \begin{bmatrix} [(X_{q\delta_{sp}} \delta_{sp} + X_{q\delta_{bp}} \delta_{bp})uq + (\dots) + F_{thruster}] \\ (Y_{\delta_{sr}} \delta_{sr} + Y_{\delta_{br}} \delta_{br})u | u | \\ (Z_{\delta_{sp}} \delta_{sp} + Z_{\delta_{bp}} \delta_{bp})u | u | \\ K_{thruster} \\ (M_{\delta_{sp}} \delta_{sp} + M_{\delta_{bp}} \delta_{bp})u | u | \\ (N_{\delta_{sr}} \delta_{sr} + N_{\delta_{br}} \delta_{br})u | u | \end{bmatrix} \quad (2.19)$$

where *sp* stands for stern planes, *sr* are the stern rudders, *bp* means bow planes and finally, *br* are the bow rudders (Figure 2.2).

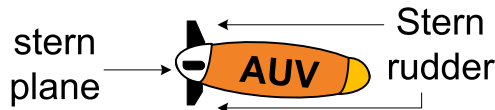


Figure 2.2: AUV standard fin arrangement

### 2.1.5.2 ROV actuator forces

For conventional ROVs the basic motion is the movement in a horizontal plane with some variation due to diving. It is possible to consider two separate planes: the motion along the horizontal plane and the motion along the vertical plane. The most often applied configuration of thrusters in the propulsion system is shown in figure 2.3 (Garus [12]). This is an overactuated system. The vertical thruster is responsible for the motions along the vertical plane, while the four remaining thrusters are responsible for the motions along the horizontal plane. Garus [12] presents some methods of thrust allocation in a propulsion system for an unmanned underwater vehicle. For further information concerning thruster allocation, the reader is referred to Webster and Sousa [13] where an algorithm using linear programming to achieve the desired force system is developed.

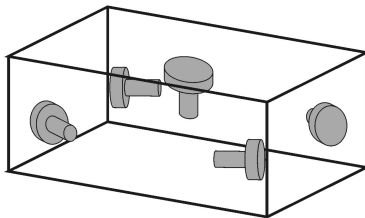


Figure 2.3: Configuration of thrusters in a typical ROV propulsion system. Source: Garus

Along the vertical plane, the thrust distribution is performed in such a way that the propeller thrust, or the sum of propellers thrusts, is equal to the demanded force  $Z_d$ . Along the horizontal plane, the forces  $X$  and  $Y$  acting in the longitudinal and transversal axis and the moment  $N$  about the vertical axis are a combination of thrusts produced by the propellers of the horizontal subsystem. The relationship between the forces and moments and the propeller thrust is a complicated function that depends on a various number of factors. In practice, the actuator forces acting in the horizontal plane can be described as a function of the thrust vector  $f$ :

$$\tau = T(\alpha)f \quad (2.20)$$

where

$$\tau = [\tau_1, \tau_2, \tau_3]^T \quad (2.21)$$

and  $\tau_1$  is force in the longitudinal axis,  $\tau_2$  is the force in the transversal axis, and finally,  $\tau_3$  is the moment about the longitudinal axis.

$$T = \begin{bmatrix} \cos \alpha_1 & \cos \alpha_2 & \dots & \cos \alpha_3 \\ \sin \alpha_1 & \sin \alpha_2 & \dots & \sin \alpha_3 \\ d_1 \sin \gamma_1 & d_2 \sin \gamma_2 & \dots & d_3 \sin \gamma_3 \end{bmatrix} \quad (2.22)$$

where  $\gamma_i = \alpha_i - \varphi_i$ . Figure 2.4 presents the layout of the thrusters responsible for the horizontal motion of the ROV.

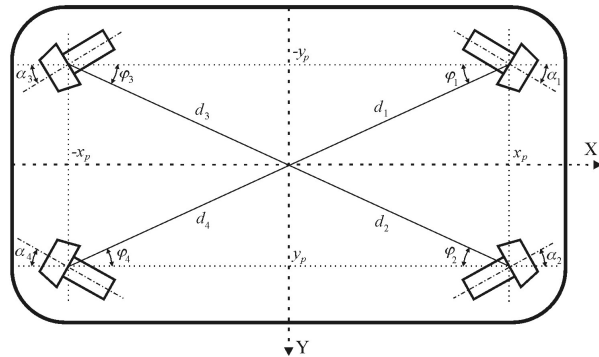


Figure 2.4: Layout of thrusters in the horizontal subsystem responsible for the horizontal motion.  
Source: Garus

## 2.2 Hybrid Systems

Modern day systems incorporate both differential equations to model the continuous behavior, and discrete event systems to model instantaneous state changes in reaction to events. System which incorporate both dynamical and discrete event models are called hybrid systems. In this section we review the formal model and make a brief introduction of some properties of hybrid automata - a formalism for specifying hybrid systems. Hybrid systems have been extensively used for intelligent vehicle control (Varaiya, [14]) and in air traffic management systems (Godbole, Sastry, Lygeros et. al. [15] and [16]). For a more in-depth study, Varaiya et. al. has an extended published work about Hybrid Systems ([17], [18], [19] etc.) and Hespanha [20] class notes are also available.

The Hybrid automaton model given next [21] is a generalization of other models introduced in the literature (Alur et. al. [22] and Puri et. al. [23])

A Hybrid transition system is a tuple

$$H = (Q, \mathbf{R}^n, \Sigma, E, \Phi) \quad (2.23)$$

where  $Q$  is the finite set of discrete states and  $\mathbf{R}^n$  is the set of continuous states.  $\Sigma$  is the finite set of discrete events.

$$E \subset Q \times \Sigma \times \{\mathbf{R}^n \rightarrow \mathbf{R}^n\} \times Q$$

$E$  is the finite set of edges<sup>2</sup>. The edges model the discrete event dynamics of the system. An edge  $e \in E$  is denoted as

$$(q_e, X_e, V_e, r_e, q_e^{new})$$

and is enabled when the discrete state is  $q_e$  and the continuous state is inside the set  $X_e$ . When a transition through  $e$  is taken, the event  $V_e \in \Sigma$  is accepted by the system. The continuous state is then reset according to the map  $r_e$ , and the system enters the discrete state  $q_e^{new}$ .

$$\Phi = \{F_q : \mathbf{R}^n \rightarrow P(\mathbf{R}^n) \setminus \emptyset | q \in Q\}$$

is a set of differential inclusions that model the continuous dynamics of the system. When the discrete state is  $q$ , the continuous state evolves according to the differential inclusion.

A hybrid automaton models a hybrid system. It consists of a graph with discrete states as vertices and with edges between the discrete states (see figure 2.5). Each discrete state ( $Q$ ) is labeled with a specific differential inclusion ( $\Phi$ ), and every edge ( $E$ ) is labeled

---

<sup>2</sup> $P(\cdot)$  denotes the power set (or, the set of all subsets) of  $(\cdot)$

with a guard condition, and a jump relation. The state of the hybrid automaton is the pair  $(q, x)$  where  $q$  is the discrete state, and  $x \in \mathbf{R}^n$  is the continuous state. The hybrid automaton starts from some initial state  $(q_0, x_0)$ . The trajectory evolves with the discrete state remaining constant and the continuous state  $x$  evolving accordingly with the differential inclusion expressed in the discrete state. When the continuous state satisfies the guard condition of an edge from some discrete state  $q_i$  to other discrete state  $q_k$ , a jump can be made to the new discrete state  $q_k$ . During the jump, the continuous state may get initialized to a new value  $x_k$  (reset condition). The new state of the hybrid system is the pair  $(q_k, x_k)$ . The continuous state  $x$  now moves with the new differential inclusion. This describes the transition between states of a hybrid system.

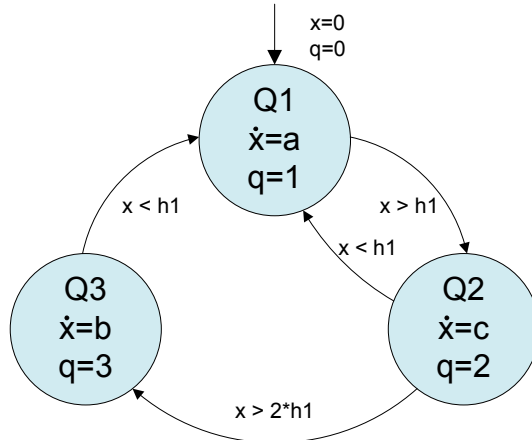


Figure 2.5: Example of a hybrid automaton

Consider for instance figure 2.5 which presents an example of a hybrid automaton. The Hybrid System starts with the continuous state  $x = 0$  and with discrete state  $q = 0$ . The system then enters state **Q1**, where the continuous state  $x$  evolves accordingly with the differential inclusion  $\dot{x} = a$ . At this point the discrete state  $q$  is  $q = 1$ . Imagine there is a limit we have to consider for  $x$  which is  $x = h_1$ . So, there is a guard condition between **Q1** and **Q2** with  $x > h_1$ . If the state of the system increases in a way that the limit is overflowed, then a jump is made to the new discrete state **Q2**. Now  $x$  evolves accordingly with  $\dot{x} = c$  and the discrete state is  $q = 2$ . In case some disturbance happens with the system that takes the state to a dangerous level (above  $2h_1$ ) then a jump is made to **Q3**, where  $\dot{x} = b$  and  $q = 3$ . When the state of the system returns to a normal level ( $x < h_1$ ), then the discrete state returns to **Q1** from either **Q2** or **Q3**.

## 2.3 Reachability results

The standard reachability problem is an essential topic in control theory. Because of its importance in applications ranging from engineering to biology and economics, questions of reachability, viability and invariance<sup>3</sup> have been studied extensively in the dynamics and control literature. Most recently, the study of these concepts has received renewed attention through the study of safety problems in hybrid systems ([17], [21], [24]). Reachability computations have been used in this context to address problems in the safety of ground transportation systems ([25]), air traffic management systems ([26], [27], [28]), flight control ([29], [30]) etc. We can define the reachability problem as the computation of the set of states reachable by a controlled process through available controls. This section follows closely João Sousa ([31], [32]).

### 2.3.1 Reach Sets

#### 2.3.1.1 Continuous-time systems

Consider the following continuous model of a system whose state evolves in  $\mathbb{R}^n$

$$\dot{x}(t) = f(t, x, u) \quad (2.24)$$

where  $x \in \mathbb{R}^n$ ,  $u \in U(t) \subset \mathbb{R}^p : \mathbb{R}^n \times U \rightarrow \mathbb{R}^n$ . Assume that the system is *Lipschitz* (see section 2.4.1 for an appropriate definition) in  $x$  and continuous in  $u$ ; in this case there is an equivalent description:

$$\dot{x}(t) \in F(t, x(t)) \subset \mathbb{R}^p \quad (2.25)$$

which is a differential inclusion, where  $F(t, x) = \{s : s = f(t, x, u), u \in U(t)\}$ . The set-valued map  $F$  maps  $(t, z)$  onto the set of admissible velocities at  $(t, x)$ . The local properties of the system depend on the geometry of this set (e.g., if we consider the differential inclusion  $\dot{x} \in F(x) \subset \mathbb{R}^n$  describing a Lipschitz system, then the system is locally controllable only when the origin is an interior point of  $F$ ).

In control theory there is the interest to know the set of points that can be reached at time  $t > t_0$  starting from  $x_0$ . A state of a dynamical system is defined to be reachable if there is a sequence of control signals  $u(\cdot)$  that drive the system to the state. Consider, as examples, the following applications in vehicle control:

1. When will the vehicle collide with an obstacle (figure 2.6) ?

---

<sup>3</sup>Viability theory deals with two fundamental properties of sets of states of a dynamical system. Roughly speaking, a set of states,  $S$ , is called viable if for all initial conditions in  $S$ , there exists a solution of the dynamical system that remains in  $S$ ; it is called invariant if for all initial conditions in  $S$  all solutions of the system remain in  $S$ .

2. When and where is it feasible for two vehicles to rendez-vous ?
3. When and where is it feasible for the AUV to dock into the ROV ?
4. What is the set of initial positions such that if the AUV departs from this set it will be able to reach the dock station in a given time interval ?

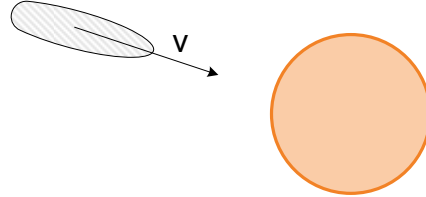


Figure 2.6: Possible collision between an AUV with an obstacle

### 2.3.1.2 Forward reachability

Consider the system described by equation (2.24).

**Definition 1 (Reach set starting at a given point).** Suppose the initial position and time  $(x_0, t_0)$  are given. The reach set  $R(t, t_0, x_0)$  of system (2.24) at time  $t \geq t_0$ , starting at position and time  $(x_0, t_0)$  is given by:

$$R(t, t_0, x_0) = \bigcup \{x(t), u(s, x(s)) \in U(s), s \in (t_0, t]\} \quad (2.26)$$

**Definition 2 (Reach set starting at a given set).** The reach set at time  $t > t_0$  starting from set  $X_0$  (see figure 2.7) is defined as:

$$R(t, t_0, X_0) = \bigcup_{x_0 \in X_0} R(t, t_0, x_0) \quad (2.27)$$

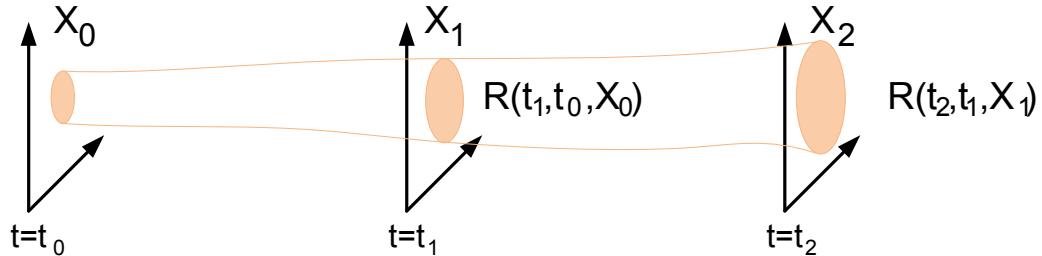


Figure 2.7: Reach set for a system starting from set  $X_0$

### 2.3.1.3 Backward reachability

Until now, we have only discussed the problem of forward reachability - the set of all reachable states for a system described by equation (2.24), starting at a given position and time. In control applications there is interest of calculating the backward reach set - the set of all states at time  $t < t_0$  that drive the state of the system to a given set  $X_f$  at time  $t = t_0$ .

**Definition 3 (Backward reach set at a given point).** The backward reach set  $BR(t_1, t, x_1)$  for the target position  $(t_1, x_1)$  is the set of all states  $x(t)$  for which there exists some control  $u(s, x(s)) \in U(s), t \leq s < t_1$ , that drives the system (2.24) to the state  $x_1$  at time  $t_1$ .

$$BR(t_1, t, x_1) = \bigcup \{x(t), u(s, x(s)) \in U(s), s \in (t, t_1]\} \quad (2.28)$$

**Definition 4 (Backward reach set at a given set).** For the target set  $X_1$  at time  $t_1$ , the backward reach set  $BR(t_1, t, X_1)$  (see figure 2.8) is

$$BR(t_1, t, X_1) = \bigcup_{x_1 \in X_1} BR(t_1, t, x_1) \quad (2.29)$$

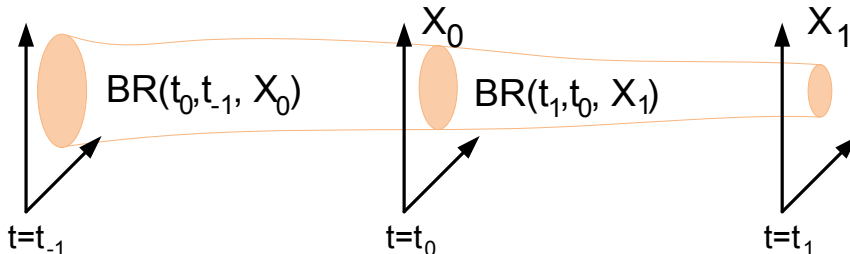


Figure 2.8: Backward reach set for the target set  $(t_1, X_1)$

### 2.3.1.4 Useful properties

The reach set describes the motion capabilities of a dynamic system. In control applications, we are interested in synthesizing a controller such that the composition of the dynamic system and the controller satisfies a number of properties. Consider a dynamic system and a closed and compact set  $S$ . Some properties of interest:

- **Invariance** - the trajectories of the system do not leave  $S$ .

- *Weak Invariance* - the pair  $(S, F^4)$  is weakly invariant if there exist controls such that a trajectory starting inside  $S$  remains inside  $S$ . Notice that there exists other controls such that the trajectory leaves  $S$ .
- *Strong Invariance* - the pair  $(S, F)$  is strongly invariant if the trajectories starting inside  $S$  **never** leave  $S$ .
- **Attainability** - the trajectories of the system will enter  $S$ .
- **Safety** - the trajectories of the system do not enter  $S$ .

Checking for those properties amounts to solving reachability problems.

### 2.3.2 Dynamic optimization for reach set computation

#### 2.3.2.1 Introduction

The relation between dynamic optimization and reachability was first presented by Leitmann [33]. The original reachability problems do not involve optimization criteria, and are reformulated in terms of optimization problems solved through the Hamilton-Jacobi-Bellman equations. The reach sets are the level sets of the *value function* solutions to these equations. Kurzhanski and Varaiya ([34], [35]) discussed optimization techniques for reachability problems. Some notions about differential games will also be introduced (for a thorough study see Krasovskii *et. al.* [36]).

#### 2.3.2.2 Dynamic programming

Dynamic programming is one of the techniques used to solve optimal control problems. The optimal control problem is embedded into a family of optimization problems which are state dependent. This dependency is characterized by value functions. This section introduces the concept of value function which is associated to optimal control problems and show how to derive the Hamilton-Jacobi-Bellman equation (which is satisfied by the value function) from the Principle of Optimality. The theory involved in viscosity solutions of first order partial differential equations (PDE) of HJB is given in [37].

Next, a simple example of minimum-time optimal control will be presented.

Consider that the model of the system is given by equation (2.24). Furthermore, we will assume that the system is locally controllable, which means that the origin is an interior point of  $F$  of the differential inclusion (2.25).

Consider a bounded and closed set  $S$  with non-empty interior. Let  $t_f$  denote the first time when the trajectory of the system reaches the target set  $S$ .

---

<sup>4</sup> $F$  is the set-valued map from equation (2.25)

$$t_f = \inf\{t : x(t) \in S\} \quad (2.30)$$

A possible problem is to reach the target in minimum time possible (minimum-time optimal control problem).

**Problem 1** – Let  $x(0) = x_0$ . Find:

$$\inf_{u(\cdot)} t_f \quad (2.31)$$

where  $u(\cdot) : \mathbb{R} \rightarrow \mathbb{R}^p$  is an admissible control function.

Under the assumptions considered for the system and for the target set, the infimum is attained at a time  $T \in \mathbb{R}$ . Introduce the value function  $T : \mathbb{R}^n \rightarrow \mathbb{R}$  as

$$T(x) = \inf_{u(\cdot)} t_f \quad (2.32)$$

Consider a pair  $(x^*; t)$  somewhere along a trajectory departing from  $(x_0, 0)$ . The **principle of optimality** for problem 1 can be expressed as follows:

$$T(x_0) \leq t + T(x^*) \quad (2.33)$$



Figure 2.9: Principle of optimality

For optimal trajectories equality holds. The interpretation is simple. For a point on the optimal trajectory, it is optimal to stay on the optimal trajectory (see figure 2.9).

One can find the Hamilton-Jacobi-Bellman equation for this problem with one further assumption: the value function  $T$  is differentiable. The HJB equation can be interpreted as an infinitesimal version of the principle of optimality described in equation (2.33) for problem 1. For this purpose we must divide both terms of equation (2.33) by  $t$  and take limits when  $t \rightarrow 0$ . Keep in mind that we are taking the total derivative of  $T$  with respect to  $t$ . One can make use of the **chain rule**<sup>5</sup> to first take the derivative with respect to  $x$  and

---

<sup>5</sup>Consider that a variable  $y$ , depends on a second variable,  $u$ , which in turn depends on a third variable,  $x$ , that is  $y = y(u(x))$ , then the rate of change of  $y$  with respect to  $x$  can be computed as the rate of change of  $y$  with respect to  $u$

multiply it by the derivative of  $x$  with respect to time. Finally, we have:

$$\inf_{u \in U} -\nabla T(x_0).f(x, u) = 1 \quad (2.34)$$

This is a partial differential equation. The boundary condition is  $T(x) = 0, x \in S$ .

### 2.3.2.3 Value functions for reach set computations

In the previous section we have defined value functions, and HJB equations. Therefore, it is possible to formulate the problem of reach set computation through as an optimization problem (Kurzhanski and Varaiya [34], [35]). The key factor is the knowledge that the reach set is the level set of an appropriate value function ([38], [39], [40]). To illustrate this point we can consider the following value function:

$$V(\tau, x) = \min_{u(\cdot)} \{d^2(x(t_0), X^0) | x(\tau) = x\} \quad (2.35)$$

$$V(t_f, x) = d^2(x, X^f) \quad (2.36)$$

where  $u(\cdot)$  is an admissible control function defined for  $[t_0, \tau]$  and  $d(x(t_0), X^0)$  is the Euclidean distance between the state of the system starting at time  $t_0$  and the initial set  $X^0$  for a trajectory finishing at  $(\tau, x)$ . It is a simple observation, that  $(\tau, x)$  belongs to the forward reach set when this distance is zero. Furthermore, this also means that the forward reach set is the zero level set of the value function  $V$ :

$$X(\tau, t_0, X^0) = \{x : V(\tau, x) \leq 0\} \quad (2.37)$$

For the value function  $V(t, x)$  it is also possible to use the notation

$$V(t, x) = V(t, x | t_0, V(t_0, \cdot)) \quad (2.38)$$

emphasizing the dependence on the boundary condition  $V(t_0, x) = d^2(x, X^0)$ .

**Theorem 1.**  $V(t, x)$  satisfies the principle of optimality:

$$V(\tau, x | t_0, V(t_0, \cdot)) = V(t, x | \tau, V(\tau, \cdot | t_0, V(t_0, \cdot))), \quad t_0 \leq \tau \leq t_1 \quad (2.39)$$

the principle of optimality states that the value function satisfies a semi-group property, inherited from the semi-group property of the reach set.

---

multipled by the rate of change of  $u$  with respect to  $x$ .

The question at hands is how to compute an appropriate value function. The goal is to transform the global problem into a local one. This is achieved by transforming the global problem onto a partial differential equation.

The solution of the reachability problem now depends on the properties of the "classical" or "viscosity" solutions of the forward HJB equation<sup>6</sup>:

$$V_t(t, x) + \max_{u \in U(t)} (V_x(t, x) \cdot f(t, x, u)) = 0 \quad (2.40)$$

$$V(t_0), x = 0, x \in X^0 \quad (2.41)$$

Here  $V_t$ ,  $V_x$  stand for the partial derivatives of  $V(t, x)$ , if these exist. Otherwise, equation (2.40) is a symbolic relation for the generalized HJB equation which has to be described in terms of subdifferentials, Dini derivatives or their equivalents. However, the typical situation is that the value function is not differentiable. This leads to the use of generalized notions of derivatives. Therefore, we consider generalized "viscosity", or equivalent concepts, of solutions for this equation (Krasovskii et. al. [36], Bardi and Capuzzo-Dolcetta [37]).

**Theorem 2 (Viscosity solution to the HJB equation).** If the value function  $V(t, x)$  is continuous in  $\{t, x\}$  then it is a (unique) viscosity solution to the "forward" HJB equation (2.40) with boundary condition (2.41). In particular, it may be a classical solution if it is differentiable in  $\{t, x\}$ .

This approach is very interesting because it is possible to express state constraints into the value functions (for more information regarding state constraints in reach set computations see Sousa [31], Kurzhanski and Varaiya [41]). Keep in mind, state constraints are an important factor in every real world system, and reach set computations must take them into account.

#### 2.3.2.4 Reach set computation through differential games

A direct method for reach set computation is with differential games theory. This section follows very closely Sousa notes [31]. For a more in-depth study consult Krasovskii and Subbotin [36].

Consider the following dynamic system with state  $x \in \mathbb{R}$  controlled by two adversarial control inputs  $u$  and  $v$ :

$$\dot{x} = f(t, x, u, v), \quad u \in P, v \in Q \quad (2.42)$$

where the following hypotheses hold:

---

<sup>6</sup>Computation of the backward reach set is achieved with the backward HJB equation

1.  $f$  is continuous in all variables and  $t \in T = (-\infty, \theta]$ .
2. For any bounded region  $D$  in  $\mathbb{R} \times \mathbb{R}$ ,  $f$  satisfies the following *Lipschitz* condition:

$$\|f(t, x_1, u, v) - f(t, x_2, u, v)\| \leq \lambda(D) \|x_1 - x_2\|$$

for any  $(t, x_i) \in D$ ,  $(u, v) \in P \times Q$

3. For any  $(t, x, u, v) \in T \times \mathbb{R} \times P \times Q$  the following inequality, where  $\sigma$  is a constant, is valid:

$$xf(t, x, u, v) \leq \sigma(1 + \|x\|^2)$$

4. For any  $(t, x) \in T \times \mathbb{R}$  and  $s \in \mathbb{R}$  the so-called "saddle point condition in a small game" is valid<sup>7</sup>:

$$\min_{u \in P} \max_{v \in Q} sf(t, x, u, v) = \max_{v \in Q} \min_{u \in P} sf(t, x, u, v)$$

Consider now the target set  $M$ :

$$M = \{(t, x) \in T \times \mathbb{R} : t = \theta; l_1 \leq x \leq l_2\} \quad (2.43)$$

Now we must consider a differential game with two players controlling  $u$  and  $v$  respectively. The objective of  $u$  is to steer the state of the system,  $x(\cdot)$ , to the target set  $M$ . The objective of  $v$  is exactly the opposite. More formally, consider the following cost functional:

$$\gamma(x(t_0, x_0, U(\cdot), V(\cdot))) = \begin{cases} 0 & \text{if } x(\cdot) \text{ intersects } M \\ 1 & \text{otherwise} \end{cases} \quad (2.44)$$

where  $U(\cdot)$  is a control function for the first player and  $V(\cdot)$  is a control function for the second player. Note that  $\gamma(x(t_0, x_0, U(\cdot), V(\cdot))) = 0$  means that the trajectory  $x(\cdot)$  departing from  $(t_0, x_0)$  under controls  $U(\cdot)$  and  $V(\cdot)$  enters the target set  $M$  at time  $\theta$ .

The adversarial aspect is captured in an optimization problem where  $u$  seeks to minimize  $\gamma$  and  $v$  seeks to maximize it (figure 2.10). Under the hypotheses stated, a value  $V_g(t_0, x_0)$  can be defined. This means that:

$$V_g(t_0, x_0) = \inf_{U(\cdot)} \sup_{V(\cdot)} \gamma(x(t_0, x_0, U(\cdot), V(\cdot))) = \sup_{V(\cdot)} \inf_{U(\cdot)} \gamma(x(t_0, x_0, U(\cdot), V(\cdot))) \quad (2.45)$$

---

<sup>7</sup>this condition holds, for example, for linear systems

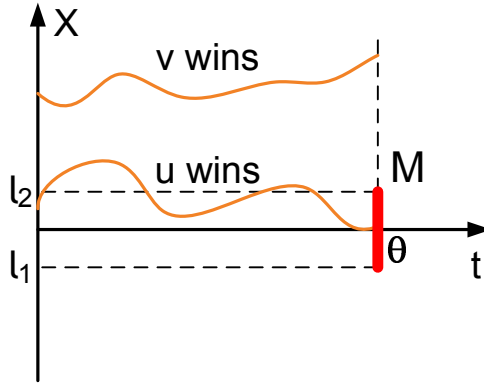


Figure 2.10: Antagonistic player in differential games

Moreover, the game has a saddle point, i.e., there exist strategies  $U^*(\cdot), V^*(\cdot)$  such that for any feedback strategies  $U(\cdot), V(\cdot)$  the following holds:

$$\gamma(x(t_0, x_0, U^*(\cdot), V(\cdot))) \leq \gamma(x(t_0, x_0, U^*(\cdot), V^*(\cdot))) \leq \gamma(x(t_0, x_0, U(\cdot), V^*(\cdot))) \quad (2.46)$$

One can summarize this notions on the following theorem 3

**Theorem 3 (Value of the game).** For any closed set  $M$  and for any initial position  $(t_0, x_0)$ , one and only one of the following assertions is valid:

1. The value of the game is 0 and any  $(U^*, V)$  is a saddle point ( $V$  is any feedback strategy)
2. The value of the game is 1. Furthermore, the optimal strategies  $U^*$  and  $V^*$  are feedback strategies.

Furthermore, Krasovskii and Subbotin [36] define the notion of **u-stable bridge**. The u-stable bridge  $W_0$  can be defined as the set of all points  $(t_0, x_0)$  such that there exists an optimal strategy  $U^*$  that keeps the motion of the system departing from  $(t_0, x_0)$  inside  $W_0$  until the target set  $M$  is reached. The v-stable bridge is exactly the opposite. In other words, the **u-stable bridge** can be seen as the backward reach set under adversarial behavior.

In this problem setup it is possible to derive a closed form for the u-stable bridge. First set:

$$f_1(t, x) := \max_{u \in P} \min_{v \in Q} f(t, x, u, v) \quad (2.47)$$

$$f_2(t, x) := \min_{u \in P} \max_{v \in Q} f(t, x, u, v) \quad (2.48)$$

Consider solutions  $w_1$  and  $w_2$  to the following ordinary differential equations (ODE):

$$\dot{w}_1(t) = f_1(t; w_1(t)); \quad w_1(\theta) = l_1 \quad (2.49)$$

$$\dot{w}_2(t) = f_2(t; w_2(t)); \quad w_2(\theta) = l_2 \quad (2.50)$$

The u-stable bridge (figure 2.11) is the set:

$$W_0 := \{(t, x) \in T \times \mathbb{R} : t \in T_*, x \in [w_1(t), w_2(t)]\} \quad (2.51)$$

where  $T_* = [\tau_*, \theta]$ ,  $\tau_* = \sup\{t \in T : w_2(t) > w_1(t)\}$ .

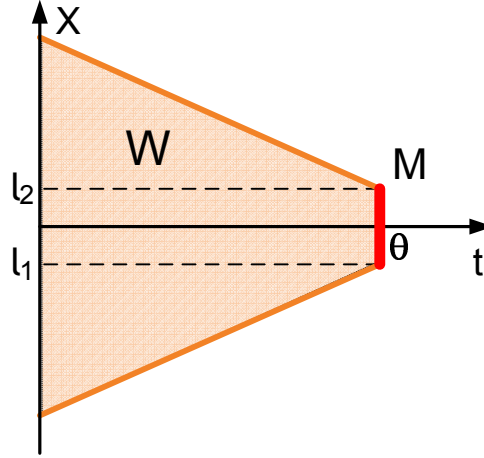


Figure 2.11: The u-stable bridge

Equations (2.49) and (2.50) describe the evolution (in reverse time) of the boundaries  $(l_1, l_2)$  of the target set  $M$  when both players adopt optimal control strategies (given by the argmax and argmin in equations (2.47) and (2.48)).

This construction can be extended to a Multiple-input multiple-output (MIMO) problem when the target set is a closed ball centered at the origin since this involves working with a norm (1-dim function).

In conclusion, reach set computation through differential games is a very interesting technique for the docking problem, since the objective of the control strategy is to drive the AUV to the origin<sup>8</sup>. In other words, we are using the distance between the two vehicles to express the backward reach set.

---

<sup>8</sup>It is possible since the AUV state can be expressed in the ROV body-fixed reference frame

## 2.4 Lyapunov stability

This section gives a brief introduction to Lyapunov theory. If a system is initially in an equilibrium point<sup>9</sup>, it remains in the same state thereafter. However, in control systems theory, there is interest in studying the behavior of the state of the system, when it is not in the equilibrium point. Therefore, Lyapunov stability deals with the behavior of the trajectories of a system when its initial state is not an equilibrium, but is near an equilibrium (the state is in the vicinity of the equilibrium point).

It is possible to find many references about Lyapunov theory in the literature. Slotine and Li [42], Vidyasagar [43] and Khalil [44] present an extended study about Lyapunov stability.

For a simple overview about the topic the reader may refer to Sastry and Robson [45] or Girard [46]. The theory presented in this section will follow more closely both Vidyasagar's and Slotine and Li's books.

### 2.4.1 Nonlinear systems and Equilibrium points

Given a system described by:

$$\dot{\mathbf{x}}(t) = f(t, \mathbf{x}(t)) \quad , \quad t \geq 0 \quad (2.52)$$

where  $\mathbf{x}(t) \in \mathbb{R}^n$ , and  $f = \mathbb{R} \times \mathbb{R}^n \rightarrow \mathbb{R}^n$  is continuous. A particular value of the state vector is also called a point because it corresponds to a point in the state-space. The number of states  $n$  is called the order of the system. A solution  $x(t)$  of the equation (2.52) usually corresponds to a curve in state space as  $t$  varies from zero to infinity. This curve is generally referred to as a state trajectory or a system trajectory.

The function  $f$  is said to be *Lipschitz* in  $x$  if, for some  $h > 0$ , there exists  $l \geq 0$  such that

$$|f(t, x_1) - f(t, x_2)| \leq l|x_1 - x_2| \quad (2.53)$$

for all  $x_1, x_2 \in B_h$ ,  $t \geq 0$ .  $B_h$  is the closed ball of radius  $h$  centered at 0 in  $\mathbb{R}$ . The constant  $l$  is called the *Lipschitz constant*. This is the local definition for the Lipschitz condition. A global Lipschitz function satisfies equation (2.53) for all  $x_1, x_2 \in \mathbb{R}$ . The Lipschitz property is usually assumed to be satisfied uniformly, i.e.,  $l$  does not depend on time  $t$ .

---

<sup>9</sup>Informally, an equilibrium (or equilibrium point) of a dynamical system is a solution that does not change with time

The meaning of the Lipschitz condition is that if  $f$  is Lipschitz in  $x$ , then it is continuous in  $x$ . On the other hand, if  $f$  has continuous and bounded partial derivatives in  $x$ , then it is Lipschitz. More formally, we can express

$$\nabla f = \left[ \frac{\partial f_1}{\partial x_j} \right] \quad (2.54)$$

so that if  $\|\nabla f\| \leq l$ , then  $f$  is Lipschitz with constant  $l$ .

From the theory of ordinary differential equations it is known that  $f$  locally bounded, and  $f$  locally Lipschitz in  $x$  implies the existence and uniqueness of the solutions of (2.52) for some time interval (for as long as  $x \in B_h$ ).

#### 2.4.1.1 Autonomous and non-autonomous systems

**Definition 5 (Autonomous system).** The nonlinear system (2.52) is said to be autonomous if  $f$  does not depend explicitly on time, i.e., if the system's state equation can be written

$$\dot{\mathbf{x}} = f(\mathbf{x}) \quad (2.55)$$

Otherwise, the system is called non-autonomous.

Obviously, linear time-invariant (LTI) systems are autonomous and linear time-varying (LTV) systems are non-autonomous.

#### 2.4.1.2 Equilibrium Points

It is possible for a system trajectory to correspond only to a single point. Such a point is called an **equilibrium point**.

**Definition 6 (Equilibrium point).** A state  $\mathbf{x}_0$  is an equilibrium state (or equilibrium point) of the system if once  $\mathbf{x}(t) = \mathbf{x}_0$ , it remains equal to  $\mathbf{x}_0$  for all future time.

$$f(t, \mathbf{x}_0) = \mathbf{0} \quad , \quad \forall t \geq 0 \quad (2.56)$$

which means, if the system starts at an equilibrium point, it stays there forever in the absence of disturbances. This section assumes that  $\mathbf{0}$  is an equilibrium of the system (2.52). Keep in mind, that if the equilibrium under study is not the origin, one can always introduce a coordinate transformation on  $\mathbb{R}^n$  in such a way that the equilibrium of interest becomes the new origin.

### 2.4.2 Stability definitions

Consider the system described by (2.52). We have seen in section 2.4.1 that a vector  $\mathbf{x}_0 \in \mathbb{R}^n$  is an equilibrium of the system if condition (2.56) is satisfied.

**Definition 7 (Stable equilibrium).** The equilibrium  $\mathbf{x}_0 = \mathbf{0}$  is *stable* if, for each  $\varepsilon > 0$  and each  $t_0 \in \mathbb{R}$ , there exists a  $\delta = \delta(\varepsilon, t_0)$  such that

$$\|\mathbf{x}_0\| < \delta(\varepsilon, t_0) \Rightarrow \|\mathbf{x}(t)\| < \varepsilon \quad , \quad \forall t \geq t_0 \quad (2.57)$$

Figure 2.12 illustrates a stable equilibrium. The equilibrium is stable, as long as for all  $\varepsilon$ , there is a  $\delta$  such that if  $|\mathbf{x}_0|$  is less than  $\delta$ , then  $|\mathbf{x}(t)|$  is less than  $\varepsilon$  for all  $t > t_0$ . The equilibrium is *unstable* if it is not stable.

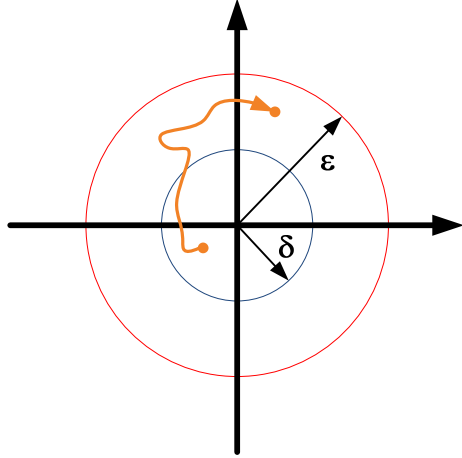


Figure 2.12: A stable equilibrium

**Definition 8 (Uniform stability).** The equilibrium  $\mathbf{x}_0 = \mathbf{0}$  is *uniformly stable* if, for each  $\varepsilon > 0$ , there exists a  $\delta = \delta(\varepsilon)$  such that

$$\|\mathbf{x}_0\| < \delta(\varepsilon) \Rightarrow \|\mathbf{x}(t)\| < \varepsilon \quad , \quad \forall t \geq t_0 \quad (2.58)$$

In other words, the system is stable for time-varying systems.

**Definition 9 (Attractive equilibrium).** The equilibrium  $\mathbf{x}_0 = \mathbf{0}$  is *attractive* if, for each  $t_0 \in \mathbb{R}$ , there is an  $\eta(t_0) > 0$  such that

$$\|\mathbf{x}_0\| < \eta(t_0) \Rightarrow \|\mathbf{x}(t)\| \rightarrow 0 \text{ as } t \rightarrow \infty \quad (2.59)$$

**Definition 10 (Uniformly attractive equilibrium).** The equilibrium state  $\mathbf{x}_0 = \mathbf{0}$  is *uniformly attractive* if there is a number  $\eta(t_0) > 0$  such that

$$\|\mathbf{x}_0\| < \eta \Rightarrow \|\mathbf{x}(t)\| \rightarrow 0 \text{ as } t \rightarrow \infty, \text{ uniformly in } \mathbf{x}_0, t. \quad (2.60)$$

Thus attractivity simply means that, at each initial  $t_0 \in \mathbb{R}$ , every solution trajectory starting sufficiently close to  $\mathbf{0}$  ( $\|\mathbf{x}_0\| < \eta(t_0)$ ) actually approaches  $\mathbf{0}$  as  $t \rightarrow \infty$ . The size of the ‘‘ball of attraction’’  $\mathbf{B}_{\eta(t_0)}$  can depend on  $t_0$ , and for a fixed  $t_0$ , the solution trajectories starting inside the ball can approach  $\mathbf{0}$  at different rates depending of the initial states. The ball of attraction  $\mathbf{B}_{\eta(t_0)}$  is called a **domain of attraction** of the equilibrium point. On the other hand, **uniform attractivity** requires that the ball of attraction is independent of  $t_0$ , and that all the trajectories starting inside the ball approach  $\mathbf{0}$  at a uniform rate.

**Definition 11 (Asymptotic stability).** The equilibrium  $\mathbf{x}_0 = \mathbf{0}$  is *asymptotically stable* if it is stable and attractive. It is *uniformly asymptotically stable* if it is uniformly stable and uniformly attractive.

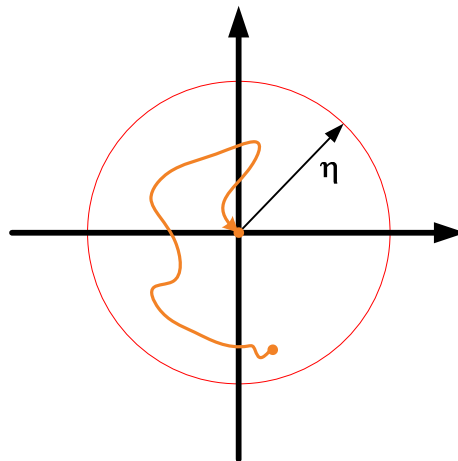


Figure 2.13: A asymptotically stable equilibrium

For asymptotic stability (see figure 2.13), we specify a  $\eta$ , such that  $\|\mathbf{x}_0\| < \eta$ , result in convergence to  $\mathbf{0}$  (a local property). We can define asymptotic stability with: If  $\eta = \infty$ , then the equilibrium is **globally asymptotically stable**.

An equilibrium point Lyapunov stable but not asymptotically stable is *marginally stable*.

**Definition 12 (Exponential stability).** The equilibrium  $\mathbf{x}_0 = \mathbf{0}$  is *exponentially stable* if there exists two strictly positive numbers  $\alpha$  and  $\beta$  such that

$$\|\mathbf{x}(t)\| \leq \alpha \|\mathbf{x}(0)\| e^{\beta t}, \quad \forall t > 0 \quad (2.61)$$

in some ball  $\mathbf{B}_\gamma$  in the neighborhood of the origin

Here we introduce the notion of quadratic stability with degree  $\alpha > 0$ . Roughly speaking, an uncertain system is quadratically stable with degree  $\alpha$  if the system is exponentially stable with rate of convergence  $\alpha$  and this stability is guaranteed by an uncertainty independent quadratic form Lyapunov function.

**Definition 13 (Quadratrical stability).** The equilibrium  $\mathbf{x}_0 = \mathbf{0}$  is *quadratically stable* if there exist a matrix  $P \in \mathbb{R}^{n \times n}$ , with  $P^T = P > 0$ , and  $\mu > 0$  such that

$$\mathbf{x}^T(t)Pf(t, \mathbf{x}(t)) \leq -\mu \|\mathbf{x}(t)\|^2 \quad \forall t > 0 \quad (2.62)$$

in some ball  $\mathbf{B}_\gamma$  in the neighborhood of the origin

**Definition 14 (Quadratrical stability with degree of stability  $\alpha > 0$ ).** The equilibrium  $\mathbf{x}_0 = \mathbf{0}$  is *quadratically stable with degree of stability  $\alpha > 0$*  if there exist a matrix  $P \in \mathbb{R}^{n \times n}$ , with  $P^T = P > 0$ , and  $\mu > 0$  such that

$$\mathbf{x}^T(t)Pf(t, \mathbf{x}(t)) \leq -\alpha \mathbf{x}^T P \mathbf{x} \quad \forall t > 0 \quad (2.63)$$

in some ball  $\mathbf{B}_\gamma$  in the neighborhood of the origin

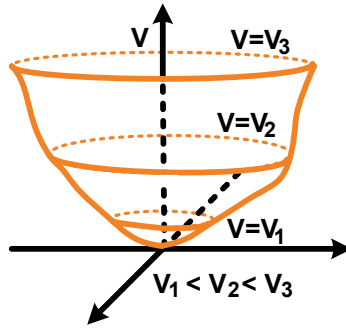
All these conditions refer to **stability** in the sense of *Lyapunov*. These conditions hold in the global sense if they are true for all  $x \in \mathbb{R}^n$ .

### 2.4.3 Lyapunov's Direct Method

The basic philosophy of Lyapunov's direct method is the mathematical extension of a fundamental physical observation: if the total energy of a system is continuously dissipated, then the system, whether linear or nonlinear, must eventually settle down to an equilibrium point. Faced with a set of ordinary differential equations describing a system, the basic procedure of *Lyapunov's direct method* is to generate a scalar "energy-like" function for the dynamic system, and examine the time variation of that scalar function. In this way, conclusions may be drawn on the stability of the set of ordinary differential equations without using the difficult stability definitions or requiring explicit knowledge of solutions.

#### 2.4.3.1 Positive definite functions and Lyapunov functions

Two very important notions for the study of Lyapunov's direct method, are the notion of positive definite functions and Lyapunov functions. A *positive definite function*  $f(x)$  is a function which is strictly positive except for  $x = 0$  where  $f(0) = 0$ . *Lyapunov functions* are functions which can be used to prove the stability of a certain fixed point in a dynamical system or autonomous differential equation.

Figure 2.14: Example of a positive definite function  $\mathbb{R}^2$ 

**Definition 15 (Positive definite functions).** A scalar continuous function  $V(\mathbf{x})$  is said to be **locally positive definite** if  $V(\mathbf{0}) = 0$  and, for a ball  $B_h$  ( $B_h$  is the closed ball of radius  $h$  centered at 0 in  $\mathbb{R}$ ) in the state space

$$\mathbf{x} \neq \mathbf{0} \Rightarrow V(\mathbf{x}) > 0$$

If  $V(\mathbf{0}) = 0$  and the above property holds over the whole state space, then  $V(\mathbf{x})$  is said to be **globally positive definite**. Figure 2.14 presents the typical shape of a positive definite function in  $\mathbb{R}^2$ .

Some concepts can be defined similarly, either in a local or global sense, i.e., a function  $V(\mathbf{x})$  is **negative definite** if  $-V(\mathbf{x})$  is positive definite;  $V(\mathbf{x})$  is **positive semi-definite** if  $V(\mathbf{0}) = 0$  and  $V(\mathbf{x}) \geq 0$  for  $\mathbf{x} \neq \mathbf{0}$ ;  $V(\mathbf{x})$  is negative semi-definite if  $-V(\mathbf{x})$  is positive semi-definite. The prefix “semi” is used to reflect the possibility of  $V$  being equal to zero for  $\mathbf{x} \neq \mathbf{0}$ .

Consider that the system state  $\mathbf{x}$  evolves accordingly with system (2.52) presented in section 2.4.1.1 and that a positive definite function is time dependent. Furthermore,  $V(t, \mathbf{x})$  has continuous partial derivatives. Thus, the function  $V(t, \mathbf{x})$  is differentiable with respect to  $t$ . Using the *Chain Rule*,

**Definition 16 (Derivative of V).** Let  $V : \mathbb{R} \times \mathbb{R}^n \rightarrow \mathbb{R}$  be continuously differentiable with respect to all of its arguments, and let  $\nabla V$  denote the gradient of  $V$  with respect to  $\mathbf{x}$  (written as a row vector). Then the function  $\dot{V} : \mathbb{R} \times \mathbb{R}^n \rightarrow \mathbb{R}$  is defined by

$$\dot{V} = \frac{dV(t, \mathbf{x})}{dt} = \frac{\partial V}{\partial t}(t, \mathbf{x}) + \nabla V(t, \mathbf{x}) \dot{\mathbf{x}} = \frac{\partial V}{\partial t}(t, \mathbf{x}) + \nabla V(t, \mathbf{x}) f(t, \mathbf{x}) \quad (2.64)$$

and is called the **derivative of  $V$  along the trajectories of (2.52)**

From this point forward, we will only consider autonomous systems as described in equation (2.55). Therefore the time derivative for  $V(\mathbf{x})$  is,

$$\dot{V} = \nabla V(\mathbf{x}) \cdot f(\mathbf{x}) \quad (2.65)$$

Since  $\mathbf{x}$  is required to satisfy the autonomous state equation (2.55),  $\dot{V}$  only depends on  $\mathbf{x}$ . At an equilibrium point,  $\dot{V} = 0$ . We can now derive a very important definition for the study of Lyapunov stability.

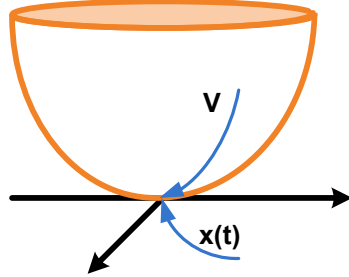


Figure 2.15: Lyapunov function in  $\mathbb{R}^2$

**Definition 17 (Lyapunov function).** If, in a ball of attraction  $B_{\eta(t_0)}$ , some function  $V(\mathbf{x})$  is positive definite and has continuous partial derivatives, and if its time derivative along any state trajectory of system (2.52) is negative semi-definite, i.e.,

$$\dot{V}(\mathbf{x}) \leq 0$$

then  $V(\mathbf{x})$  is said to be a Lyapunov function for the system (2.52). Figure 2.15 presents a typical Lyapunov function where the  $-\nabla V$  is seen to always point down. In figure 2.16, a trajectory is seen to move across contour curves corresponding to different values of  $V$ .

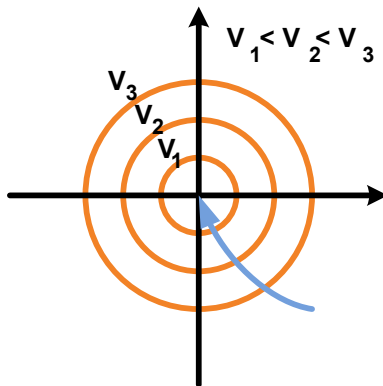


Figure 2.16: Lyapunov function for  $\mathbb{R}^2$  in contour curves

### 2.4.3.2 Equilibrium point theorems

The relations between Lyapunov functions and the stability of systems are made precise in a number of theorems in **Lyapunov's direct method**. Those theorems have local and global properties. The local properties are concerned with stability in the vicinity of an equilibrium point and usually involve a locally positive definite function.

**Theorem 4 (Lyapunov theorem for local stability).** If, in a ball of attraction  $B_{\eta(t_0)}$ , there exists a scalar function  $V(\mathbf{x})$  with continuous first partial derivatives such that

- $V(\mathbf{x})$  is positive definite (locally in  $B_{\eta(t_0)}$ )
- $\dot{V}(\mathbf{x})$  is negative semi-definite (locally in  $B_{\eta(t_0)}$ )

then the equilibrium point **0** is **stable**. If, actually, the derivative  $\dot{V}(\mathbf{x})$  is locally negative definite in  $B_{\eta(t_0)}$ , then the stability is **asymptotic**.

**Theorem 5 (Lyapunov theorem for global stability).** Assume that there exists a scalar function  $V$  of the state  $\mathbf{x}$ , with continuous first order derivatives such that

- $V(\mathbf{x})$  is positive definite
- $\dot{V}(\mathbf{x})$  is negative definite
- $V(\mathbf{x}) \rightarrow \infty$  as  $\|\mathbf{x}\| \rightarrow \infty$

then the equilibrium at the origin is **globally asymptotically stable**.

## 2.5 Nonlinear Control techniques

This section discusses some nonlinear control techniques and its application to the docking operation control problem.

During the past several decades, great advances in control theory and techniques have been made in the area of controller design for nonlinear uncertain systems. **Sliding Mode Control** (SMC), also known as Variable Structure Control (VSC) uses a discontinuous controller structure [47] to guarantee perfect tracking for a class of systems satisfying the well known “matching conditions” (known as *matched* systems). The classic sliding mode controller can be found in Slotine and Li [42] and in Utkin [48]. The “matching conditions” can be found in Swei and Corless [49] for Linear Systems and in Chen [50] for Nonlinear systems. There have been several “smoothing” extensions to sliding mode control that still retain the concept of an “attractive” surface but eliminate the discontinuous nature of the control. In general, the smoothing nature also eliminates the perfect tracking condition and results in a definable boundary layer around the desired surface.

More recently, the area of robust nonlinear control has received a great deal of attention in the literature which resulted in several new approaches. Most methods employ a Lyapunov synthesis approach. Corless and Leitmann [51] applied this method to open-loop stable, mismatched systems (systems that do not satisfy the “matching conditions”). The “integrator backstepping” methodology [52] is a popular step-by-step design procedure for dealing with uncertain nonlinear mismatched systems; however, it requires repeated differentiation of nonlinear functions as well as the need to bound the uncertainties in these higher derivatives. This problem led to the development of two related methods, the method of “Multiple Sliding Surfaces” (Hedrick et. al. [53], [54], [55]) and the method of “Dynamic Surface Control” (Gerdes et. al. [56], [57], [58]).

There are a varied number of applications of nonlinear control techniques to underwater vehicles. Yoerger and Slotine [59] developed a sliding mode controller to robust trajectory control of underwater vehicles. Healey and Lienard [60] developed the models for a multivariable Sliding Mode Controller for autonomous diving and steering of underwater vehicles. More recently, Girard, Sousa and Silva [61] reviewed dynamics, configurations and control strategies for underwater vehicle autopilots using sliding mode control techniques.

### 2.5.1 Sliding Mode Control

The models of the underwater vehicles (presented in section 2.1) are affected by imprecisions on the parameters due to the complex nature of underwater vehicle dynamics.

Therefore, simplified representation of the system's dynamics are used. Modeling inaccuracies can have strong adverse effects on nonlinear control systems. Uncertainties also come from disturbances, such as ocean currents and wave surging. To address this difficulty, the design of the controllers must explicitly consider the system uncertainties.

Two major approaches to deal with model uncertainty are *robust control* and *adaptive control*. The typical structure of a robust controller is composed of a nominal part, similar to a feedback linearizing or inverse control law, and of additional terms that counteract the model uncertainty. Adaptive control is similar, however the model is updated *online*, during operation.

Sliding mode control constitute a simple approach to robust control. SMC uses a discontinuous controller structure to guarantee perfect tracking for a class of systems satisfying the "matching conditions" (presented in section 2.5.1.3). It comes from the notion that it is easier to control a 1<sup>st</sup>-order system (*i.e.*, systems described by 1<sup>st</sup>-order differential equations), than it is to control general n<sup>th</sup>-order systems. Therefore, a notational simplification is introduced to allow the n<sup>th</sup>-order problems to be replaced by equivalent 1<sup>st</sup>-order problems. It is then possible to demonstrate that "perfect" performance can be achieved even in the presence of arbitrary parameter uncertainties. Such performance, unfortunately, is obtained at the cost of extremely high control activity. A modification can be introduced to decrease the control activity in the interest of achieving a better trade-off between tracking performance and parametric uncertainty.

### 2.5.1.1 Definition

Consider the single-input dynamic system

$$x^{(n)} = f(\mathbf{x}) + b(\mathbf{x})u \quad (2.66)$$

where the scalar  $x$  is the output of interest (for instance, the position of an AUV in the longitudinal axis),  $n$  is the order of the system, the scalar  $u$  is the control input (for instance, thruster force), and  $\mathbf{x} = [x, \dot{x}, \dots, x^{n-1}]^T$  is the state vector; the function  $f(\mathbf{x})$  (in general nonlinear) is not exactly known, but is upper bounded by a known continuous function of  $\mathbf{x}$ ; similarly, the control gain  $b(\mathbf{x})$  is not exactly known, but it is of known sign and is bounded by known, continuous functions in  $\mathbf{x}$ .

The control problem is to get the state  $\mathbf{x}$  to track a specific time-varying reference  $\mathbf{x}_d = [x_d, \dot{x}_d, \dots, x_d^{n-1}]^T$  even in the presence of model imprecision on  $f(\mathbf{x})$  and  $b(\mathbf{x})$ .

Let  $\tilde{x} = x - x_d$  be the tracking error in the variable  $x$ , and let  $\tilde{\mathbf{x}} = \mathbf{x} - \mathbf{x}_d$  be the tracking error vector. Furthermore, let us define a time-varying surface  $S(t) \in \mathbb{R}$  by the scalar equation  $s(\mathbf{x}, t) = 0$ , where

$$s(\mathbf{x}, t) = \left( \frac{d}{dt} + \lambda \right)^{n-1} \tilde{x} \quad (2.67)$$

where  $\lambda$  is a strictly positive constant. For  $n = 2$ , we have

$$s = \dot{\tilde{x}} + \lambda \tilde{x} \quad (2.68)$$

i.e.,  $s$  is a weighted sum of the position error and the velocity error.

The problem of tracking  $\mathbf{x} \equiv \mathbf{x}_d$  is equivalent to that of remaining on the surface  $S(t)$  for all  $t > 0$ . Thus, the problem of tracking the  $n$ -dimensional vector  $\mathbf{x}_d$  can be reduced to that of keeping the scalar quantity  $s$  at zero. The original  $n^{\text{th}}$ -order tracking problem is replaced by a 1<sup>st</sup>-order stabilization problem in  $s$ . Therefore the scalar  $s$  represents a true measure of tracking performance.

The simplified 1<sup>st</sup>-order problem of keeping the scalar  $s$  at zero can be achieved if one chooses the appropriate control law  $u$  of equation (2.66) such that outside of  $S(t)$

$$\frac{1}{2} \frac{d}{dt} s^2 \leq -\eta |s| \quad (2.69)$$

where  $\eta$  is a strictly positive constant. Condition (2.69) states that the squared "distance" to the surface (measured by  $s^2$ ), decreases along all system trajectories, guaranteeing convergence to the desired state. Therefore, it constraints the system trajectories to point towards the surface  $S(t)$ , as it is possible to see in figure 2.17. Once on the surface, the trajectories remain on the surface. Satisfying condition (2.69), known as sliding condition, makes the surface an *invariant set*.

The sliding condition also implies that some disturbances or dynamic uncertainties can be tolerated while the surface still remains an invariant set. If the surface  $S(t)$  verifies the sliding condition (2.69) then it is referred to as sliding surface, and the system's behavior once on the surface is called sliding mode.

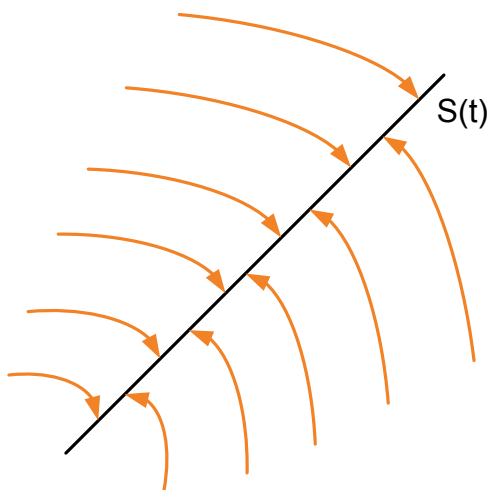


Figure 2.17: The sliding condition

If the system initial state is not the desired state, the surface  $S(t)$  will nonetheless be reached in a finite time  $t_{reach}$

$$t_{reach} \leq \frac{|s(t=0)|}{\eta}. \quad (2.70)$$

The purpose behind equations (2.67) and (2.69) is to select a well-behaved function of the tracking error,  $s$ , according to (2.67), and then select the feedback control law  $u$  in system (2.66) such that  $s^2$  remains a Lyapunov-like function of the closed-loop system, even in the presence of model imprecisions and of disturbances. Figure 2.18 represents an example of a sliding mode for a system with  $n = 2$ .

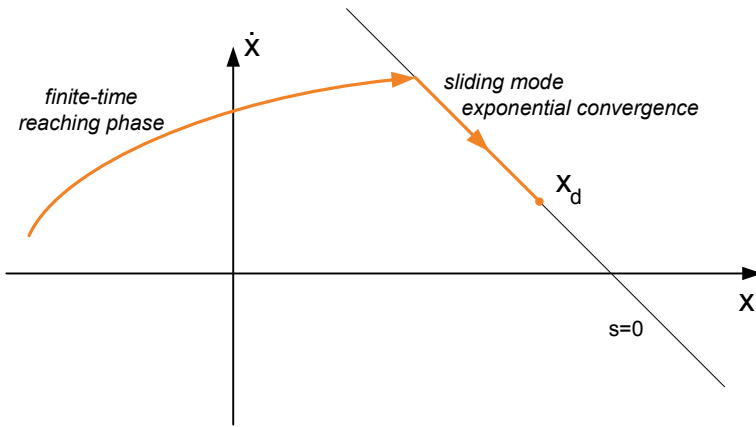


Figure 2.18: The sliding mode for a system with  $n=2$

The controller design is a twofold procedure. First, a feedback control law  $u$  is selected to satisfy sliding condition (2.69). Nonetheless, in order to counteract modeling imprecisions and disturbances, the control law has to be discontinuous across  $S(t)$ . Since the control switchings are not instantaneous and the value of  $s$  is not known with infinite precision, this leads to *chattering*, as illustrated by figure 2.19. In general, chattering is undesirable in practice, because it involves high control activity and further may excite high-frequency dynamics neglected during modeling. Accordingly, the second step involves smoothing the discontinuous control law  $u$  to achieve an optimal trade-off between control bandwidth and tracking precision. In conclusion, the first step accounts for parametric uncertainty, and the second step achieves robustness to high frequency unmodeled dynamics.

The dynamics while in sliding mode can be written as

$$\dot{s} = 0 \quad (2.71)$$

Solving the equation formally for the control input, we obtain an expression for  $u$  called the equivalent control,  $u_{eq}$ , which can be interpreted as the continuous control

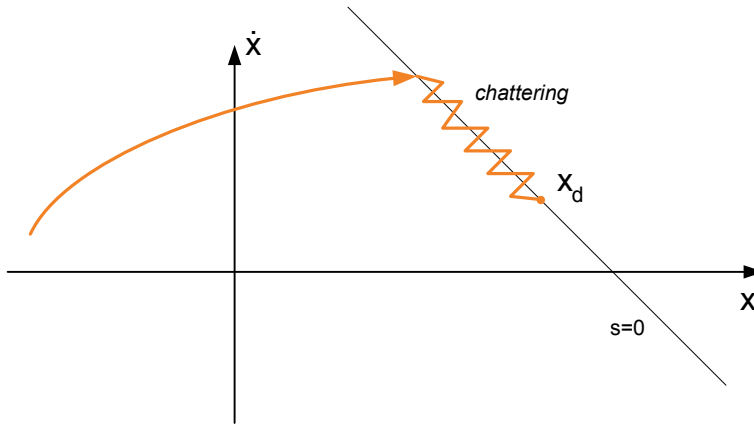


Figure 2.19: Chattering as a result of imperfect control switchings

law that would maintain  $\dot{s} = 0$  if the dynamics were exactly known. In the interest of satisfying sliding condition (2.69) despite uncertainties on the system, we add to  $u_{eq}$  a term discontinuous across the surface  $s = 0$

$$u = u_{eq} - \eta \operatorname{sgn}(s) \quad (2.72)$$

where  $\operatorname{sgn}$  is the *sign* function:

$$\begin{aligned} \operatorname{sgn}(s) &= +1 && \text{if } s > 0 \\ \operatorname{sgn}(s) &= -1 && \text{if } s < 0 \end{aligned}$$

By choosing the switching gain  $\eta = \eta(x, \dot{x})$  large enough, we can guarantee that the sliding condition is verified.

To prevent chattering (figure 2.19), one can introduce a boundary layer  $\phi$  (figure 2.20), used to retain continuity of control as motion trajectories cross the sliding surface. Also, it is possible to use a continuous function to define "practical" sliding surface dynamics such as a *sat* or a *tanh* function instead of the *sign* function. Therefore we now have:

$$u = u_{eq} - \eta \tanh(s/\phi) \quad (2.73)$$

### 2.5.1.2 Multivariable Sliding Mode Control

A similar control law may be found for a multivariable system model that is predominantly linear, where the control law contains a cancellation term, a linear dynamics substitution term, and a switching term to provide robustness to model uncertainty and disturbances.

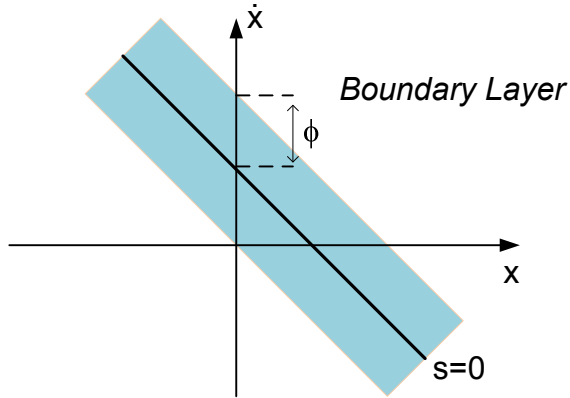


Figure 2.20: Boundary Layer

Suppose we have a linear system described by the usual general form

$$\dot{\mathbf{x}} = A\mathbf{x} + Bu \quad (2.74)$$

where  $\mathbf{x} \in \mathbb{R}^{n \times 1}$ ,  $A \in \mathbb{R}^{n \times n}$ ,  $B \in \mathbb{R}^{n \times r}$  and  $u \in \mathbb{R}^{r \times 1}$ .

The design of a SMC servo to track a reference state,  $\mathbf{x}_{ref}(t) \in \mathbb{R}^{n \times 1}$  is approached by designing a control to drive the state to the surface  $s = 0$  where  $s \in \mathbb{R}^{r \times 1}$ . The surface has to be a stable surface.

Therefore, it is possible to define a state error  $\tilde{\mathbf{x}}$ , and a sliding surface  $s$ , such that

$$\tilde{\mathbf{x}} = \mathbf{x} - \mathbf{x}_{ref} \quad (2.75)$$

$$s = k^T \tilde{\mathbf{x}} \quad (2.76)$$

The vectors  $k$  define directions in the state error space upon which the elements of  $s$ , are lengths of the projection of the state error vector ( $k$  can be defined as unit vectors without loss of generality). Basically, it is a requirement of the method that the condition

$$s \rightarrow 0 \Rightarrow \dot{s} \rightarrow 0 \implies \tilde{x} \rightarrow 0 \text{ as } t \rightarrow \infty \quad (2.77)$$

Also, since the objective is to design control laws for the inputs,  $u(t)$ , the dimension of  $s$  will be equal to the dimension of  $u(t)$ . Then, the control design procedure is to employ the reaching condition and substituting it in the dynamics model to extract the control law.

Lets define a Lyapunov function

$$V = 0.5s^T s \quad (2.78)$$

$$\dot{V} = \dot{s}^T s = \sum_{i=1}^r \dot{s}_i s_i < 0 \quad (2.79)$$

$$\dot{s}_i = -\eta \tanh(s_i/\phi), \quad i = 1, \dots, r \quad (2.80)$$

which leads to

$$k_i^T(Ax + Bu - \dot{\mathbf{x}}_{ref}) = -\eta \tanh(s_i/\phi) \quad (2.81)$$

where it is intended that  $k_i^T$  is the  $i$ -th row of  $k$ , and corresponds to the  $i$ -th sliding surface. It is possible to define  $-\eta \tanh(s_i/\phi)$  as the  $i$ -th column in a column vector of switching functions  $F(s)$  with size  $1 \times r$ .

It may now be shown by substitution of the system dynamics equations into the reaching condition, that the control law is

$$k^T(A\mathbf{x} + Bu) - k^T\dot{\mathbf{x}}_{ref} = -F(s) \quad (2.82)$$

$$\therefore u = [k^T B]^{-1}[k^T \dot{\mathbf{x}}_{ref} - k^T A\mathbf{x} - F(s)] \quad (2.83)$$

The control law has three components:

$$k_1\dot{\mathbf{x}}_{ref} \quad k_2\mathbf{x} \quad k_3F(s)$$

The first, provides a feedforward control action to follow the reference, the second, a feedback to correct for errors, and the third, a switching term to provide robustness for model uncertainty and disturbances.

The values of  $k$  are found by the requirement that when  $s = 0$  the system dynamics must exhibit stable sliding on the surface to the origin in the error space. By inspection of the above it is seen that if  $s = 0$ , then the closed loop dynamics are driven by the poles of the closed loop matrix,

$$(A - BK) = A_c \quad \text{with} \quad K = [k^T B]^{-1}s^T A \quad (2.84)$$

Therefore,  $K$  is chosen by *pole placement* or other means to make  $A_c$  stable subject to the additional constraints imposed by

$$s^T(A - BK) = s^T(A - B([k^T B]^{-1}s^T A)) = s^T A_c = 0 \quad (2.85)$$

Equation (2.85) means that  $A_c$  must have a sufficient number of poles at the origin to allow the system to remain on the sliding surface ( $s = 0$ ), while the remaining poles must have stable dynamics. This is accomplished through a choice of  $K$  that produces the requisite pole placement.

Since the purpose is to have  $k^T A_c = 0$ , then  $A_c^T k = 0$  and the particular design values of  $k$  are found as the normalized eigenvectors<sup>10</sup> of  $A_c$  corresponding to the  $r$  eigenvalues at the origin required by the  $r$  constraints.

---

<sup>10</sup>Let  $A$  be a square matrix. A non-zero vector  $s$  is called an eigenvector of  $A$  if and only if there exists a number (real or complex)  $\lambda$  such that  $Ax = \lambda x$ . If such a number  $\lambda$  exists, it is called an eigenvalue of  $A$ . The vector  $x$  is called eigenvector associated to the eigenvalue  $\lambda$ .

### 2.5.1.3 Matching Conditions

As stated previously, Sliding Mode Control (or Variable Structure Control) uses a discontinuous controller structure to guarantee perfect tracking for a class of systems satisfying the *matching conditions*.

In the past, the design has been mainly based on a structural condition in the system, namely, the matching condition (Corless and Leitmann [51]). Swei and Corless [49] study the necessity of the matching condition for robust stabilization of linear systems and for nonlinear systems, Chen [50] introduced a new matching condition for robust control design. The main idea of the matching condition is to configure the possible route through which the uncertainty may affect the stability of a system. Once the matching condition is satisfied, the control law can be constructively synthesized.

The following gives a brief introduction of the theory behind the matching conditions for nonlinear systems. The main reference is Levine [62].

Consider the following nonlinear system which contains a structured uncertain term

$$\dot{x} = F(x) + G(x)u + \Delta(x, t) \quad (2.86)$$

where  $F$  and  $G$  are known functions comprising the nominal system and  $\Delta$  is an unknown function known only to lie within some bounds. For instance,  $\Delta$  may be bounded by some function  $\rho(x)$ , i.e.,  $|\Delta(x, t)| \leq \rho(x)$ . For simplicity it is assumed that  $\Delta$  does not depend on the control variable  $u$ . Furthermore, it is assumed that the nominal system is stabilizable, which means, that some state feedback  $u_{nom}(x)$  exists so that the nominal closed-loop system,

$$\dot{x} = F(x) + G(x)u_{nom}(x) \quad (2.87)$$

has a globally asymptotically stable equilibrium at  $x = 0$ . We further assume knowledge of a Lyapunov function  $V$  for this system so that

$$\nabla V(x)[F(x) + G(x)u_{nom}(x)] < 0 \quad \forall x \neq 0 \quad (2.88)$$

The problem now is to design an additional robustifying feedback  $u_{rob}(x)$  so that the composite feedback  $u = u_{nom} + u_{rob}$  robustly stabilizes the system (2.86), thus, guaranteeing stability for every admissible uncertainty  $\Delta$ . It suffices that the derivative of  $V$  along closed-loop trajectories is negative for all such uncertainties. The derivative is computed as follows

$$\dot{V} = \nabla V(x)[F(x) + G(x)u_{nom}(x)] + \nabla V(x)[G(x)u_{rob}(x) + \Delta(x, t)] \quad (2.89)$$

Is it possible to make this derivative negative by some choice of  $u_{rob}(x)$ ? Equation (2.88) proves that the first of the two terms in equation (2.89) is negative; it remains to examine

the second of these terms. A special case occurs when  $\nabla V(x) \cdot G(x) = 0$ , because on this set

$$\dot{V} = \nabla V(x) \cdot F(x) + \nabla V(x) \cdot \Delta(x, t) \quad (2.90)$$

regardless of our choice for the control. Hence, to guarantee the negativity of  $V$ , the uncertainty  $\Delta$  must satisfy

$$\nabla V(x) \cdot F(x) + \nabla V(x) \cdot \Delta(x, t) \leq 0 \quad (2.91)$$

at all points where  $\nabla V(x) \cdot G(x) = 0$ . This inequality constraint on the uncertainty  $\Delta$  is necessary for the Lyapunov redesign method to succeed. If we require that the uncertainty  $\Delta$  is of the form,

$$\Delta(x, t) = G(x) \cdot \bar{\Delta}(x, t) \quad (2.92)$$

for some unknown function  $\bar{\Delta}$ , then clearly  $\nabla V \cdot \Delta = 0$  at all points where  $\nabla V(x) \cdot G(x) = 0$ , and therefore the sufficient condition (2.91) is satisfied. In the literature, equation (2.92) is called the **matching condition** because it allows the system (2.86) to be written

$$\dot{x} = F(x) + G(x)[u + \bar{\Delta}(x, t)] \quad (2.93)$$

where now the uncertainty  $\bar{\Delta}$  is matched with the control input  $u$ .

### 2.5.2 Multiple Sliding Surface

This section gives a brief introduction to the Multiple Sliding Surface (MSS) nonlinear control technique. Multiple Surface Sliding control was developed to simplify the controller design of systems where model differentiation was difficult. A “multiple-surface” method was suggested by Green and Hedrick [53] when sliding mode control was applied to a speed tracking controller of an automobile engine whose model does not satisfy the matching condition. For a more complete study the reader is referred to Won and Hedrick [54] and Hedrick and Yip [55]. An example of the implementation of the technique for an automated vehicle can be found in Hedrick [63].

The principle of multiple sliding surface is illustrated in the following nonlinear system

$$\left. \begin{array}{l} \dot{x}_1 = f_1(x_1) + x_2 + \Delta f_1(x_1) \\ \dot{x}_2 = u \end{array} \right\} \quad (2.94)$$

where  $f_1$  and  $\Delta f_1$  are non-Lipschitz nonlinearities. We assume that function  $f_1(x_1)$  is known while  $\Delta f_1(x_1)$  is not. However,  $\Delta f_1$  is bounded by a known nonlinearity  $\rho_1(x_1)$ . The purpose of the controller is to make  $x_1$  track a desired trajectory  $x_{1d}(t)$ . Applying MSS control to this system, the first sliding surface is defined as

$$S_1 = x_1 - x_{1d} \quad (2.95)$$

Thus,

$$\dot{S}_1 = f_1 + x_2 + \Delta f_1(S_1) - \dot{x}_{1d} \quad (2.96)$$

A second sliding surface is defined as

$$S_2 = x_2 - x_{2d} \quad (2.97)$$

where the desired state,  $x_{2d}$ , is chosen to make  $S_1 \dot{S}_1 < 0$ . It is possible to define  $\dot{S}_1 = -K_1 S_1$ . A reasonable choice for  $x_{2d}$  is achieved by substituting (2.97) in (2.96).

$$x_{2d} = \dot{x}_{1d} - f_1 - K_1 S_1 - \rho_1 \operatorname{sgn}(S_1) \quad (2.98)$$

The control  $u$  is chosen to drive  $S_2$  to zero (defining  $S_2 \dot{S}_2 < 0$ )

$$\dot{S}_2 = u - \dot{x}_{2d} = -K_2 S_2 \quad (2.99)$$

Therefore,

$$u = \dot{x}_{2d} - K_2 S_2 \quad (2.100)$$

Choosing a Lyapunov function candidate

$$V = \frac{S_1^2 + S_2^2}{2} \quad (2.101)$$

we have

$$\dot{V} = S_1 \dot{S}_1 + S_2 \dot{S}_2 \leq -K_1 S_1^2 - K_2 S_2^2 + S_1 S_2 \quad (2.102)$$

$\dot{V}$  can be made negative definite by picking  $K_1, K_2 > 1/2$ . The time derivatives of the desired state  $\dot{x}_{2d}$  can be computed by numerical differentiation, i.e.,

$$\dot{x}_{2d} \approx \frac{x_{2d}[n] - x_{2d}[n-1]}{\Delta T} \quad (2.103)$$

where  $\Delta T$  is the sample time.

A more comprehensive study is presented in Won and Hedrick [54].

### 2.5.3 Dynamic Surface Control

This section gives a brief introduction to the Dynamic Surface Control (DSC) nonlinear control technique. DSC is a dynamic extension to MSS control introduced in Swaroop *et al.* [57] to overcome the problem of finding derivatives of reference (desired) trajectories for the  $i$ -th state for the MSS scheme in Green and Hedrick [53]. It is also more intuitive

and applies to a more general class of system as compared to the MSS scheme in Won and Hedrick [54]. The first structured approach to the use of dynamic filters can be found in the dissertation of Gerdes [64].

To illustrate how DSC overcomes the shortcomings of the previous methods, a controller is designed for the example discussed in the MSS section 2.5.2. The first sliding surface is defined the same way as before,  $S_1 = x_1 - x_{1d}$ . Thus,  $\dot{S}_1$  is also given by equation (2.96). The difference arises in the desired state,  $x_{2d}$ , which is generated by a first-order filter,

$$\tau \dot{x}_{2d} + x_{2d} = \bar{x}_2 \quad (2.104)$$

$$x_{2d}(0) = \bar{x}_2(0) \quad (2.105)$$

with the input of the filter,  $\bar{x}_2$ , given by

$$\bar{x}_2 = -f_1(x_1) - K_1 S_1 - S_1 \frac{\rho_1^2}{2\epsilon} + \dot{x}_{1d} \quad (2.106)$$

where  $\epsilon$  is a design parameter specifying the tracking accuracy. Once again, the second surface is defined as  $S_2 = x_2 - x_{2d}$ . Differentiation of  $x_{2d}$  is now possible and  $u$  is chosen to drive  $S_2$  to zero. Therefore, we have

$$u = \dot{x}_2 - K_2 S_2 = \frac{\bar{x}_2 - x_{2d}}{\tau} - K_2 S_2 \quad (2.107)$$

It is important to mention that this control law does not involve model differentiation and therefore has prevented the explosion of terms. Furthermore, the requirement on the smoothness of  $f_1$  and  $\rho_1$  is relaxed with this method. To design a DSC,  $f_1$  and  $\rho_1$  are required to be  $C^1$  functions<sup>11</sup>, irrespective of the order of the system.

It is possible to synthesize the design procedure of the dynamic surface control for  $n$ -th order system, as follows,

We define the  $i$ -th surface as

$$S_i = x_i - x_{id} \quad (2.108)$$

with

$$\dot{S}_i = x_{i+1} + f_i(x_1, \dots, x_i) - \dot{x}_{id} + \Delta f_i(x_1, \dots, x_i) \quad (2.109)$$

$\bar{x}_{i+1}$  is chosen to drive  $S_i$  to zero

$$\bar{x}_{i+1} = -f_i(x_1, \dots, x_i) - K_i S_i + \dot{x}_{id} \quad (2.110)$$

---

<sup>11</sup>The function  $f$  is said to be of class  $C^k$  if the derivatives  $f^{(1)}, f^{(2)}, \dots, f^{(k)}$  exist and are continuous.

Filtering  $\bar{x}_{i+1}$  we obtain  $x_{i+1,d}$

$$\tau_{i+1}\dot{x}_{i+1,d} + x_{i+1,d} = \bar{x}_{i+1} \quad (2.111)$$

The final surface is defined

$$S_n = x_n - x_{nd} \quad (2.112)$$

Finally, the control law is chosen to be

$$u = \dot{x}_{nd} - K_n S_n \quad (2.113)$$

so that  $\dot{S}_n = -K_n S_n$ , with  $K_n > 0$ , in order to  $S_n \dot{S}_n < 0$ .



# **Chapter 3**

## **State of the art in autonomous docking systems**

### **3.1 Introduction**

This section summarizes the background work related to Autonomous Docking Systems (ADS) for underwater vehicles. Improvements relative to performance of energy storage technology, precision of navigation instruments and reliability of acoustic communication devices enabled a tremendous development on homing/docking systems throughout the last two decades. Such advances have made a positive and profound impact on ocean exploration. Many research institutes have been involved in the development of autonomous docking systems for underwater vehicles.

This overview addresses various techniques involved with docking systems, although special attention is given to the control strategy.

### **3.2 Problem description**

One of the main obstacles for the exploration of the vast oceanic environment is the shortcoming of the present technology, *i.e.*, non-availability of affordable and suitable platforms that can be deployed for various science missions. The Autonomous Docking Systems enhance the capability of underwater exploration and data collection by increasing the level of autonomy of the AUVs. With an ADS, the AUVs can be deployed for extended times, data can be uploaded, instructions can be downloaded and the battery can be recharged.

### 3.3 Overview

Autonomous docking using an ultra-short baseline<sup>1</sup> (USBL) acoustic homing array were demonstrated by Stokey, Purcell, and et. al. [65] when they built a docking system for REMUS (Remote Environmental Monitoring UnitS), a low cost torpedo shaped AUV designed by the Oceanographic Systems Laboratory at the Woods Hole Oceanographic Institution (WHOI) to dock inside a stationary conical shaped docking station (figure 3.1). Their work discusses solutions for enabling the vehicle to acoustically find and then home on the docking system; procedures for mechanically latching the vehicle to the dock; some electro-mechanical techniques for power and data transfer from the docking system to the vehicle; remote data download from the vehicle and mission upload to the vehicle; and in situ battery recharge without opening the vehicle housing.

They also developed an algorithm for the docking sequence using state machines. The algorithm used the techniques of waypoint following and minimization of cross-track error<sup>2</sup>. The docking algorithm can be summarized as follows: the first state was to navigate to a position 50 meters from the dock along the track into the dock; once that criteria had been met, the vehicle attempted to follow the trackline into the dock; when the vehicle determined it is entering the dock it straightens the fins out, and continues thrusting at constant RPM for 15 seconds. That period forced the vehicle all the way into the guide tube.

This work is very important because it addresses all components of a docking system, which includes the dock, charging and communication circuitry, AUV navigation, the vehicle software and the docking algorithm. Some of the disadvantages with this system resulted from a navigational problem, since the vehicle could not merely head towards the dock; the vehicle had to orient itself on a proper glide path, much as an airplane must align itself with a runway; it required a priori knowledge of which way the dock was facing; it required either an electronic compass on the dock and/or calibration at installation; and finally, it suffered from susceptibility to problems with currents, which could move the vehicle off its desired approach path. The system was tested at Woods Hole harbor.

This docking system did not consider a model of the AUV nor the ocean currents in the control loop, therefore it was not a robust control method. Thus, convergence was not guaranteed.

They further expanded their work in [66] and [67].

An electromagnetic (EM) homing system was proposed by Feezor et. al. [68] for a torpedo shaped AUV named SeaGrant Odyssey IIb to dock inside a stationary conical shaped docking station. The sensing technique consisted of a magnetic field generated by

---

<sup>1</sup>USBL is a method of underwater acoustic positioning. A complete USBL system consists of a transceiver, which is mounted on a pole under a ship, and a transponder/responder on the seafloor or in an underwater vehicle.

<sup>2</sup>Cross-track error is the minimum distance between the vehicle and the line connecting two waypoints

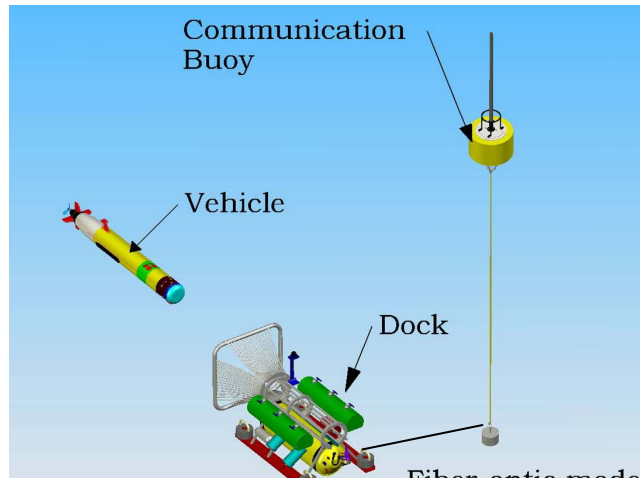


Figure 3.1: REMUS Docking system. Source: Allen et. al.

coils on the dock. When the AUV was ready to dock it sensed this magnetic field and was guided to the dock. This sensing system provides precise, better than 20cm homing position into dock, with precise control of the AUV in final stages of homing. A further advantage is that common oceanographic phenomena, such as turbidity, bubbles, floating organic materials, fouling, and boundaries at the surface of bottom do not alter the field lines. However, the range of the EM system was limited to a range of 25 to 30m. In this docking technique, there were no communications between the underwater vehicle and the dock.

A straightforward Proportional Integral Derivative (PID) control loop supplied the control response of the AUV. The docking sequence can be described as follows: The AUV was programmed to travel outbound from the launch point for 60s, execute a  $180^\circ$  turn to point towards the dock station, and travel back toward the ship and dock. The AUV remained under internal compass<sup>3</sup> control until the magnetic field sense coils detected a predetermined magnetic field strength. At this point, control of the AUV was shifted from the compass and depth sensors to the homing system.

A series of tests were conducted in Buzzards Bay, near Woods Hole Oceanographic Institution. The tests failed when the AUV was aligned more than  $30^\circ$  off the dock axis when it acquired the EM signal. In these cases, the AUV side slipped during the turn to the dock and hit the outside edge of the dock during homing.

An optical terminal guidance system which tracks the light source on the dock was also introduced by Cowen et. al. [69] using two torpedo shaped AUVs for the sea trials, more specifically, the SeaGrant Odyssey IIb and the NRaD Flying Plug. The system was simple but highly effective. The optical docking system was demonstrated to be

---

<sup>3</sup>An internal mechanism that allows vehicles to orient themselves so as to proceed in the proper direction during long-distance movements.

accurate and robust for vehicle terminal guidance during field operations, and provided targeting accuracy on the order of 1cm under real-world conditions, even in the presence of disturbances such as turbid bay water.

The control of the vehicle was achieved using a conventional closed loop PID control. One of the main disadvantages of this optical technique was the susceptibility to the sunlight when docking in shallow waters (It was found that false detections occurred when the vehicle operated at depths of less than about 1.5 m and simultaneously faced into the sun when it was low on the horizon, specially in the late afternoon). Also, the range of the system was significantly related to the turbidity of water. They obtained reliable acquisition range of 20-28m according to the rate of turbidity. Successful tests were performed in Buzzard's Bay with the vehicle docking in the dock station with nominal speeds of 1 to 1.5 meters per second.

All the above systems use a cone dock for docking system (also known as *funnel docking*). Singh, Bellingham, Hover, and et. al. [70] presented a omni-directional docking system for the Odyssey vehicle (see figure 3.2), using an USBL system for AUV to approach the dock from any direction by determining the range and bearing to the transponder mounted on the dock. After the vehicle reached the dock, an appendage mounted on the front of the vehicle latched on to a pole mounted on the dock (a method known as *cable latching docking*). The advantage of the system is robustness to the errors (two dominant sources of error of previous docking systems in the oceanic environment - namely, the presence of currents and magnetic anomalies). This work presented solutions for several failure modes to ensure reliability of the system, including failure of a task to complete, communications failure, mechanical failures, conflicting sensor data, missing AUV and software lockups. They developed a layered hierarchical control architecture for the autonomous control of the AUV during the docking procedures using a high level Finite-State Machine (FSM) model to monitor and supervise the whole operation. The system was divided into 4 different states in a higher level of abstraction:

**State 0 - The power on sequence** - the vehicle checks its condition, startups the systems and goes to the appropriate state.

**State 1 - Dock and Vehicle Ready for Mission** - This is the state where the underwater vehicle is docked inside the docking station and ready for mission deployment. When a mission is assigned, the dock transfers to the AUV a file, telling the vehicle to launch a mission at a specified time. Then, the dock checks if the vehicle actually left the dock and transitions to State 2.

**State 2 - Vehicle in Mission, Dock Station Empty** - In this state the dock is empty, while the vehicle is on mission. When the mission timer expires, the AUV

turns on the homing beacon and returns to the dock. After docking the state transitions to State 3.

**State 3 - Vehicle Returns to Dock Station** - After successful docking, the status of the system is checked and logged.

The homing algorithm for the AUV involved a Line-of-Sight (LoS) technique. An ultra-short baseline system on the vehicle uses this signal to calculate an azimuth<sup>4</sup> and elevation<sup>5</sup> to the dock. The LoS method works by nullifying the bearing<sup>6</sup> to the dock. The heading control law was of the inner-outer loop type, wherein a traditional PID (the inner loop) ensured that the actual vehicle heading  $\psi$  followed the desired heading  $\psi_d$ . The algorithm for the homing system is explained as follows: homing was typically initiated from 100 to 200 meters away from the dock. When the AUV picked up the homing beacon, it attempted to null the bearing to the dock. The docking was successfully tested with cross currents to test system for robustness in the presence of strong disturbances.

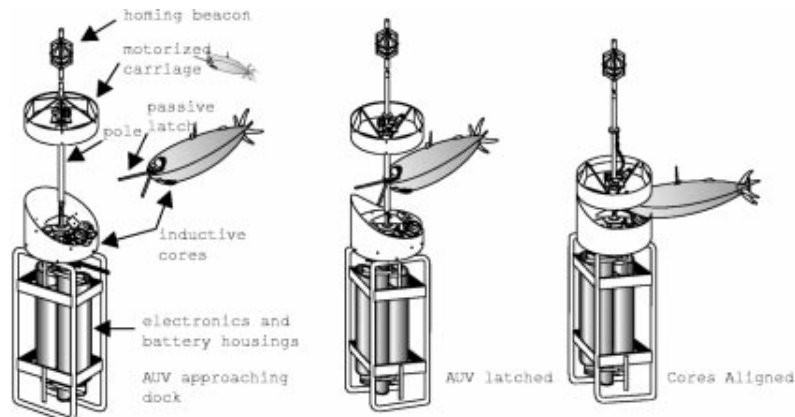


Figure 3.2: An omni-directional docking system. Source: Singh et. al.

Lee, Jeon and Lee [71] presented a docking system for a torpedo shaped AUV to dock into an underwater station with a camera. In their paper, they derived an optical flow model of a camera mounted on a AUV, where a charge-coupled device (CCD) camera was installed at the nose center of the AUV to monitor the docking condition. They combined the optical flow equation of the camera with the AUV linearized equations of motion (EOM), deriving a state equation for the visual servoing AUV. This way, they not only took into account the AUV model, but also the optical flow equation which allows a more accurate control of the docking sequence. The mathematical model of the visual

<sup>4</sup>The horizontal angular distance between the heading of a vehicle and a reference direction

<sup>5</sup>The vertical angular distance between the pitch angle of a vehicle and a reference direction

<sup>6</sup>Direction, especially angular direction measured from one position to another using geographical or celestial reference lines

servoing AUV included a system disturbances vector, to account for modeling errors and uncertainties of the AUV, and a white noise vector for measurement disturbances.

The control objective was to move the AUV to the docking station while holding the center of the camera to the target point. A control law was designed on the basis of an optimal one-step ahead predictive controller by minimizing a cost function, that reflected the distance between  $y(k+1)$  and  $y_d(k+1)$ , where  $y_d$  is the desired position in the CCD plane for an object and the attitude of the AUV in one step ahead. The purpose of the cost function was to achieve a trade-off between the control objective, and the necessary control efforts involved. In the simulation they neglected the roll-induced ( $\phi$ ) velocities. Numerical integration was conducted with the Euler method.

The results were presented by docking the AUV to a target station using the 6 degrees of freedom (DOF) nonlinear equations of REMUS of WHOI and a CCD camera. They depicted the effectiveness of the modeling and the control law for the visual servoing AUV.

A completely different strategy is implemented on the SWIMMER AUV [72] - their deployment configuration mounts a work class ROV above a heavy weight AUV. The SWIMMER AUV is not a small torpedo shaped vehicle, instead it is a 2.5 tons and 6 meters length vehicle, built for deep water (1000m to 10km) operations, and in this case, the AUV is the dock station. The techniques employed are restricted to very structured environments, aimed typically for intervention missions (e.g.: valve manipulation in oil platforms). For the positioning of the AUV they use an Active Sonar Object Prediction (ASOP). The principle behind ASOP is to use a 3-D map or model, and use that to drive an active search for significant sonar features (landmarks) in the live sonar data.

Evans et. al. [73] used sonar and video-based real-time 3D pose estimation on a Intervention-AUV (I-AUV), the Autonomous Light Intervention Vehicle (ALIVE). The purpose was to latch the underwater vehicle onto a fixed subsea structure. In order to guarantee a precise positioning of the AUV for the docking sequence, they combined the following techniques: Embedded, real-time sonar-based feature tracking, high precision video-based position control, Inertial Navigation Systems (INS) and video-based Dynamic Positioning (DP) and high-bandwidth acoustic video transmission.

The docking algorithm used a three-stage process:

**Transit** - During this stage the position of the vehicle is monitored at the surface station by periodic data transmitted using the acoustic modems.

**Approach** - In the approach phase, the AUV's Docking System uses repeated sonar scans to continuously track and calculate the vehicle's position relative to the docking panel. The vehicle's control system uses this information to maneuver within the safe landing zone to approximately 2-3m from the docking

panel. Once the vehicle is close enough to observe the panel using the onboard video systems, the state of the system transitions into the docking phase.

**Docking** - During the docking phase, the combined sonar and video control systems stabilized the vehicle to within 10cm of the docking panel. Docking manipulators then extended to perform the latch.

They presented successful results on deep water trials.

The ‘‘Marine Bird’’ [74] is another heavy weight AUV intended for deep water surveys. The docking system for the ‘‘Marine Bird’’ employs a slightly similar strategy with the glide path performed by an airplane while performing the landing sequence. This AUV can dock with an underwater base built on the bottom of the sea to charge batteries and transfer data with the base. Sea Trials were performed in Wakayama, Japan.

A similar approach was presented recently by Brignone, Perrier and Viala [75] where they introduced a comprehensive control architecture designed to dock an I-AUV on a receiving structure, using sonar and video image processing alongside navigation data from conventional sensors. They also used a station installed at the bottom of the sea, although in their project, docking is performed by thrusting to maintain contact between two passive grabbers at the front end of the vehicle (fitted with dampers) and a docking ring located in the topmost section of the structure. Their results were validated in real-time conditions on the Ifremer’s experimental underwater vehicle VORTEX.

Jantapremjit and Wilson [76] presented a very interesting and complete study about optimal control and guidance of homing/docking operations, because they introduced every necessary step for the development of a robust controller to perform optimal control during the docking sequence. The docking platform is not completely stationary.

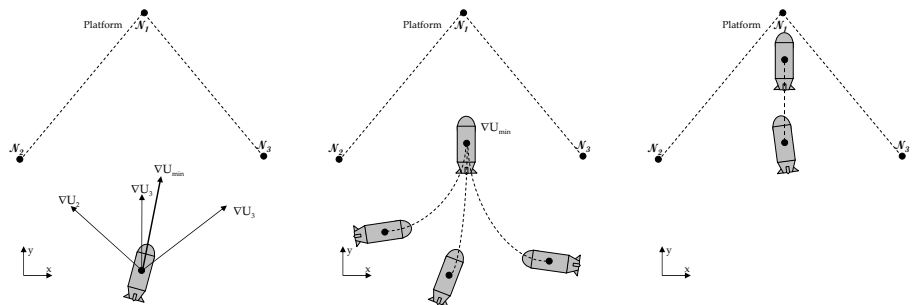


Figure 3.3: Trajectory planning for the AUV. Source: Jantapremjit and Wilson

This paper uses an approximate model of the dynamics of the 6 degrees of freedom AUV (from Fossen [1]). The motion controller is decoupled into two subsystems of heading and depth (Healey and Lienard [60]). The low level control is accomplished using

robust control techniques to provide stability in the presence of model uncertainty and disturbances. Three techniques are implemented and compared, namely, Sliding Mode Control, High-order Sliding Mode Control (HOSMC), and a State-Dependent Riccati Equation Model (SDREM). The methods provided robustness of motion control including elimination of chattering effect for the decoupled systems of the AUV. Comparisons between them were presented in simulation with depth control in the presence of disturbances.

The homing and docking strategy is divided in different stages. The homing trajectory was modeled with a conventional artificial *potential method*. This approach breaks up the free space into a fine grid which is then searched for a free path. Each grid element is assigned a *potential*, where the goal and neighboring elements are assigned an attractive potential and obstacles possess a repulsive potential. This ensures that the path created moves towards the goal while steering clear of any obstacles. In order to track the gradient field it is used an acoustic sensor network such as Long Baseline<sup>7</sup> (LBL).

The docking strategy was divided into two stages. In the first stage, a precise tracking was used for relative position and motion between an AUV and the platform. In the second stage, the docking velocity was kept within a safe range in order to avoid a possible serious impact with the platform, and the trajectory was derived using an *Average Vector Field* (AVF). AVF is a method that uses the data from the sensor networks in the workspace to compute a potential field function, in order to derive a smooth trajectory for the docking sequence (see figure 3.3). Then, a LoS path following is implemented to drive the AUV to the docking station. The results were presented in MATLAB.

McEwen et. al. [77] from the Monterey Bay Aquarium Research Institute (MBARI) developed a 54-cm-diameter torpedo shaped docking AUV and companion docking station (see figure 3.4). The AUV homes to the dock using an ultra-short baseline (USBL). The dock was a benthic<sup>8</sup>, fixed-heading cone with minimal moving parts and electronics.

The homing and docking sequence consisted of the following steps:

1. *Locate and home to the dock.* The vehicle locates the dock station and then homes to the dock using pure pursuit guidance (LoS path following), where the heading control system continuously points the vehicle at the beacon. The downside of this method is that it does not compensate for ocean current and thus the vehicle can be blown downwind while approaching. The main advantage is that it keeps the USBL pointed at the beacon for maximum signal strength.

---

<sup>7</sup>LBL, is a method of acoustic positioning commonly used in deep water (water depth of greater than 900 meters). A typical LBL positioning system consists of a transceiver and several beacons arranged into a structure called an array. The LBL transceiver pings each beacon and uses the 2-way travel time to calculate its position within the array

<sup>8</sup>happening on the bottom under a body of water

2. *Compute a position fix.* When the USBL attains good signal strength, the vehicle uses its compass heading and the USBL bearing and range to compute a position fix.
3. *Fly to the start of the final approach path.* The approach path is along the cone centerline, and begins about 300 meters out. The disadvantage of this method is that it may require the vehicle to turn away from the dock and temporarily lose USBL contact.
4. *Execute final approach.* The vehicle approaches along the cone centerline using a cross-track controller instead of pure pursuit. This method accounts for external disturbances since it acquires a drift correction angle if the ocean current has a lateral component. The vehicle slows to 1 m/s about 200m from the dock. This serves two purposes: first, it allows time for the control loop to zero the cross-track error, and second, it also prevents the vehicle from hitting the dock with too much force.
5. *Latch the vehicle when it enters the dock.*

The high level control of the homing and docking sequence was achieved with hybrid systems theory. The low level control consisted of outer and inner proportional-integral-derivative (PID) loops for both heading and depth (using decoupled control design as explained in section 5.9).

The system was successfully tested in the Monterey Inner Shelf Observatory operated by the Naval Postgraduate School.



Figure 3.4: MBARI docking system for a 54-cm diameter AUV. Source: McEwen et. al.

Sotiropoulos et. al. [78] discussed the benefits and draw backs of the existing docking methods, either for survey AUVs (torpedo shaped) and for intervention AUVs. For the survey AUVs the options presented are pole docking, funnel docking and cable latch docking.

Palmer et. al. [79] presented a reliable technique for robust localization of an under-water vehicle on the boundaries of a subsea intervention panel, based on computer vision

as well as traditional navigation sensors. In their work, they demonstrated that the prior knowledge of the structure where the vehicle has to dock on, allows the use of model based pose estimation techniques that rely on a list of detected features. Their system was mainly based on a sensor fusion scheme, that produced pose estimation in 6 degrees of freedom using the information from different sensors and the vision module.

Park, Jun, Lee et. al. [80] further expanded the work in [71], by presenting a vision guided underwater docking algorithm for an AUV, using lights at the dock to guide the vehicle during the last stage of the docking sequence (see figure 3.5). The dock remained stationary during docking. The algorithm allowed the tested AUV to identify dock lights, eliminate interfering luminary noises and successfully estimate both the center of the dock and the distance to it. The control was implemented based on the decoupled equations of

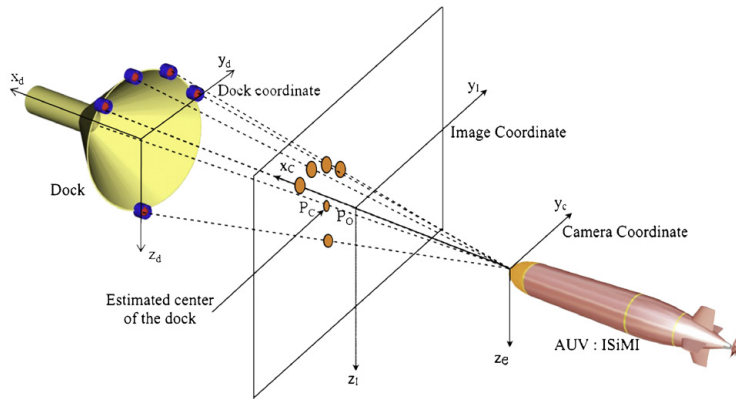


Fig. 10. Coordinates of the vision system.

Figure 3.5: Vision guided docking system. Source: Park et. al.

motions for steering and for diving (Healey and Lienard [60]). To track the heading and depth references a conventional PID control loop was applied. The developed algorithm was based on pure pursuit guidance law. In pure pursuit guidance law, there is an absence of compensation against environmental disturbance, especially ocean current. Moreover, no alignment of the AUV's heading with dock direction was applied. In [81] a conceptual idea was derived to overcome these two problems. If there is an ocean current, the AUV approaches to the dock with side slip angle ( $\beta$ ). The torpedo-type AUV is an under-actuated system. Hence, the agreement of three states (vehicle heading, course and the dock heading) at the moment of docking is impossible. They assumed that a final approach and docking with the side slip angle is more dangerous than docking with discrepancy between the course and the dock heading. It is further assumed that the dock heading is fixed at  $\psi_{dock} = 0$  and the AUV knows this heading. The current is also assumed to be regular and uniform. Only lateral current was considered. The main idea is to generate an intentional cross-track error to compensate the effect of cross currents, combined with a predetermined heading relative to the ocean currents that will drive the

state of the AUV to a final state inside the docking station, perfectly aligned. Park et. al. [81] presents the necessary equations to derive the references for the cross-track error and the desired heading ( $\psi_{AUV}$ ). Figure 3.6 presents the method to compensate the effect of lateral currents.

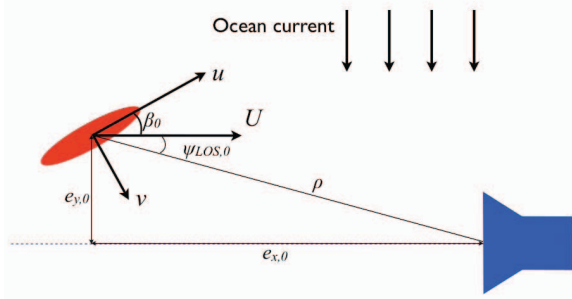


Figure 3.6: Method to compensate the effect of cross currents. Source: Park et. al.

This related work is essential to properly define the problem and to derive a solution for the control of underwater vehicles in autonomous underwater docking maneuvers.



# Chapter 4

## Problem statement

This chapter formally describes the docking control problem. The concept for this section is largely influenced by the work methodology presented for the Mobile Offshore Base (MOB) [82] by Girard, Sousa and Hedrick ([83], [84], and [85]).

### 4.1 Introduction

To expand an AUV's autonomy it is important to dock into a station that it is able to transfer power and data. This work aims to develop a control strategy to successfully dock an AUV into a ROV. Figure 4.1 illustrates the docking problem. In order to achieve this goal the AUV is required to:

- Reach a position inside the ROV, with a given forward speed (surge,  $u$ ), and aligned with the dock structure (same heading and elevation).
- Connect with the ROV with the purpose of transferring data and power.
- Undock and start a new mission assignment.

The following sections in this chapter present the docking requirements, scenarios of operation during the docking sequence, assumptions considered in the approach, and finally, the problems formulated to be solved in chapter 5.

### 4.2 Requirements

The formal solution for the docking problem has to consider the vehicles involved in the memorandum of understanding (MOU) between the Underwater Systems and Technology Laboratory (LSTS) and the Portuguese Task Group for the Extension of the Continental

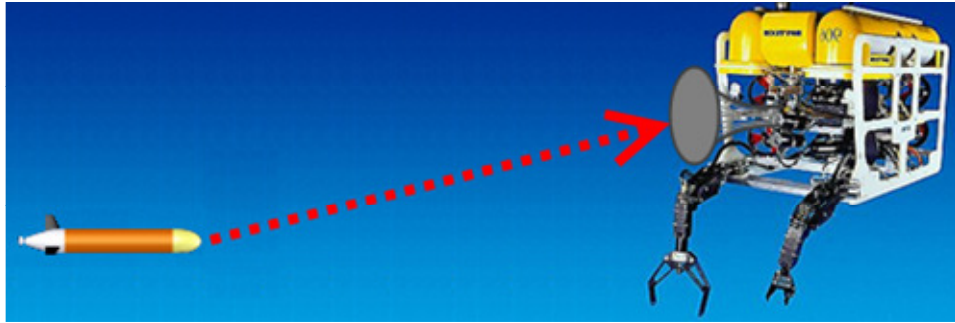


Figure 4.1: The docking problem

Shelf (EMEPC). Hence, the vehicles to consider are the LSTS's LAUV and the EMEPC's ROV Luso. Technical specifications for both vehicles are presented in the following sections.

#### 4.2.1 LAUV

The Light Autonomous Underwater Vehicle (LAUV) [7] designed and built at the LSTS is a small underwater vehicle (figure 4.2) optimized for a low cost mechanical structure. The main goal of the vehicle is to test new control and software methodologies without the concern of high monetary impact in the case of catastrophic failure.



Figure 4.2: The Light Autonomous Underwater Vehicle

The LAUV is a torpedo shaped vehicle, with a length of 108cm, a diameter of 15cm and a mass of approximately 18kg. The actuator system is composed of one propeller and 3 or 4 control fins (depending on the vehicle version), all electrically driven. It has a miniaturized computer system running the control system software. It uses an inertial measurement unit (IMU), a depth sensor and long baseline (LBL) system for navigation. The maximum velocity is 2m/s. Table 4.1 presents the LAUV technical specifications.

Table 4.1: LAUV technical specifications

LAUV Technical Specifications	
Dimensions	108 × 15cm
Weight	18kg
Mass depth	50 meters
Max Forward Velocity	2m/s
Autonomy	up to 8 hours
Communications	GSM, Wi-Fi
Standard sensors	CTD, GPS/GSM
Navigation	IMU, LBL module
Computer systems	Gumstix (Xscale), running Linux

#### 4.2.2 ROV Luso

Portugal has now the capability to explore the deep ocean with a 6000 meter rated ROV (figure 4.3). The ROV, named Luso, was acquired by the EMEPC. Luso is a medium work class Bathysaurus XL, developed by ARGUS Remote Systems AS. Its main application focuses on both fundamental and applied research in deep waters.



Figure 4.3: ROV Luso

The ROV Luso is a medium size vehicle, with a length of 2.1m, a width of 1.6m and a height of 1.7m. It weights approximately 1700kg. Its standard equipment include several manipulators, cameras, a sonar, depth sensor and compass. The maximum expected velocity is 1.5m/s forward and 1m/s vertical. Table 4.2 presents some of ROV Luso technical specifications.

Table 4.2: ROV Luso technical specifications

ROV Luso Technical Specifications	
Dimensions	2.1 × 1.6 × 1.7m
Weight	1700kg
Mass depth	6000 meters
Max Forward Velocity	1.5m/s
Max Vertical Velocity	1m/s
Thrusters	7 × 5.5kW, 4 horizontal and 3 vertical
Umbilical	Kevlar armoured, 4000m

## 4.3 Models of the vehicles

The models presented in this section are intended to model the dynamic behavior of the LAUV and the ROV Luso.

### 4.3.1 Model for the LAUV

The model of the LAUV presented in this section [7] uses a lift matrix,  $L(v)$  (some authors include these terms on the damping matrix,  $D(v)$ ). Therefore, we change the equations of motion (2.15) presented in section 2.1.4 to

$$M\dot{v}_R + C(v_R)v_R + D(v_R)v_R + L(v_R)v_R + g(\eta) = Bu \quad (4.1)$$

$$\dot{\eta} = J(\eta_2)(v_R + v_c) \quad (4.2)$$

The LAUV shape and weight leads to some simplifications in the equation of motion (4.1):

1. The origin of the body-fixed reference frame is the center of buoyancy. When the AUV is fully submerged, the vehicle's center of buoyancy will be coincident with the vehicle's center. Hence,

$$x_B = y_B = z_B = 0m \quad (4.3)$$

2. With the origin of the body-fixed referential at the AUV's center of buoyancy, the vehicle possesses symmetry in the planes  $xz$  and  $xy$ , i.e., longitudinal and lateral symmetry. The fins at the bow of the vehicle introduce small asymmetries in the  $yz$  plane.

3. The inertia operator ( $M$ ) of the vehicle can be approximated by an prolate ellipsoid.

The last assumption is supported by Arnold [9].

"If a body is stretched out along some axis, then the moment of inertia with respect to this axis is small, and consequently, the inertia ellipsoid is also stretched out along this axis; thus, the inertia ellipsoid may resemble the shape of the body" [9, chap 2, p. 139]

The inertia ellipsoid of the body is the ellipsoid  $(\Omega : (M\Omega, \Omega) = 1)$ , where  $\Omega$  is the angular velocity in the body reference frame,  $M$  is the inertia operator and  $(a,b)$  is the interior product between  $a$  and  $b$ .

If the vehicle has three planes of symmetry, this suggests that the contribution from the off-diagonal elements in the added mass matrix  $M_A$  [1] can be neglected. This is due to the fact that the off-diagonal elements of a positive matrix (inertia) will be much smaller than their diagonal counterparts. Hence, the following simpler expressions for  $M_A$  and  $C_A(v)$  hold:

$$M_A = -\text{diag}(X_{\dot{u}}, Y_{\dot{v}}, Z_{\dot{w}}, K_{\dot{p}}, M_{\dot{q}}, N_{\dot{r}}) \quad (4.4)$$

$$C_A(v) = \begin{bmatrix} 0 & 0 & 0 & 0 & -Z_{\dot{w}}w & Y_{\dot{v}}v \\ 0 & 0 & 0 & -Z_{\dot{w}}w & 0 & -X_{\dot{u}}u \\ 0 & 0 & 0 & -Y_{\dot{v}}v & X_{\dot{u}}u & 0 \\ 0 & -Z_{\dot{w}}w & Y_{\dot{v}}v & 0 & -N_{\dot{r}}r & M_{\dot{q}}q \\ Z_{\dot{w}}w & 0 & -X_{\dot{u}}u & N_{\dot{r}}r & 0 & -K_{\dot{p}}p \\ -Y_{\dot{v}}v & X_{\dot{u}}u & 0 & -M_{\dot{q}}q & K_{\dot{p}}p & 0 \end{bmatrix} \quad (4.5)$$

However, the objective is to derive simplified matrices for  $M(\dot{v})$  and  $C(v)$ . Taking into account the first and the third assumption that the inertia tensor is approximated by an prolate ellipsoid, and with equation (4.4), it is possible to derive:

$$M = \begin{bmatrix} m - X_{\dot{u}} & 0 & 0 & 0 & mz_G & 0 \\ 0 & m - Y_{\dot{v}} & 0 & -mz_G & 0 & 0 \\ 0 & 0 & m - Z_{\dot{w}} & 0 & 0 & 0 \\ 0 & -mz_G & 0 & I_x - K_{\dot{p}} & 0 & 0 \\ mz_G & 0 & 0 & 0 & I_y - M_{\dot{q}} & 0 \\ 0 & 0 & 0 & 0 & 0 & I_z - N_{\dot{r}} \end{bmatrix} \quad (4.6)$$

The Coriolis and centripetal matrix  $C(v)$  will be given by:

$$C(v) = \begin{bmatrix} \mathbf{0} & C_{12}(v) \\ C_{21}(v) & C_{22}(v) \end{bmatrix} \quad (4.7)$$

with

$$C_{12}(v) = \begin{bmatrix} mz_Gr & (m - Z_{\dot{w}})w & -(m - Y_{\dot{v}})v \\ -(m - Z_{\dot{w}})w & mz_Gr & (m - X_{\dot{u}})u \\ -mz_Gp - Y_{\dot{v}}v & -mz_Gq + X_{\dot{u}}u & 0 \end{bmatrix}$$

$$C_{21}(v) = \begin{bmatrix} -mz_Gr & (m - Z_{\dot{w}})w & (mz_Gp - (m - Y_{\dot{v}})v \\ -(m - Z_{\dot{w}})w & -mz_Gr & (mz_Gq - (m - X_{\dot{u}})u \\ (m - Y_{\dot{v}})v & -(m - X_{\dot{u}})u & 0 \end{bmatrix}$$

$$C_{22}(v) = \begin{bmatrix} 0 & (I_z - N_r)r & -(I_y - M_{\dot{q}})q \\ -(I_z - N_r)r & 0 & (I_x - K_{\dot{p}})p \\ (I_y - M_{\dot{q}})q & -(I_x - K_{\dot{p}})p & 0 \end{bmatrix}$$

The Coriolis additional force and moment terms induced by ocean currents,  $C(v_r)v_r$  will be given by:

$$C(v_r)v_r = C(v)v_r + \begin{bmatrix} mS(\omega)J_1^{-1}(\eta_2)U_c \\ mS(\rho_G)S(\omega)J_1^{-1}(\eta_2)U_c \end{bmatrix}$$

where  $S(\cdot)$  is the skew symmetric matrix involving the vector cross product of  $(\cdot)$  with other vectors.  $\omega = [p, q, r]^T$ , and  $\rho_G = [x_G, y_G, z_G]$  which are the coordinates of the vehicle's center of gravity (CG) expressed in the body-fixed reference frame. Thus, we have

$$S(\omega) = \begin{bmatrix} 0 & -r & q \\ r & 0 & -p \\ -q & p & 0 \end{bmatrix}$$

and

$$S(\rho_G) = \begin{bmatrix} 0 & -z_G & y_G \\ z_G & 0 & -x_G \\ -y_G & x_G & 0 \end{bmatrix}$$

For the damping matrix  $D(v)$ , Fossen [1] derives a rough approximation if we assume that a vehicle is performing non-coupled motion, has three planes of symmetry and that terms higher than second order are negligible. The previous assumptions suggests a diagonal structure for the damping matrix  $D(v)$  with only linear and quadratic damping terms on the diagonal.

$$\begin{aligned} D(v) = & -\text{diag}[X_u, Y_v, Z_w, K_p, M_q, N_r] \\ & -\text{diag}[X_{u|u}|u|, Y_{v|v}|v|, Z_{w|w}|w|, K_{p|p}|p|, M_{q|q}|q|, N_{r|r}|r|] \end{aligned} \quad (4.8)$$

A more accurate approximation would be to consider the asymmetry existent in the  $yz$  plane, which makes the damping matrix non-diagonal [7].

$$D(v) = - \begin{bmatrix} X_u & 0 & 0 & 0 & 0 & 0 \\ 0 & Y_v & 0 & 0 & 0 & Y_r \\ 0 & 0 & Z_w & 0 & Z_q & 0 \\ 0 & 0 & 0 & K_p & 0 & 0 \\ 0 & 0 & M_w & 0 & M_q & 0 \\ 0 & N_v & 0 & 0 & 0 & N_r \end{bmatrix} - \begin{bmatrix} X_{u|u}|u| & 0 & 0 & 0 & 0 & 0 \\ 0 & Y_{v|v}|v| & 0 & 0 & 0 & Y_{r|r}|r| \\ 0 & 0 & Z_{w|w}|w| & 0 & Z_{q|q}|q| & 0 \\ 0 & 0 & 0 & K_{p|p}|p| & 0 & 0 \\ 0 & 0 & M_{w|w}|w| & 0 & M_{q|q}|q| & 0 \\ 0 & N_{v|v}|v| & 0 & 0 & 0 & N_{r|r}|r| \end{bmatrix} \quad (4.9)$$

There is no change in the damping matrix, when one considers the influence of ocean currents, hence  $D(v_R) = D(v)$ .

The Lift matrix  $L(v_R)$  comes as follows

$$L(v_R) = \begin{bmatrix} 0 & 0 & 0 & 0 & 0 & 0 \\ 0 & Y_{uv} & 0 & 0 & 0 & Y_{ur} \\ 0 & 0 & Z_{uw} & 0 & Z_{uq} & 0 \\ 0 & 0 & 0 & 0 & 0 & 0 \\ 0 & 0 & M_{uw} & 0 & M_{uq} & 0 \\ 0 & N_{uv} & 0 & 0 & 0 & N_{ur} \end{bmatrix} \quad (4.10)$$

In what concerns the restoring terms, the vector  $g(\eta_2)$  will be given by:

$$g(\eta_2) = \begin{bmatrix} (W - B) \sin \theta \\ -(W - B) \cos \theta \sin \phi \\ -(W - B) \cos \theta \cos \phi \\ z_G W \cos \theta \sin \phi \\ z_G W \sin \theta \\ 0 \end{bmatrix} \quad (4.11)$$

where  $W$  is the body weight and  $B$  is the body's buoyancy force.

The control matrix  $B$  is given by

$$B = \begin{bmatrix} 1 & 0 & 0 \\ 0 & Y_{uu}\delta_r * u^2 & 0 \\ 0 & 0 & Z_{uu}\delta_s * u^2 \\ \frac{K_{prop0}}{X_{prop0}} & 0 & 0 \\ 0 & 0 & M_{uu}\delta_s * u^2 \\ 0 & N_{uu}\delta_r * u^2 & 0 \end{bmatrix} \quad (4.12)$$

Finally, the control vector  $u$  is

$$u = [X_{prop}, \delta_R, \delta_S]^T \quad (4.13)$$

where  $X_{prop}$  is the propeller force acting on the longitudinal axes and  $\delta_R$  and  $\delta_S$  are the rudder and stern planes angles of deflection, respectively.

### 4.3.2 Model for the ROV

The model used in the ROV Luso is a very simplified one, due to the low complexity of the required maneuvers for the ROV during the docking procedures. For the ROV Luso the equations of motion considered are

$$M\dot{v}_R + C(v_R)v_R + D(v_R)v_R + g(\eta) = Bu \quad (4.14)$$

$$\dot{\eta} = J(\eta_2)(v_R + v_c) \quad (4.15)$$

Furthermore, the following assumptions are considered:

1. The origin of the body-fixed reference frame is the center of gravity. When the ROV Luso is fully submerged, the vehicle's center of gravity will be coincident with the vehicle's center.

$$x_G = y_G = z_G = 0m \quad (4.16)$$

2. The ROV Luso has three vertical thrusters to perform heave motions. For simplicity, only one vertical thruster will be considered. All the four horizontal thrusters will be considered during the modeling process. The thruster allocation used is equal to the thruster allocation of the ROV-KOS [86].

3. The thruster allocation will follow the solution introduced in section 2.1.5.2.

Thus, the constant added mass and inertia matrix,  $M$  is

$$M = diag(m - X_{\dot{u}}, m - Y_{\dot{v}}, m - Z_{\dot{w}}, m - K_{\dot{p}}, m - M_{\dot{q}}, m - N_{\dot{r}}) \quad (4.17)$$

The Coriolis and centripetal matrix  $C(v_R)$  will be given by:

$$C = \begin{bmatrix} 0 & 0 & 0 & 0 & mw - Z_{\dot{w}}w & -mv + Y_{\dot{v}}v \\ 0 & 0 & 0 & -mw + Z_{\dot{w}}w & 0 & mu - X_{\dot{u}}u \\ 0 & 0 & 0 & mv - Y_{\dot{v}}v & -mu + X_{\dot{u}}u & 0 \\ 0 & mw - Z_{\dot{w}}w & -mv + Y_{\dot{v}}v & 0 & -I_zr - N_{\dot{r}}r & -I_yq + M_{\dot{q}}q \\ -mw + Z_{\dot{w}}w & 0 & mu - X_{\dot{u}}u & -I_zr + N_{\dot{r}}r & 0 & -I_xp - K_{\dot{p}}p \\ mv - Y_{\dot{v}}v & -mu + X_{\dot{u}}u & 0 & -I_yr - M_{\dot{q}}q & -I_xp + K_{\dot{p}}p & 0 \end{bmatrix} - \begin{bmatrix} 0 & 0 & 0 & 0 & -mw_c & mv_c \\ 0 & 0 & 0 & mw_c & 0 & -mu_c \\ 0 & 0 & 0 & -mv_c & mu_c & 0 \\ 0 & 0 & 0 & 0 & 0 & 0 \\ 0 & 0 & 0 & 0 & mz_Bw_c & -mz_Bv_c \\ 0 & 0 & 0 & 0 & 0 & 0 \end{bmatrix} \quad (4.18)$$

Due to the low complexity of the maneuvers required for the ROV Luso, the Damping matrix,  $D(v_R)$  is

$$D(v_R) = -\text{diag}[X_u, Y_v, Z_w, K_p, M_q, N_r] - \text{diag}[X_{u|u}|u|, Y_{v|v}|v|, Z_{w|w}|w|, K_{p|p}|p|, M_{q|q}|q|, N_{r|r}|r|] \quad (4.19)$$

In what concerns the restoring terms, the vector  $g(\eta_2)$  will be given by:

$$g(\eta_2) = [0, 0, 0, -z_B W \cos \theta \sin \phi, -z_B W \sin \theta, 0]^T \quad (4.20)$$

where  $z_B$  is the ROV center of buoyancy.

The control matrix  $B$  is given by

$$B = \begin{bmatrix} \cos(\alpha_1) & \cos(\alpha_2) & \cos(\alpha_3) & \cos(\alpha_4) & 0 \\ \sin(\alpha_1) & \sin(\alpha_2) & \sin(\alpha_3) & \sin(\alpha_4) & 0 \\ 0 & 0 & 0 & 0 & 1 \\ 0 & 0 & 0 & 0 & 0 \\ D_{1z} & D_{2z} & -D_{3z} & -D_{4z} & D_{5x} \\ d_1 \sin(\gamma_1) & d_2 \sin(\gamma_2) & d_3 \sin(\gamma_3) & d_4 \sin(\gamma_4) & 0 \end{bmatrix} \quad (4.21)$$

where  $\alpha_i$ ,  $\gamma_i$  and  $d_i$  were explained in section 2.1.5.2.  $D_{ij}$  is the position of thruster  $i$  in the  $j$ -axes.

Finally, the control vector  $u$

$$u = [F_{1h}, F_{2h}, F_{3h}, F_{4h}, F_{5v}]^T \quad (4.22)$$

where the subscript  $h$  stands for horizontal force, and the subscript  $v$  stands for vertical force.

## 4.4 Scenarios

In the interest of defining different scenarios involved with the docking operation one can define a proper set of modes of operation:

- **Unassembled mode** – the AUV and ROV are two independent modules, with different position and orientation and with different mission assignments (prior to the docking operation).
- **Homing mode** – when the AUV is performing a homing sequence to reach a state where it is aligned and pointed to the entry of the dock structure, without the risk of frontal collision between both vehicles.
- **Docking mode** – the AUV is performing the motion plan to dock inside the dock structure.
- **Docked mode** – the LAUV is docked inside the ROV.
- **Abort mode** – set of maneuvers that allow the AUV to retrieve.

A problem when the vehicle is in the *unassembled* or the *homing mode* is the possibility of collisions between both vehicles, which can lead to serious mechanical malfunction. Therefore the docking system must be able to avoid collisions between both vehicles.

During the *docking mode* there is the need for the controller to track the motion plan that drives the AUV to the dock structure. Thus, external disturbances such as ocean currents have to be considered in order to develop robust and safe controllers.

During the final moments of the docking operation, there is the possibility that the external disturbances move the LAUV away from the motion plan with risk of collisions. Hence, the control must be able to stop the docking sequence and drive the state of the LAUV away from the ROV - the *abort mode*.

## 4.5 Assumptions

This section introduces some **assumptions** that will hold for the remainder of the problems formulated in the following sections.

- The problems will be formulated in the horizontal plane only (XY) - therefore only the following state variables will be considered (AUV position coordinates in the earth-fixed frame,  $x$  and  $y$ , AUV heading,  $\psi$  and their respective time derivatives, surge,  $u$ , sway,  $v$ , and turn ratio about the z-axes,  $r$ ).

- The AUV knows its exact position and orientation, and also its time-derivatives (the first two are relative to the earth-fixed reference frame and the latter is relative to the body-fixed reference frame).
- The AUV knows the exact position and orientation of the ROV.
- The AUV must approach the ROV from behind, *i.e.*, if one considers the AUV expressed in the ROV body-fixed reference frame, then the dock structure entry is in the origin of the reference frame, aligned positively with the x-axes. Therefore the AUV must perform the motion plan to reach the origin of the frame along the negative x-axes. Figure 4.4 illustrates this assumption.

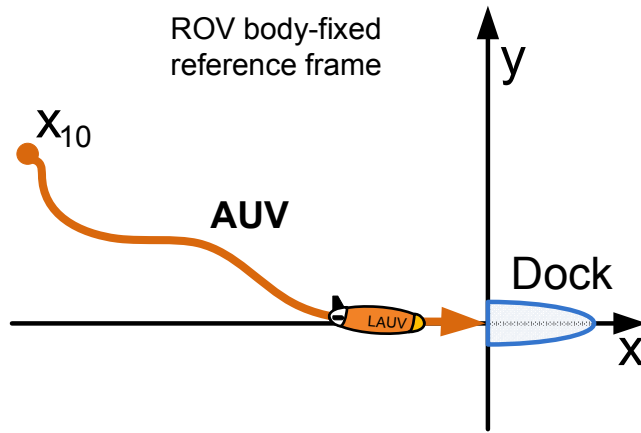


Figure 4.4: The docking problem expressed in the ROV body-fixed reference frame

## 4.6 Problem 1 – Docking without disturbances with the ROV fixed

This problem intends to develop a control strategy to dock the torpedo shaped underwater vehicle inside the ROV, while the ROV is in a fixed position.

### 4.6.1 Assumptions

In addition to the assumptions described in section 4.5, this problems considers the following assumptions:

- The ROV is in a fixed position and orientation relative do the earth-fixed reference frame (*i.e.*, the ROV is performing dynamic positioning).
- No disturbances will be considered (such as ocean currents or wave surge).

The objective is to reach a position in the vicinity of the ROV, with the AUV correctly aligned with the heading of the dock structure. The surge of the AUV must be above a predefined value. This objective holds for the rest of the problems to be defined.

#### 4.6.2 Formal statement

Given the AUV state,  $\mathbf{x}_1 \in \mathbb{R}^n$ , and the ROV state,  $\mathbf{x}_2 \in \mathbb{R}^n$ , where:

$$\begin{aligned}\dot{\mathbf{x}}_1 &= f_1(\mathbf{x}_1, u_1) && \text{with } u_1 \in \Omega_1 \in \mathbb{R}^p \\ \dot{\mathbf{x}}_2 &= f_2(\mathbf{x}_2, u_2) = 0 && \text{with } u_2 \in \Omega_2 \in \mathbb{R}^q \\ \mathbf{x}_1(t_0) &= \mathbf{x}_{10} && \text{is the AUV initial state} \\ \mathbf{x}_2(t) &= \mathbf{x}_{20} && \text{is the ROV state during the docking sequence}\end{aligned}$$

In the above equation  $u_1$  and  $u_2$  are the AUV and ROV input controls (such as control surfaces or thrusters), respectively, and,  $\Omega_1$  and  $\Omega_2$  are both closed and bounded sets.

The objective is to find a control strategy that drives the AUV into the docking position inside the ROV, such that:

$$\exists u_1(\cdot) : \quad \mathbf{x}_1(t_d) \in C \quad \text{and} \quad x_{1\text{surge}}(t_d) > K_{\text{minspeed}} \quad (4.23)$$

Where  $u_1(\cdot)$  is the AUV control strategy along time,  $t_d$  is the moment in time where the docking occurs, and  $C$  is a bounded and closed set in the neighborhood of the ROV state  $\mathbf{x}_2$ .  $x_{1\text{surge}}(t_d)$  is the AUV forward speed, during the moment of docking,  $t_d$ , and  $K_{\text{minspeed}}$  is a positive constant.

Expression (4.23) reads that there exists a control strategy for the AUV, that allows its state to enter a set  $C$ , which is a close vicinity to the state of the ROV. The AUV surge,  $u$ , must be above a predetermined value  $K_{\text{minspeed}}$ . Figure 4.5 illustrates the docking problem.

### 4.7 Problem 2 – Docking without disturbances with the ROV in motion

#### 4.7.1 Assumptions

In addition to the assumptions described in section 4.5, this problems considers the following assumptions:

- The ROV is in motion.
- No disturbances will be considered (such as ocean currents or wave surge).

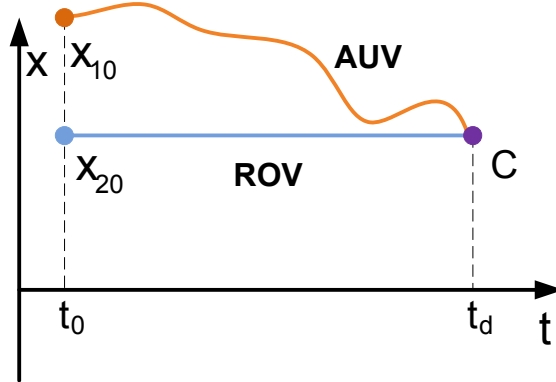


Figure 4.5: The docking problem when the ROV is performing dynamic positioning

- The AUV is aware of the ROV strategy throughout the docking procedures.

#### 4.7.2 Formal statement

Given AUV state,  $\mathbf{x}_1 \in \mathbb{R}^n$ , and ROV state,  $\mathbf{x}_2 \in \mathbb{R}^n$ , where:

$$\begin{aligned}\dot{\mathbf{x}}_1 &= f_1(\mathbf{x}_1, u_1) && \text{with } u_1 \in \Omega_1 \in \mathbb{R}^p \\ \dot{\mathbf{x}}_2 &= f_2(\mathbf{x}_2, u_2) && \text{with } u_2 \in \Omega_2 \in \mathbb{R}^q \\ \mathbf{x}_1(t_0) &= \mathbf{x}_{10} && \text{is the AUV initial position} \\ \mathbf{x}_2(t_0) &= \mathbf{x}_{20} && \text{is the ROV initial position}\end{aligned}$$

The objective is to find a control strategy that drives the AUV into the docking position inside the ROV, such that:

$$\exists u_1(\cdot), u_2(\cdot) : \quad \mathbf{x}_1(t_d) \in C(t_d) \quad \text{and} \quad x_{1\text{surge}}(t_d) > K_{\text{minspeed}} + x_{2\text{surge}}(t_d) \quad (4.24)$$

Where  $u_1(\cdot)$  and  $u_2(\cdot)$  are the AUV and ROV control strategies along time, respectively,  $t_d$  is the moment in time where the docking occurs, and  $C(t)$  is a bounded and closed set in the neighborhood of the ROV state  $x_2$ .  $x_{1\text{surge}}(t_d)$  and  $x_{2\text{surge}}(t_d)$  are the AUV and ROV forward speeds, respectively, during the moment of docking,  $t_d$ , and  $K_{\text{minspeed}}$  is a positive constant.

Expression 4.24 reads that there exists a control strategy for each of both vehicles, that allows the state of the AUV to enter a set  $C(t)$ , which is a close vicinity to the state of the ROV. The ROV state evolves in time.

The other difference between Problem 2 and Problem 1 (4.6), is that it is not enough for the AUV surge,  $u$ , to be above  $K_{\text{minspeed}}$ . Now, AUV surge must be above ROV surge

plus  $K_{\min speed}$  and  $C$  is now time varying. Figure 4.6 illustrates the docking problem when the ROV is in motion.

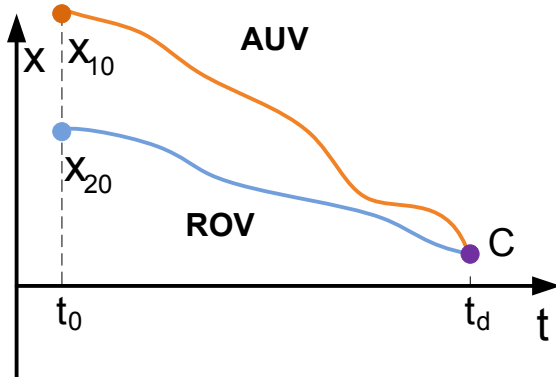


Figure 4.6: The docking problem when the ROV in motion

## 4.8 Problem 3 – Docking with disturbances

The purpose of this problem is to verify the robustness of the control strategy developed in the previous problems, since for this problem, the tests will be performed in the presence of external disturbances.

### 4.8.1 Assumptions

This problems considers the following assumptions:

- The ROV is in motion. Hence, the LAUV can dock with a higher velocity (while maintaining a low velocity relative to the ROV).
- The AUV is aware of the ROV strategy throughout the docking procedures.
- The external disturbances can be measured offline, prior to the beginning of the docking sequence.
- Disturbances will be considered (ocean currents) that satisfy the matching condition.

### 4.8.2 Formal statement

The difference in the formal statement lies in

$$\begin{aligned}\dot{\mathbf{x}} &= f_1(\mathbf{x}_1, u_1, v_1) && \text{with } u_1 \in \Omega_1 \in \mathbb{R}^p \\ \dot{\mathbf{x}} &= f_2(\mathbf{x}_2, u_2, v_2) && \text{with } u_2 \in \Omega_2 \in \mathbb{R}^q\end{aligned}$$

where  $v_1, v_2 \in \Upsilon$  are unknown, but closed and bounded disturbances. More precisely, only ocean currents will be considered for this problem.

The objective is the same of the previous problem.

$$\exists u_1(\cdot), u_2(\cdot) : \quad \mathbf{x}_1(t_d) \in C(t_d) \quad \text{and} \quad x_{1_{\text{surge}}}(t_d) > K_{\text{minspeed}} + x_{2_{\text{surge}}}(t_d) \quad (4.25)$$

Figure 4.7 illustrates the docking problem with ocean currents (external disturbances).

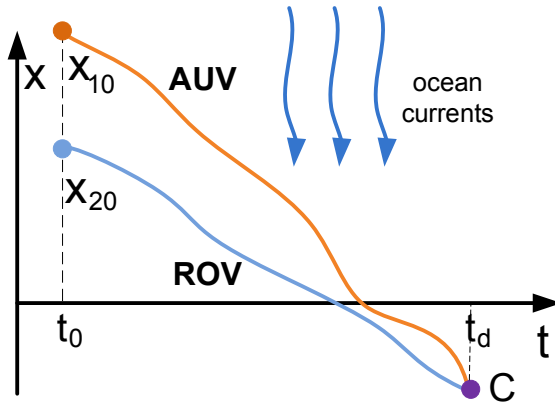


Figure 4.7: The docking problem with ocean currents

## 4.9 Problem 4 – Collision Avoidance in the early stages of the operation

The moment of the final docking happens when the dock structure inside the ROV is in the line-of-sight of the AUV, and when the AUV orientation is aligned with the orientation of the dock structure. Nonetheless, there is the need to develop a collision avoidance controller for the early stages of the docking operation.

### 4.9.1 Assumptions

This problems considers the following assumptions:

- The ROV is in motion.
- The AUV is aware of the ROV strategy throughout the docking procedures.
- The external disturbances can be measured offline, prior to the beginning of the docking sequence.
- Disturbances will be considered (ocean currents) that satisfy the matching condition.

### 4.9.2 Formal statement

Given AUV state,  $\mathbf{x}_1 \in \mathbb{R}^n$ , and ROV state,  $\mathbf{x}_2 \in \mathbb{R}^n$ , where:

$$\dot{\mathbf{x}}_1 = f_1(\mathbf{x}_1, u_1, v_1) \quad \text{with} \quad u_1 \in \Omega_1 \in \mathbb{R}^p$$

$$\dot{\mathbf{x}}_2 = f_2(\mathbf{x}_2, u_2, v_2) \quad \text{with} \quad u_2 \in \Omega_2 \in \mathbb{R}^q$$

$\mathbf{x}_1(t_0) = \mathbf{x}_{10}$  is the AUV initial position

$\mathbf{x}_2(t_0) = \mathbf{x}_{20}$  is the ROV initial position

The objective is to find a control strategy that drives the AUV into the docking position inside the ROV, such that:

$$\exists u_1(\cdot), u_2(\cdot) : \quad \mathbf{x}_1(t_d) \in C(t_d) \quad (4.26)$$

$$x_{1\text{surge}}(t_d) > K_{\text{minspeed}} + x_{2\text{surge}}(t_d) \quad (4.27)$$

$$\mathbf{x}_1(t) \notin D(t) \quad \forall t < t_d \quad (4.28)$$

where set  $D$ , which is a bounded and closed set in the vicinity of the ROV state,  $x_2$ . Hence, the objective is to reach a position in  $C$  only during the final docking moment (when the vehicle performs the motion plan). Previously, the AUV is required to avoid the set surrounding the ROV, to avoid collisions. Hence,  $D$  is considered a safety zone. In practice the purpose is to prevent the AUV to collide with the ROV while the dock structure is not in the AUV line of sight. Figure 4.8 illustrates the collision avoidance problem.

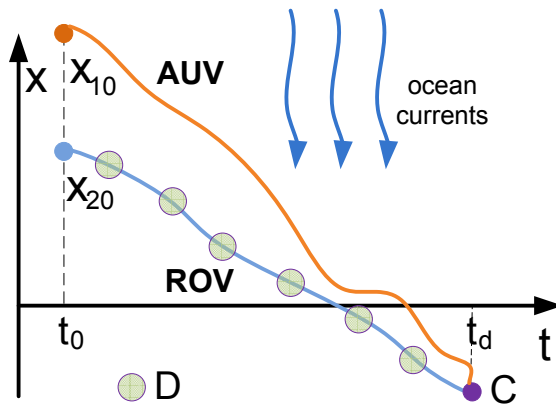


Figure 4.8: The collision avoidance problem

## 4.10 Problem 5 – Abort sequence

### 4.10.1 Assumptions

This problems considers the following assumptions:

- The ROV is in motion.
- The AUV is aware of the ROV strategy throughout the docking procedures.
- The external disturbances can be measured offline, prior to the beginning of the docking sequence.
- Disturbances will be considered (ocean currents) that satisfy the matching condition.
- The docking sequence can be aborted.

### 4.10.2 Formal statement

Given AUV state,  $\mathbf{x}_1 \in \mathbb{R}^n$ , and ROV state,  $\mathbf{x}_2 \in \mathbb{R}^n$ , where:

$$\begin{aligned}\dot{\mathbf{x}}_1 &= f_1(\mathbf{x}_1, u_1, v_1) && \text{with} && u_1 \in \Omega_1 \in \mathbb{R}^p \\ \dot{\mathbf{x}}_2 &= f_2(\mathbf{x}_2, u_2, v_2) && \text{with} && u_2 \in \Omega_2 \in \mathbb{R}^q \\ \mathbf{x}_1(t_0) &= \mathbf{x}_{10} && \text{is the AUV initial position} \\ \mathbf{x}_2(t_0) &= \mathbf{x}_{20} && \text{is the ROV initial position}\end{aligned}$$

After receiving the abort signal, the objective is to find a control strategy such that

$$\mathbf{x}_1(t) \notin D(t) \quad \forall t \quad (4.29)$$

The AUV is required to avoid the set  $D$  (bounded and closed set in the vicinity of the ROV states). Figure 4.9 illustrates this problem.

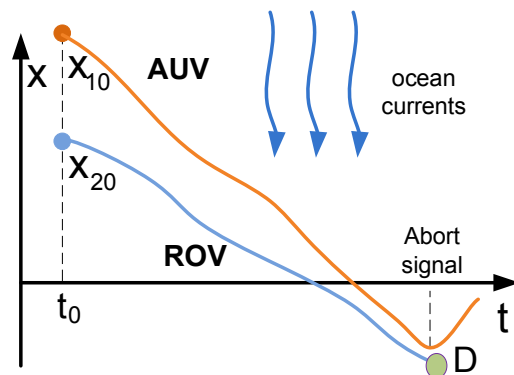


Figure 4.9: The abort docking problem



# Chapter 5

## Approach

### 5.1 Introduction

This chapter presents the approach to solve the problems described in chapter 4. The docking will be divided into basic maneuvers that intend to guide the vehicle with a determined heading and depth. The control architecture for the LAUV will be explained, as well as the controllers used to perform the basic maneuvers. Finally, each one of the problems will be addressed individually, and a solution will be derived.

### 5.2 Basic maneuvers

The docking mission is a complex problem that can be divided into smaller operations, designated here as *basic maneuvers*. The interest is to define a set of basic maneuvers, that can be easily combined to perform maneuvers with a higher degree of complexity [87]. Notice that the following basic maneuvers involve driving the vehicle to a specific region while using state feedback references for guidance.

- **Maneuver 1: Line of sight guidance** – Reaching a region in bounded time, while moving inside some prescribed area.
- **Maneuver 2: Follow Track** – Follow a line between two prescribed points with some additional constraints.
- **Maneuver 3: Roundabout** – Perform a circle around the ROV to avoid collisions and to reach a position behind him<sup>1</sup>.

The control activities follow a specific logical pattern that results from interactions with other entities in the environment, and that are not completely known in advance.

---

<sup>1</sup>A position behind the ROV is a position with a negative value on the x-axis, if we consider the ROV body-fixed reference frame

Maneuver automation entails the realm of logic, and of discrete event models interacting with nonlinear ordinary differential equations that model vehicle dynamics. This suggests the need for concepts and theories from hybrid systems and the use of a **hierarchical control architecture** [83] to allow for a higher degree of abstraction.

### 5.3 Architecture

In section 5.2 we suggest the need for a hierarchical control architecture for the docking operation. This is due to the need to control dynamic motions of the AUV and the ROV that are expressed through nonlinear ordinary differential equations which interact with discrete event models. Hierarchical control architectures have been largely implemented in multi-agent vehicle system such as air traffic control (Tomlin et. al. [88], [24] and [28], Sastry et. al. [16]) and automated highway systems (Varaiya [14], Godbole et. al. [15], Lygeros et. al. [25], Carbaugh et. al. [89]).

For the docking operation, a three-level control architecture similar to the MOB control architecture is considered ([82] - [85]).

**Supervisory Layer** - This level is responsible for the correct execution of the docking operation. At the beginning of the operation this layer receives the waypoint definitions (described in detail in section 5.5), the initial states of both vehicles and the boundary of the ocean currents. The ocean currents boundary is used to compute the backreach set under adversarial behavior. Afterwards, the motion planning (section 5.5) uses the backreach set information, the waypoints definitions and the initial states of the vehicles to derive the set of basic maneuvers for the vehicle to perform (section 5.2). If there is no information regarding the boundary of the ocean currents, the backreach set computation can be skipped.

While the docking operation is being performed, the supervisory layer is responsible for providing high level control to the system. This is achieved using hybrid systems theory (introduced in section 2.2). Hence, this level interacts directly with the maneuver layer dispatching the basic maneuvers and receiving events concerning their completion or failure.

**Maneuver Layer** - This level is responsible for the correct execution of the basic maneuvers. Each one of the maneuvers has a dedicated controller. Hence, this layer receives the maneuver definitions from the supervisory layer and activates the respective controller to perform the maneuver. The controllers are responsible for sending low-level commands, as state references, to the regulation layer and receive state feedback. Finally, this layer sends events concerning the completion or failure of the maneuvers.

**Regulation Layer** - This level is the lower level of automation, therefore, it deals with continuous signals, and interfaces directly with the vehicle hardware. This layer receives

control laws given as state references and sends input references to control the vehicle dynamics. The regulation layer has access to sensor information about the actual state of the vehicle, and is able to calculate tracking errors.

The control is achieved using a dynamic model of the LAUV. To decrease the computational costs, simplified decoupled systems (section 5.9) are implemented to model the dynamics of the vehicle. In the absence of external disturbances, tracking should be nearly perfect. Nonetheless, in the presence of large external disturbances (such as ocean currents), tracking can severely deteriorate. Thus, nonlinear control techniques (section 2.5) are implemented to provide robustness.

Figure 5.1 presents the complete control architecture. The indispensable blocks are represented with thicker lines. The layers are conceived in a way that they work in a completely transparent manner. Each layer can be expanded without changing interactions between them.

The following sections describe all the blocks of the control architecture, except the *high level control* block in the supervisory layer. The high level solution will be presented for each one of the problems stated in chapter 4.

## 5.4 Backward reach set computation

### 5.4.1 Introduction

The presence of external disturbances such as ocean currents, makes it harder for the controllers to track their prescribed motion plan, and therefore, increases the risk of an unsuccessful docking. Furthermore, the presence of disturbances increases the risk of mechanical malfunction in the case of collision, if the LAUV misses the docking approach.

In this problem we assume that the estimate of the bounds of the external disturbances can be measured prior to the docking sequence. Hence, there is the need to analyze the effects of those disturbances and to find a method to compensate for them to ensure safe docking.

A valuable resource to solve this problem is the reachability theory presented in section 2.3. Most specifically, backward reachability (section 2.3.1.3) which is the set of all states at time  $t < t_0$  that drive the state of the system to a given set  $X_f$  at time  $t = t_0$ .

In principle, the knowledge of the nonlinear dynamics equations of motion of the vehicle allows us to determine the backward reach set for this particular problem.

The actual computation of the backward reach set is however difficult. Some tools can do this for linear systems (Kurzhanskiy and Varaiya [90] and Ian Mitchell [91]). Observe that it is not possible to describe the behavior of underwater vehicles expressed in the earth-fixed reference frame using linearized approximations.

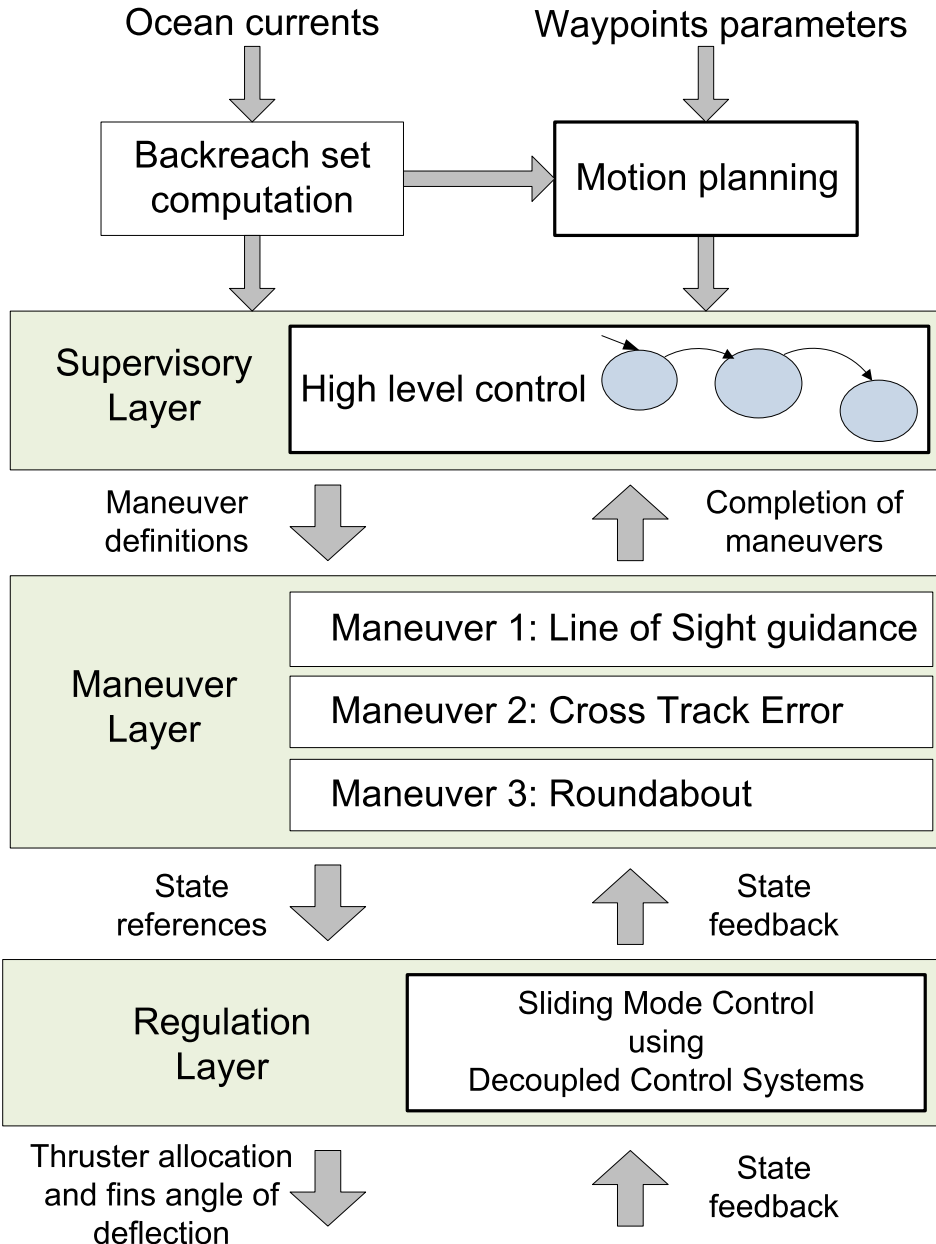


Figure 5.1: Architecture of the control

Hence, another technique must be applied. Krasovskii and Subbotin [36] introduced a construction setup that can be used for this purpose. (section 2.3.2.4).

### 5.4.2 Backreach Set under adversarial behavior

This section will introduce the necessary guidelines to compute the system backreach set under adversarial behavior (bounded ocean currents).

The goal is to maximize (minimize) the distance between both vehicles. In order to maximize (minimize) the distance value, it is necessary to drive the system backward in time and try to maximize (minimize) the distance function. The calculation of the bounds of the backreach set under adversarial behavior set contain the evolution of the state of the system as also the necessary control inputs. The differential games theory is applied since  $u$  is the control input responsible to drive the vehicle to the dock structure, and the external disturbances  $v$ , can be considered as the adversarial player, responsible to drive the vehicle off of the dock structure.

The state variables to consider are  $\mathbf{x} = [x, y, r, \psi]^T$  (horizontal plane only). An approximation can be made if one considers the body-fixed velocities constant. Hence, the surge of the vehicle will be the nominal speed value, and the sway motion will be neglected.

Then, from section 2.3.2.4 we have

$$\dot{x} = f(t, x, u, v), \quad u \in P, v \in Q \quad (5.1)$$

where  $u$  is the control input,  $v$  is the external disturbance (adversarial player) and  $x$  is the system state vector. The disturbance  $v$  is bounded. To compute the bounds of the backreach set under adversarial behavior we have

$$d_1(t, x) := \max_{u \in P} \min_{v \in Q} f(t, x, u, v) \quad (5.2)$$

$$d_2(t, x) := \min_{u \in P} \max_{v \in Q} f(t, x, u, v) \quad (5.3)$$

To efficiently compute the distance value bounds it is necessary to use numerical integration. Using Euler's method of numerical integration backwards in time it is possible to define:

$$x[k-1] = x[k] - \frac{x[k] - x[k-1]}{\delta t} \delta t \quad (5.4)$$

Equation (5.4) allows us to compute the state of the system backwards in time.

The necessary linearized equations of motion are

$$x[k-1] = x[k] - (U \cos \psi[k] + u_{cx})t_{\text{step}} \quad (5.5)$$

$$y[k-1] = y[k] - (U \sin \psi[k] + v_{cy})t_{\text{step}} \quad (5.6)$$

$$\psi[k-1] = \psi[k] - r[k]t_{\text{step}} \quad (5.7)$$

$$\left[ \frac{r[k] - r[k-1]}{t_{\text{step}}} \right] = \frac{N_r + N_{rr\text{abs}}(r) + N_{ur}U}{I_z - N_r} r + \frac{N_{uu}\delta_r U^2}{I_z - N_r} \delta_r \quad (5.8)$$

$$r[k-1] = r[k] - \left[ \frac{r[k] - r[k-1]}{t_{\text{step}}} \right] t_{\text{step}} \quad (5.9)$$

Then, several iterations are required to find the necessary control inputs that maximize and minimize the backreach set ( $d_1$  and  $d_2$ , respectively) which are the bounds of the de-

sired reach set. Finally, the vehicle state information is therefore contained in the vectors  $x$ ,  $y$ ,  $\psi$  and  $r$ , as also the necessary optimal control inputs that lead the state of the vehicle along the bounds of the reach set to the goal.

Figure 5.2 present the distance between the vehicles and the bounds of the backward reach set under adversarial behavior, when no external disturbances are considered. The time used in the computation is  $t = -5$  (s). The distance between both vehicles is defined as

$$d[k] = \sqrt{x[k]^2 + y[k]^2 + k\psi[k]^2} \quad (5.10)$$

where the constant  $k$  ranges between  $[0.1, 0.5]$  to guarantee results with practical meaning.

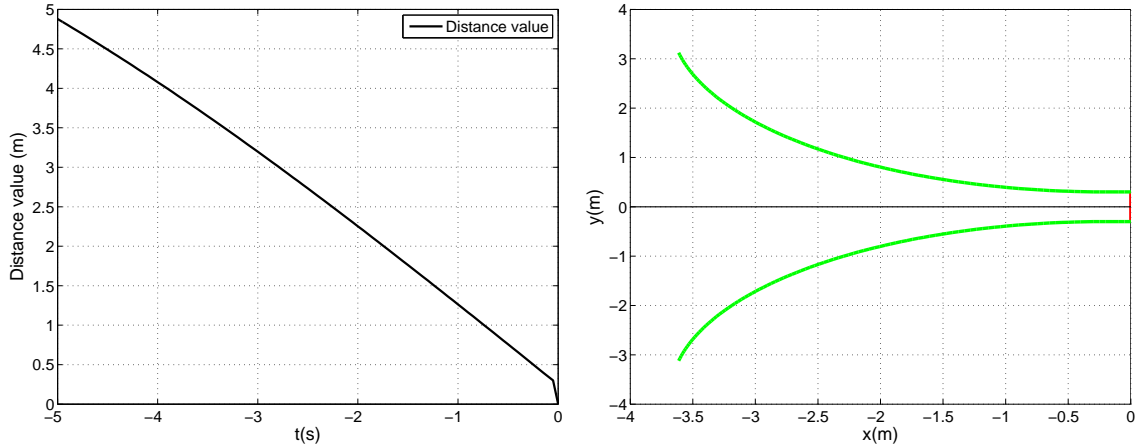


Figure 5.2: Distance between the vehicles and backward reach set under adversarial behavior without disturbances

Figure 5.3 also present the distance between the vehicles and the backward reach set, but considering a constant lateral (along the  $y$ -axis) ocean current with  $v_c = 0.4$  (m/s). Once again, the time is  $t = -5$  (s). It is possible to observe that the "cone" shaped set turned in order to compensate the effects of the ocean currents. This is a useful indication for the motion planning (section 5.5).

#### 5.4.3 Switch controllers at the boundary of the reach set

An important question arises when the LAUV is performing the maneuver inside the backward reach set. What happens if the trajectory performed by the vehicle reaches the boundary of the reach set ? This question should not be overlooked, since we know that while inside the backward reach set, there exists a feasible sequence of control inputs that lead the state of the vehicle to the goal set. If the state is outside the backward reach set, then there are no guarantees that a feasible sequence of controls exists.

A possible solution to solve the problem of the vehicle reaching the bounds of the reach set is

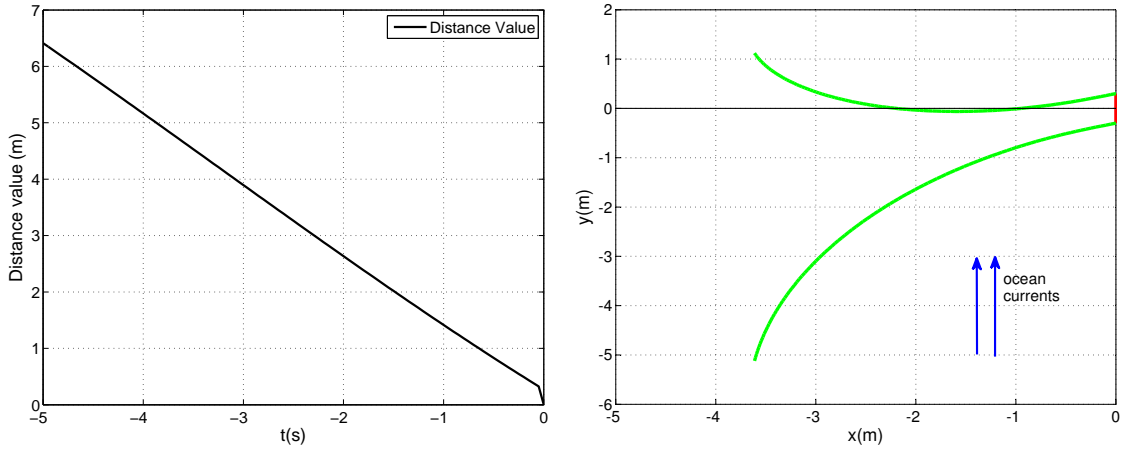


Figure 5.3: Distance between the vehicles and backward reach set under adversarial behavior with lateral ocean current  $v_c = 0.4 \text{ m/s}$

- **Switch to optimal controller** – During the computation of the backward reach set, the control inputs that drive the vehicle from the bounds of the reach set to the goal set were calculated. These control inputs are optimal in the sense that they maximize (or minimize) the bounds of the reach set. Thus, it is possible to **switch** the controller, once the vehicle reaches the bounds of the backreach set.

This solution guarantees convergence (if the bounds of the external disturbances are known). Figure 5.4 presents a possible state during the docking sequence when the vehicle enters the reach set. Notice that while the vehicle is inside the set, the controller used is the controller defined in the *maneuver layer*. In figure 5.4, and without loss of generality, it is assumed a sliding mode controller. However, once the vehicle reaches the upper bound of the set, it is not guaranteed convergence if the vehicle leaves the set, hence, a switch of controllers happens. While the state of the vehicle is on the bound, an optimal control strategy is applied to the vehicle while it remains on the bound. The optimal controller simply uses the control inputs previously defined during the backreach set computation, which are known to drive the state of the system along the boundary to the goal. If the vehicle reaches a position inside the set, another switch can take place to the sliding mode controller.

## 5.5 Motion planning

This section presents the motion planning for the docking operation. The motion plan is a set of **waypoints** that the LAUV has to reach in order to successfully dock inside the ROV. Notice that this motion plan only computes the necessary waypoints to ensure a safe docking. Then, the supervisory layer is responsible to define the maneuvers to guarantee that the AUV performs the desired motion.

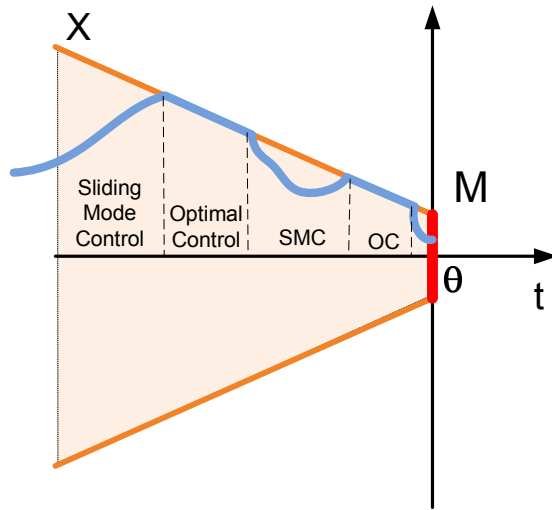


Figure 5.4: Switch between controllers using backward reachability

This block receives the following inputs

- Initial set of waypoints (indispensable).
- Backreach set under adversarial behavior (section 5.4).

The initial set of waypoint parameters define a possible motion for the LAUV, if one neglects the presence of the external disturbances, *i.e.*, the backward reach set under adversarial behavior. Figure 5.5 illustrates a possible motion plan using the initial set of waypoints.

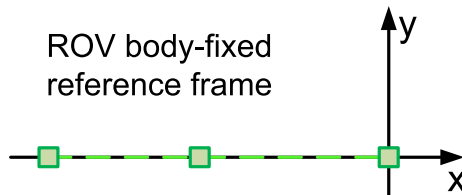


Figure 5.5: Motion plan with the initial set of waypoints

The backward reach set of the system (right hand side of the figures 5.2 and 5.3), allows to improve the motion planning of the LAUV since it combines the set of initial and the backreach set information. Figure 5.6 presents two possible solutions to define a path using the reach set information.

The blue colored line in figure 5.6 presents a possible path using the cone heading. Another solution is to use all the information contained in the reach set cone to derive a smoother path (magenta line). The final motion uses the first solution (information regarding the cone heading) combined with the initial set of waypoints to derive the final

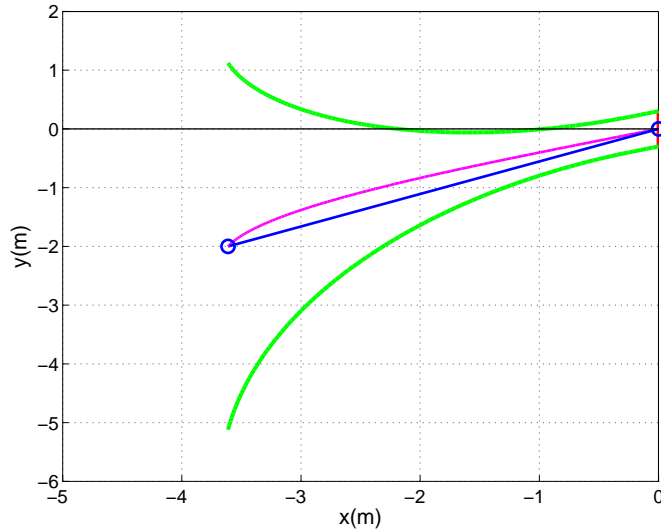


Figure 5.6: Motion planning with reach set information

motion for the LAUV. An example is presented in figure 5.7. The motion plan is then sent to the supervisory layer to define the proper set of maneuvers that satisfy the motion plan requirements.

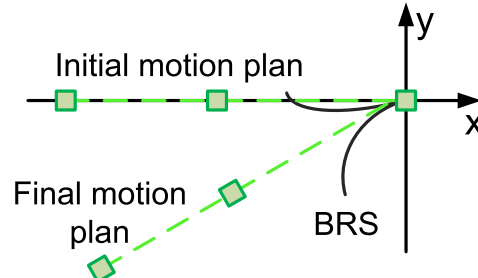


Figure 5.7: Final motion plan using backreach set under adversarial behavior information

The low-level controllers usually present an offset while tracking a state reference that is dependent to the presence of external disturbances. This information can be studied and introduced in the initial waypoints parameters plan, to allow for the motion planning block to compensate the estimated offset effects in the docking operation.

For instance, the waypoints can be defined along the  $y$ -axis as follows

$$y_{wp} = -kv_{cy} \quad (5.11)$$

where  $k$  is a positive constant that can be tuned to overcome the offset, and  $v_{cy}$  is a transversal external disturbance to the vehicle.

The following sections present the controllers of the basic maneuvers defined in section 5.2.

## 5.6 Maneuver 1: Line of Sight guidance

This is the controller implemented to perform the following maneuver

- **Maneuver 1** – Reaching a region in bounded time, while moving inside some prescribed area.

The Line-Of-Sight guidance controller (LoS) uses the vehicle state and the next waypoint coordinates (from the motion plan) and returns a heading reference necessary to reach the waypoint. Hence, this is a controller used in the horizontal plane of motion. The heading reference,  $\psi(t)_{\text{ref(LoS)}}$  can be determined from

$$\psi(t)_{\text{ref(LoS)}} = \text{atan2}(\tilde{Y}(t)_{\text{wpt(i)}}, \tilde{X}(t)_{\text{wpt(i)}}) \quad (5.12)$$

where  $\tilde{Y}(t)_{\text{wpt(i)}}$  and  $\tilde{X}(t)_{\text{wpt(i)}}$  are the difference between the current vehicle position and the next waypoint, thus

$$\tilde{X}(t)_{\text{wpt(i)}} = X_{\text{wpt(i)}} - x(t) \quad (5.13)$$

$$\tilde{Y}(t)_{\text{wpt(i)}} = Y_{\text{wpt(i)}} - y(t) \quad (5.14)$$

The Line-of-Sight heading error,  $\tilde{\psi}(t)_{\text{LoS}}$  can be computed from

$$\tilde{\psi}(t)_{\text{LoS}} = \psi(t)_{\text{ref(LoS)}} - \psi(t) \quad (5.15)$$

When performing waypoint navigation, two conditions may be true for the way point index to be incremented. The first and most usual case is if the vehicle has reached the way point watch radius  $R_{w(i)}$ . Secondly, if a large amount of cross track error is present, the next way point will become active if the projected distance to the way point, along the  $i$ -axis,  $S(t)_i$  reaches some minimum value  $S_{\min(i)}$ , such that

**if**  $(D \leq R_{w(i)} \text{ } \parallel S(t)_i \leq S_{\min(i)})$  **then** Activate next Way Point

where  $D$  is the distance between the vehicle and the way point,  $D = \sqrt{(\tilde{X}(t)_{\text{wpt(i)}})^2 + (\tilde{Y}(t)_{\text{wpt(i)}})^2}$ .

## 5.7 Maneuver 2: Follow Track

To perform the Follow Track maneuver, the *cross-track error controller* is introduced.

- **Maneuver 2** – Follow a line between two prescribed points with some additional constraints.

To follow a track prescribed between two points, a sliding mode controller is considered. This implementation uses a combination of Line-Of-Sight guidance and cross track

error control. One of the shortcomings of the LoS controller defined in section 5.6, is that it has no ability to track a straight line path between two way points. With the following controller, the goal is to command the vehicle to track a line between two way points with both a minimum error from the track and heading error between the vehicle and the track. Figure 5.8 introduces the definitions involved with this technique.

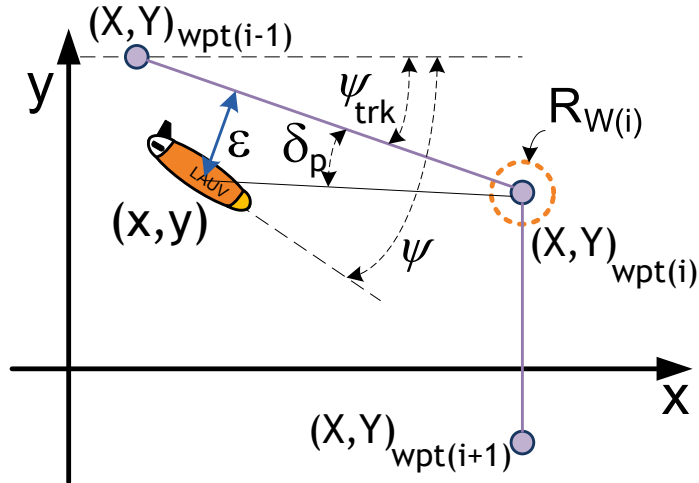


Figure 5.8: Cross Track Error definitions

The variable of interest to minimize is the cross track error,  $\varepsilon(t)$ , and is defined as the perpendicular distance between the center of the vehicle (located at  $(x(t), y(t))$ ) and the adjacent track line defined between the previous way point  $(X, Y)_{wpt(i-1)}$  and the current way point  $(X, Y)_{wpt(i)}$ . The track angle,  $\psi_{trk(i)}$ , is defined by

$$\psi_{trk(i)} = \text{atan}2(Y_{wpt(i)} - Y_{wpt(i-1)}, X_{wpt(i)} - X_{wpt(i-1)}) \quad (5.16)$$

The cross track heading error,  $\tilde{\psi}_{CTE(i)}(t)$  for the  $i^{th}$  segment is defined as

$$\tilde{\psi}_{CTE(i)}(t) = \psi(t) - \psi_{trk(i)} + \beta(t) \quad (5.17)$$

where  $\beta(t)$  is the angle of side slip and is defined here as  $\tan(\beta(t)) = v(t)/U$ . The cross track heading error,  $\tilde{\psi}_{CTE(i)}(t)$ , must be normalized between  $\pm 180^\circ$ .

The difference between the current vehicle position and the next way point, as seen for the LoS controller, is

$$\tilde{X}(t)_{wpt(i)} = X_{wpt(i)} - x(t) \quad (5.18)$$

$$\tilde{Y}(t)_{wpt(i)} = Y_{wpt(i)} - y(t) \quad (5.19)$$

The cross track error,  $\varepsilon(t)$ , may now be defined with

$$\varepsilon(t) = d(t) \sin \delta_p(t) \quad (5.20)$$

where  $d(t)$  is the euclidian distance between the vehicle and the current way point, i.e.,  $d(t) = \sqrt{(\tilde{X}(t)_{\text{wpt(i)}})^2 + (\tilde{Y}(t)_{\text{wpt(i)}})^2}$ .  $\delta_p(t)$  is the angle between the line of sight to the next way point and the current track line given by

$$\delta_p(t) = -\psi_{\text{trk}(i)} + \text{atan2}(\tilde{Y}(t)_{\text{wpt(i)}}, \tilde{X}(t)_{\text{wpt(i)}}) \quad (5.21)$$

and must be normalized to stay within  $\pm 180^\circ$ .

With the cross track error defined, the sliding surface can be cast in terms of the derivatives of the errors such that

$$\begin{aligned} \varepsilon(t) &= \varepsilon(t) \\ \varepsilon'(t) &= U \sin(\tilde{\psi}_{\text{CTE}(i)}(t)) \\ \varepsilon''(t) &= U(-r(t) + \dot{\beta}(t)) \cos(\tilde{\psi}_{\text{CTE}(i)}(t)) \\ \varepsilon'''(t) &= U(-\dot{r}(t) + \ddot{\beta}(t)) \cos(\tilde{\psi}_{\text{CTE}(i)}(t)) - U(-r(t) + \dot{\beta})^2 \sin(\tilde{\psi}_{\text{CTE}(i)}(t)) \end{aligned}$$

An approximation can be made if one assumes that the time rate of change of side slip,  $\dot{\beta}$ , is small compared to the turn rate,  $r(t)$ . Therefore  $\dot{\beta}$  will be neglected.

The sliding surface for the cross track error controller is selected to be a second order polynomial of the form

$$\sigma(t) = \varepsilon''(t) + \lambda_1 \varepsilon'(t) + \lambda_2 \varepsilon(t) \quad (5.22)$$

Thus, the condition for stability of the sliding mode controller is

$$\dot{\sigma}(t) = \varepsilon'''(t) + \lambda_1 \varepsilon''(t) + \lambda_2 \varepsilon'(t) = -\eta \tanh(\sigma/\phi) \quad (5.23)$$

If we extract the linearized heading equation from equation (5.38) in section 5.9.2, we obtain

$$\dot{r}(t) = a_1 r(t) + a_2 v(t) + b \delta_r(t) \quad (5.24)$$

where

$$a_1 = \frac{N_r}{I_{zz} - N_r} \quad (5.25)$$

$$a_2 = \frac{N_v}{I_{zz} - N_r} \quad (5.26)$$

$$b = \frac{N_{uu} \delta_r * U^2}{I_{zz} - N_r d} \quad (5.27)$$

The rudder input can be expressed as

$$\begin{aligned}\delta_r(t) = & \left[ \frac{-1}{Ub \cos(\tilde{\psi}_{CTE(i)}(t))} \right] \left[ U(a_1 r + a_2 v) \cos(\tilde{\psi}_{CTE(i)}(t)) + Ur^2(t) \sin(\tilde{\psi}_{CTE(i)}(t)) \right. \\ & \left. + \lambda_1 Ur(t) \cos(\tilde{\psi}_{CTE(i)}(t)) - \lambda_2 U \sin(\tilde{\psi}_{CTE(i)}(t)) - \eta \tanh(\sigma/\phi) \right]\end{aligned}\quad (5.28)$$

where  $\lambda_1$ ,  $\lambda_2$ ,  $\eta$  and  $\phi$  are parameters that can be tuned to achieve a better tracking.

The sliding surface,  $\sigma$  is

$$\sigma(t) = -Ur(t) \cos(\tilde{\psi}_{CTE(i)}(t)) + \lambda_1 U \sin(\tilde{\psi}_{CTE(i)}(t)) + \lambda_2 \varepsilon(t)\quad (5.29)$$

To avoid division by zero, in the rare case where  $\cos(\tilde{\psi}_{CTE(i)}(t)) = 0.0$ , i.e., the vehicle heading is perpendicular to the track line, the rudder command is set to zero since the condition is transient in nature.

## 5.8 Maneuver 3: Roundabout

- **Maneuver 3: Roundabout** – Perform a circle around the ROV to avoid collisions and to reach a position behind him.

This maneuver is used to avoid collisions between both vehicles. Collision avoidance techniques are studied mainly in Air Traffic Management systems (ATM) (Tomlin *et. al.* [88]), Automated Highway Systems (AHS) (Carbaugh *et. al.* [89]) and in robotic manipulators (Schiavi *et. al.* [92]). The techniques can be either in the global sense using path planning (Eichhorn [93]) or local solutions using reactive techniques and policies to avoid obstacles (Pallottino *et. al.* [94] Yang *et. al.* [95]).

The roundabout maneuver presented follows closely the work of Eichhorn ([96] and [97]) by using a reactive obstacle avoidance system for the LAUV.

### 5.8.1 Collision avoidance system using gradient lines by geometrical construction

A Collision Avoidance System (CAS), is required in the case when the vehicle has to roundabout the ROV to be able to dock. Figure 5.9 illustrates a possible collision avoidance maneuver during the docking sequence.

Remember that one of the assumptions is that the state of the ROV is known by the LAUV, as also the measurements of the external disturbances considered (ocean currents). Therefore, the following is not about sensing techniques to detect the presence of obstacles, but about defining a maneuver that avoids collisions with the ROV.

The roundabout maneuver can be defined by means of gradient lines. These gradient lines point to the goal from any position of the area of operation, being able to lead

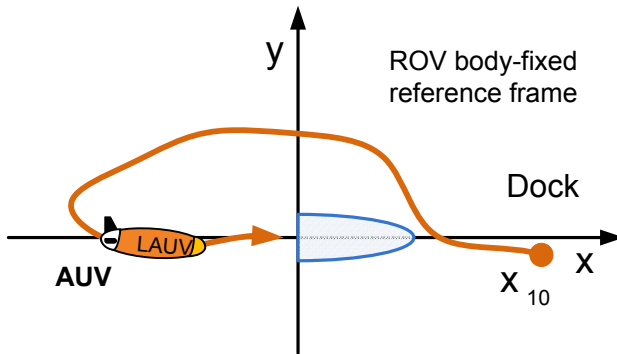


Figure 5.9: Roundabout maneuver to avoid collision

the vehicle past the obstacles to the goal from its current position. Hence, the collision avoidance technique must be treated using two separate phases. If there is the risk of collision, the ROV is treated as an obstacle, and the LAUV has to roundabout the ROV and reach a position behind him. If there is no risk of collision between both vehicles, then other maneuvers can be used to guide the LAUV. There are two methods to produce the gradient lines.

- *Production of gradient lines by harmonious dipole potentials* – If one takes the circle as a positive point charge and the goal as a negative point charge, then this structure forms a dipole and its lines of flux lead from the positive to the negative charge. The value for the negative charge in the goal is selected to  $-1$ .
- *Production of gradient lines by geometrical construction* – This technique produces the necessary gradient lines by means of dividing the state space into individual sectors. The division into sectors depends on the LAUV current position  $\mathbf{x}_{\text{auv}}$ , the ROV position  $\mathbf{x}_{\text{rov}}$  and the goal position (which is the first waypoint defined in the motion planning).

The division of the state space into different sectors can be seen in figure 5.10.

If the condition  $\mathbf{x}_{\text{auv}} < R$  is fulfilled, the vehicle is located inside the safety circle (the state of the AUV is expressed in the ROV body-fixed reference frame). The gradient can then be expressed by the following equation:

$$G = \frac{\mathbf{x}_{\text{auv}}}{|\mathbf{x}_{\text{auv}}|} \quad (5.30)$$

The radius  $R$  is  $n$  times the size of the ROV to guarantee safety. Although the purpose during the early stages of the docking sequence is (if the vehicle is not ready to dock) to keep the AUV away from the ROV, the presence of strong disturbances can lead the vehicle to penetrate the safety zone. In such a case the vehicle must be lead away from the circle, which requires a description of a gradient inside the circle.

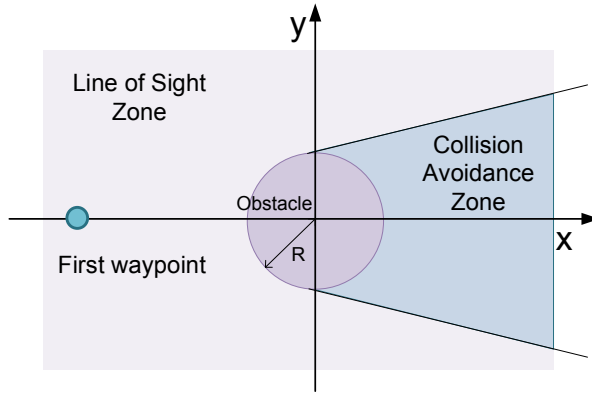


Figure 5.10: Division of the state space into sectors

The **collision avoidance zone** is active if the goal is not in the direct line of sight of the LAUV (*i.e.*, the obstacle stands between the goal and the LAUV). Hence, the direction vector of the tangent from  $\mathbf{x}_{\text{auv}}$  to the circle must be determined in dependence of the orientation of  $\mathbf{x}_{\text{auv}}$  to the symmetry axis. The gradient is thereby the unit direction vector  $x_{\text{tangent}}$ :

$$G = \frac{x_{\text{tangent}}}{|x_{\text{tangent}}|} \quad (5.31)$$

This leads the vehicle to perform the **roundabout maneuver** in order to avoid the safety zone.

If there is a direct connection between vehicle and goal, then the other basic maneuvers are used (line of sight guidance and cross track error maneuver).

To achieve a smoother transition between gradient lines it is possible to define a weighting factor  $\alpha$

$$G = \alpha G_i + (1 - \alpha) G_j \quad (5.32)$$

where  $G_i$  and  $G_j$  are the gradient lines from different sectors.

Finally, to compute the bounds of the collision avoidance zone we have

$$y_{\max} = \frac{R - y_{\text{wp}}}{-x_{\text{wp}}} (x_{\text{auv}} - x_{\text{wp}}) + y_{\text{wp}} \quad (5.33)$$

$$y_{\min} = \frac{R + y_{\text{wp}}}{x_{\text{wp}}} (x_{\text{auv}} - x_{\text{wp}}) + y_{\text{wp}} \quad (5.34)$$

$x_{\text{auv}}$  is the coordinate of the AUV in the  $x$ -axis of the ROV body frame,  $x_{\text{wp}}$  and  $y_{\text{wp}}$  are the coordinates of the goal, and  $R$  is the radius of the safety zone.

## 5.9 LAUV decoupled control systems

In this section, the focus will be the vehicle's equations of motion applied to the modeling and analysis of small motions<sup>2</sup> where the vehicle is in forward motion at a nominal speed. The action of rudders, stern or bow planes cause small motions that occur in the perpendicular directions, with respect to the longitudinal axis, which cause small angles of side slip and angles of attack<sup>3</sup>.

The LAUV is typically operated at a constant forward speed. Small variations around the nominal speed are also feasible. It is usual to assume that the vehicle is moving with a constant forward speed,  $U_0$  that is often larger than the surrounding water currents. Furthermore, when the vehicle is in steady motion conditions, there is a balance between the hydrodynamic forces from drag, the propulsion forces, the weight and buoyancy forces. Thus, in constant forward speed, some approximations can be made, if only small changes of motion to the vehicle are considered.

$$\begin{aligned}\Delta X_f &= f(u, \dot{u}, t) \\ \Delta Y_f &= f(v, \dot{v}, r, \dot{r}, p, \dot{p}, t) \\ \Delta Z_f &= f(u, \dot{u}, w, \dot{w}, q, \dot{q}, t) \\ \Delta K_f &= f(p, \dot{p}, v, \dot{v}, r, \dot{r}, t) \\ \Delta M_f &= f(u, \dot{u}, w, \dot{w}, q, \dot{q}, t) \\ \Delta N_f &= f(p, \dot{p}, v, \dot{v}, r, \dot{r}, t)\end{aligned}\quad (5.35)$$

According to the approximations made in 5.35, it is possible to assume:

1. The only variables that affect the force along the longitudinal axis,  $X_f$ , result from surge,  $u$ , and its time derivative,  $\dot{u}$ .
2. The variables affecting the force and the moment about the transversal axis, respectively  $Y_f$  and  $N_f$  are sway  $v$ ,  $\dot{v}$  and turn ratio  $r$ ,  $\dot{r}$ .
3. The variables affecting the force and the moment about the vertical axis, respectively  $Z_f$  and  $M_f$  are heave  $w$ ,  $\dot{w}$  and turn ratio  $q$ ,  $\dot{q}$ .
4. Roll  $p$  and  $\dot{p}$  are neglected since roll stabilization is usually performed in a passive fashion, by lowering the center of gravity relatively to the center of buoyancy, in order to create a restoring moment.

---

<sup>2</sup>All the changes to the motion of the vehicle are assumed to be "small" compared to the nominal speed.

<sup>3</sup>By convention, angle of side slip and angle of attack refers, respectively, to the angles formed by the horizontal sway velocity,  $v$ , and the vertical heave velocity,  $w$ , both divided by the forward speed of the body,  $u$ .

Therefore the 6-DOF equations of motion can be divided into three non-interacting subsystems for speed control, steering and diving (as suggested by Healey and Marco [98]). Each subsystem consists of the following state variables:

1. **Speed system state:**  $u(t)$
2. **Steering system states:**  $v(t)$ ,  $r(t)$  and  $\psi(t)$
3. **Diving system states:**  $w(t)$ ,  $q(t)$ ,  $\theta(t)$  and  $z(t)$

The typical AUV configuration suggests that the three subsystems can be controlled by a single propeller (speed system control), a pair of rudder planes with deflection  $\delta_R(t)$  (steering system) and a pair of stern planes with deflection  $\delta_S(t)$  (diving system). This is the configuration of the LAUV.

This simplification for three single-input single-output (SISO) subsystem facilitate the design of the control architecture of the vehicle. The following sections introduce the subsystems equations.

### 5.9.1 Forward speed control

Neglecting the interactions from sway, heave, roll, pitch and yaw, the speed equation can be written as:

$$(m - X_{\dot{u}})\dot{u} = (X_u + X_{|u|u}|u|)u + X_{prop} \quad (5.36)$$

Equation (5.36) is derived from the state matrices introduced in section 4.3.1. Most authors assume the quadratic damping  $X_{|u|u}|u|$  as the only dissipative effect, because it is dominant. However, there is also the linear damping  $X_u$  that has a dissipative effect.  $X_{prop}$  is the propeller force.

### 5.9.2 Steering system control

For the steering system control, the motions that take place in the vertical plane are neglected. This assumption allows us to consider:

$$[w, p, q, Z, \phi, \theta] = 0$$

so that the only motions of interest involve the variables  $[u, v, r]$ . For simplicity,  $u$  is assumed to be constant - the forward speed ( $U_0$ ). Furthermore, the quadratic damping terms can be neglected.

Considering the hydrodynamic forces derived in section 4.3.1, then we have:

$$\begin{aligned} m\dot{v} &= -mU_0r + Y_{\dot{v}}\dot{v} + Y_vv + Y_r\dot{r} + Y_r r + Y_\delta \delta_R \\ I_z\dot{r} &= N_{\dot{v}}\dot{v} + N_vv + N_r\dot{r} + N_r r + N_\delta \delta_R \\ \dot{\psi} &= r \\ \dot{x} &= U_0 \cos \psi - v \sin \psi + U_{cx} \\ \dot{y} &= U_0 \sin \psi + v \cos \psi + U_{cy} \end{aligned} \quad (5.37)$$

where  $U_{cx}$  and  $U_{cy}$  are the ocean currents in the x- and y-axis, respectively.

Now, it is possible to express the equations in the matrix form:

$$\begin{bmatrix} m - Y_{\dot{v}} & -Y_r & 0 \\ -N_{\dot{v}} & I_z - N_r & 0 \\ 0 & 0 & 1 \end{bmatrix} \begin{bmatrix} \dot{v} \\ \dot{r} \\ \dot{\psi} \end{bmatrix} = \begin{bmatrix} Y_v & Y_r - mU_0 & 0 \\ N_r & N_r & 0 \\ 0 & 1 & 0 \end{bmatrix} \begin{bmatrix} v \\ r \\ \psi \end{bmatrix} + \begin{bmatrix} Y_\delta \\ N_\delta \\ 0 \end{bmatrix} \delta_R \quad (5.38)$$

Where  $Y_\delta = Y_{uu}\delta_r u_0 u_0$ ,  $N_\delta = N_{uu}\delta_r u_0 u_0$  and  $\delta_R$  is the rudder input control. The equation (5.38) is slightly different from what is usually presented in the literature (Fossen [1] or Healey [6]), but that is due to the assumptions made in section 4.3.1.

The above now reduces to the familiar LTI (Linear time-invariant) form

$$\dot{x}(t) = Ax(t) + Bu(t)$$

where

$$\begin{aligned} A &= \begin{bmatrix} m - Y_{\dot{v}} & -Y_r & 0 \\ -N_{\dot{v}} & I_z - N_r & 0 \\ 0 & 0 & 1 \end{bmatrix}^{-1} \begin{bmatrix} Y_v & Y_r - mU_0 & 0 \\ N_r & N_r & 0 \\ 0 & 1 & 0 \end{bmatrix}; \\ B &= \begin{bmatrix} m - Y_{\dot{v}} & -Y_r & 0 \\ -N_{\dot{v}} & I_z - N_r & 0 \\ 0 & 0 & 1 \end{bmatrix}^{-1} \begin{bmatrix} Y_\delta \\ N_\delta \\ 0 \end{bmatrix}; \end{aligned}$$

with  $x(t) = [v, r, \psi]^T$  and  $u(t) = \delta_R$ .

### 5.9.3 Diving system control

For the Diving system control we ignore the motions that take place in the horizontal plane. This assumption allows us to consider:

$$[v, r, p, \phi, \psi, x, y] = 0$$

so that the only variables of interest involve  $[w, q, \theta, z]$ . Once again,  $u$  is assumed to be constant - the forward speed ( $U_0$ ), and the quadratic damping terms are neglected. It is primarily considered effects of vehicle inertia, hydrostatic, weight terms and hydrodynamic forces resultant from lift and added mass.

Considering the state matrices derived in section 4.3.1, then we have:

$$\begin{aligned} u &= U_0 \\ m\dot{w} &= -mU_0q + (W - B)\cos\theta + Z_{\dot{w}}\dot{w} + Z_w w + Z_{\dot{q}}\dot{q} + Z_q q + Z_\delta \delta_s \\ I_y\dot{q} &= z_G W \sin\theta + M_{\dot{q}}\dot{q} + M_q q + M_{\dot{w}}\dot{w} + M_w w + M_\delta \delta_s \\ \dot{\theta} &= q \\ \dot{z} &= w \cos\theta - U_0 \sin\theta \end{aligned} \quad (5.39)$$

The above equations retain the nonlinear trigonometric terms, as a result of the vector of restoring terms  $g(\eta_2)$  presented in equation (4.11). Nonetheless, a further assumption can be made that the pitch angles are small, and that the vehicle undergoes small motions in the vertical plane. Equation (5.40) present the linearized diving system model.

$$\begin{aligned} (m - Z_{\dot{w}})\dot{w} - Z_{\dot{q}}\dot{q} &= -mU_0q + Z_w w + Z_q q + Z_\delta \delta_s \\ (I_y - M_{\dot{q}})\dot{q} - M_{\dot{w}}\dot{w} &= (z_B B - z_G W)\theta + M_q q + M_w w + M_\delta \delta_s \\ \dot{\theta} &= q \\ \dot{z} &= w - U_0 \theta \end{aligned} \quad (5.40)$$

Therefore, the system can be expressed:

$$\begin{bmatrix} m - Z_{\dot{w}} & -Z_{\dot{q}} & 0 & 0 \\ -M_{\dot{w}} & I_y - M_{\dot{q}} & 0 & 0 \\ 0 & 0 & 1 & 0 \\ 0 & 0 & 0 & 1 \end{bmatrix} \begin{bmatrix} \dot{w} \\ \dot{q} \\ \dot{\theta} \\ \dot{z} \end{bmatrix} = \begin{bmatrix} Z_w & Z_q - mU_0 & 0 & 0 \\ M_w & M_q & z_G W & 0 \\ 0 & 1 & 0 & 0 \\ 1 & 0 & -U_0 & 0 \end{bmatrix} \begin{bmatrix} w \\ q \\ \theta \\ z \end{bmatrix} + \begin{bmatrix} Z_\delta \\ M_\delta \\ 0 \\ 0 \end{bmatrix} \delta_s \quad (5.41)$$

Where  $Z_\delta = Z_{uu}\delta_r u_0 u_0$ ,  $M_\delta = M_{uu}\delta_r u_0 u_0$  and  $\delta_s$  is the stern input control. Once again, the assumptions made in section 4.3.1, make the equation (5.41) slightly different than what is usually presented in the literature.

Reducing, as the simplified steering model, to the LTI form

$$\dot{x}(t) = Ax(t) + Bu(t)$$

where

$$A = \begin{bmatrix} m - Z_{\dot{w}} & -Z_{\dot{q}} & 0 & 0 \\ -M_{\dot{w}} & I_y - M_{\dot{q}} & 0 & 0 \\ 0 & 0 & 1 & 0 \\ 0 & 0 & 0 & 1 \end{bmatrix}^{-1} \begin{bmatrix} Z_w & Z_q - mU_0 & 0 & 0 \\ M_w & M_q & z_G W & 0 \\ 0 & 1 & 0 & 0 \\ 1 & 0 & -U_0 & 0 \end{bmatrix};$$

$$B = \begin{bmatrix} m - Z_{\dot{w}} & -Z_{\dot{q}} & 0 & 0 \\ -M_{\dot{w}} & I_y - M_{\dot{q}} & 0 & 0 \\ 0 & 0 & 1 & 0 \\ 0 & 0 & 0 & 1 \end{bmatrix}^{-1} \begin{bmatrix} Z_\delta \\ M_\delta \\ 0 \\ 0 \end{bmatrix};$$

with  $x(t) = [w, q, \theta, z]^T$  and  $u(t) = \delta_S$ .

## 5.10 Problem 1 – Docking without disturbances with the ROV fixed

This problem was introduced in section 4.6. For this problem the following assumptions hold:

- ROV is performing dynamic positioning (i.e., the ROV state is fixed in the inertial reference frame).
- No external disturbances are considered.

The *regulation layer* guarantees that the vehicles follow the state references. In a higher level of automation, the *maneuver layer* is responsible for the correct execution of the basic maneuvers. The *supervisory layer* is responsible for the correct execution of the docking mission.

Hence, the solution for this particular problem has to consider each one of the three levels of control. Notice that the other problems can be regarded as extensions of the current problem, thus, the solution will hold for the rest of the problems, except when stated otherwise.

Only the LAUV controller will be analyzed.

### 5.10.1 Hybrid systems approach for high level control

The following reasons prevents the immediate use of the ROV state as a state reference to the low-level controllers:

- **LAUV is an underactuated system** – Since the LAUV is an underactuated system, i.e., a system with a lower number of actuators than degrees of freedom, it is not locally controllable (in section 2.3.2.2).

- **dock structure orientation** – To enter the dock structure the LAUV has to approach from behind with the same orientation.

Hence, it is advised to first align the vehicle behind the dock structure, much like an airplane performing its glide path (Sprinkle et. al. [30]). The glide path is performed when the vehicle travels through the waypoints defined in the motion planning. In the absence of external disturbances, the whole docking operation can be performed using line of sight guidance (**Maneuver 1**).

The Line Of Sight guidance uses the LAUV decoupled control systems presented in section 5.9. Then, a multivariable sliding mode controller (section 2.5.1.2) is used to track the state references and to provide robustness in the presence of parametric uncertainties (keep in mind, that the decoupled control systems are linearized approximations of the vehicle nonlinear dynamics). The sliding mode controller gives the necessary references for the hardware of the vehicle (the thruster power allocation and the fins angles of deflection). Figure 5.11 presents the control block diagram. Figure 5.12 presents the

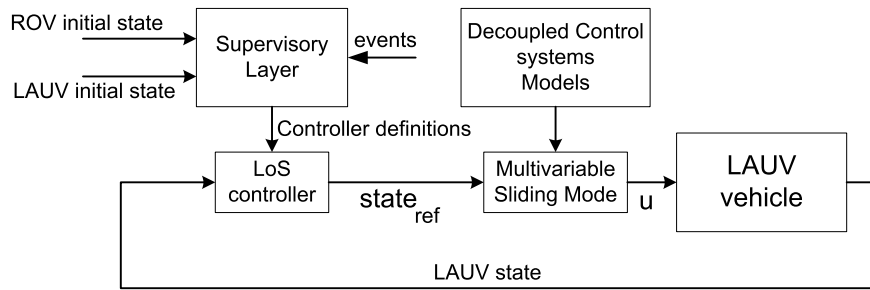


Figure 5.11: Problem 1 control block diagram

arrangement for the supervisory layer controller using hybrid automata.

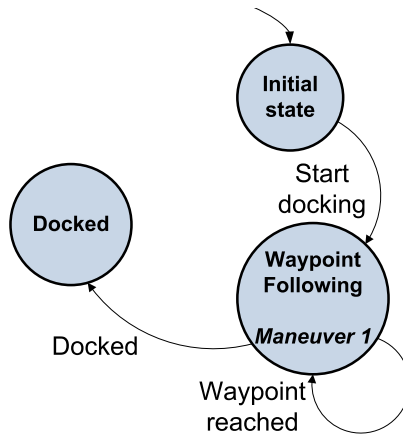


Figure 5.12: High level controller for Problem 1

### 5.10.2 Stability of the low level controllers

This section studies the stability of the provided solution. In the control scheme derived, the supervisory layer assume a passive presence, acting solely in the beginning of the docking sequence, when it derives the waypoints to perform the motion plan. The edges of the hybrid systems are automatically activated leading the discrete state of the system to the state responsible to interact with the maneuver layer. The maneuver layer for the problem 1 uses only line of sight guidance. The line of sight controllers derives the state feedback for the low level controllers to track.

The low level controllers use a multivariable sliding mode control (MSMC) (The stability of the solution is shown in section 2.5.1.2) technique combined with the decoupled linearized systems of the vehicle dynamics. The control law applied to both fins is

$$\delta_{r/s} = K\mathbf{x}_r + \frac{k\dot{x}_{\text{ref}}}{kB} - \frac{\eta}{kB} \tanh\left(\frac{k\tilde{\mathbf{x}}}{\phi}\right). \quad (5.42)$$

where matrices  $A$  and  $B$  can be found in section 5.9.2. The surge of the vehicle is considered at its nominal value  $u = 1.5$ .

For the rudder,  $K$  is the linear state feedback gain set to place the closed loop poles when in sliding condition at  $\lambda = [-15, -5, 0]$ ,  $K = [13.99, -1.41, 0]$ .  $k$  is the sliding surface  $k = [0.56, 0.10, 0.80]$ . The gain  $\eta = 0.5$ , and the boundary layer is  $\phi = 0.2$ . Therefore,

$$\begin{aligned} \delta_r = & -13.99v + 1.41r - 15.07\dot{v}_{\text{ref}} - 2.57\dot{r}_{\text{ref}} - 20.16\dot{\psi}_{\text{ref}} \\ & + 12.6 \tanh\left(\frac{0.60v + 0.10r + 0.80(\psi - \psi_{\text{ref}})}{0.2}\right) \end{aligned} \quad (5.43)$$

For the stern,  $K$  is the linear state feedback gain set to place the closed loop poles when in sliding condition at  $\lambda = [-2 + 1.2i, -2 - 1.2i, -2, 0]$ ,  $K = [-2.62, 0.23, -3.72, 0]$ .  $k$  is the sliding surface  $k = [0.90, -0.19, 0.19, 0.35]$ . The gain  $\eta = 0.5$ , and the boundary layer is  $\phi = 1.2$ . Therefore,

$$\begin{aligned} \delta_s = & 2.62w - 0.23q + 3.72\theta + 4.39\dot{w}_{\text{ref}} - 0.92\dot{q}_{\text{ref}} + 0.95\dot{\theta}_{\text{ref}} + 1.70\dot{z}_{\text{ref}} \\ & - 2.56 \tanh\left(\frac{0.90w - 0.19q + 0.19(\theta - \theta_{\text{ref}}) + 0.35(z - z_{\text{ref}})}{1.2}\right) \end{aligned} \quad (5.44)$$

## 5.11 Problem 2 – Docking without disturbances with the ROV in motion

This problem was formally introduced in section 4.7. The difference between the current problem and the previous one is that the ROV inertial state is no longer fixed. Hence, some questions arise when one looks at the solution to the previous problem.

- Is it possible to use the same control solution of Problem 1 ?
- If so, how to define the way points for the LAUV ?

The control architecture defined for the previous problem holds for this one. However there is the question of how to perform the motion plan, since the ROV position and orientation change along time.

A possible solution is to define the motion plan expressed in the ROV body-fixed reference frame. Likewise, the LAUV state has to be expressed in the ROV body frame also. The following section presents the necessary coordinate transformation.

### 5.11.1 Coordinate transformation

The main reference for the following transformation is Siciliano and Khatib [99].

Consider that  $\eta_{1_{\text{AUV}}} \in \mathbb{R}^3$  is the AUV inertial position (following the notation used in section 2.1.1). The goal is to derive the AUV state expressed in the ROV body-fixed reference frame,  $\eta_{1_{\text{AUV}}}^{\text{ROV}} \in \mathbb{R}^3$ . Hence,  $\eta_{1_{\text{AUV}}}$  can be expressed as

$$\eta_{1_{\text{AUV}}} = J_1(\eta_{2_{\text{ROV}}})\eta_{1_{\text{AUV}}}^{\text{ROV}} + \eta_{1_{\text{ROV}}} \quad (5.45)$$

where  $J_1(\eta_{2_{\text{ROV}}})$  is the transformation matrix of the ROV in the earth-fixed reference frame, and  $\eta_{1_{\text{ROV}}}$ , is the ROV inertial state. Thus,

$$\eta_{1_{\text{AUV}}}^{\text{ROV}} = J_1^{-1}(\eta_{2_{\text{ROV}}})(\eta_{1_{\text{AUV}}} - \eta_{1_{\text{ROV}}}) \quad (5.46)$$

For the AUV orientation expressed in the ROV body-fixed reference frame, it is possible to define

$$J_{1_{\text{ROV}}}(\eta_{2_{\text{AUV}}}) = J_1^{-1}(\eta_{2_{\text{ROV}}})J_1(\eta_{2_{\text{AUV}}}) \quad (5.47)$$

for simplicity, lets simply define  $J = J_{1_{\text{ROV}}}(\eta_{2_{\text{AUV}}})$ , where  $J$  is the transformation matrix of the AUV in the ROV body-fixed reference frame.

The orientation of the AUV expressed in the ROV body-fixed reference frame can be derived with

$$\begin{aligned} \theta &= \text{atan2}(-J_{31}, \sqrt{J_{11}^2 + J_{21}^2}) \\ \psi &= \text{atan2}\left(\frac{J_{21}}{\cos \theta}, \frac{J_{11}}{\cos \theta}\right) \\ \phi &= \text{atan2}\left(\frac{J_{32}}{\cos \theta}, \frac{J_{33}}{\cos \theta}\right) \end{aligned}$$

### 5.11.2 Solution

Given the state AUV expressed in the ROV body-fixed reference frame,  $\mathbf{x}_{\text{AUV}}^{\text{ROV}}$ , it is possible to perform the defined motion plan. Hence, the high level hybrid system defined for

the previous problem (figure 5.12) still holds for the present solution.

The block diagram of the control is presented in figure 5.13. Only two simple maneu-

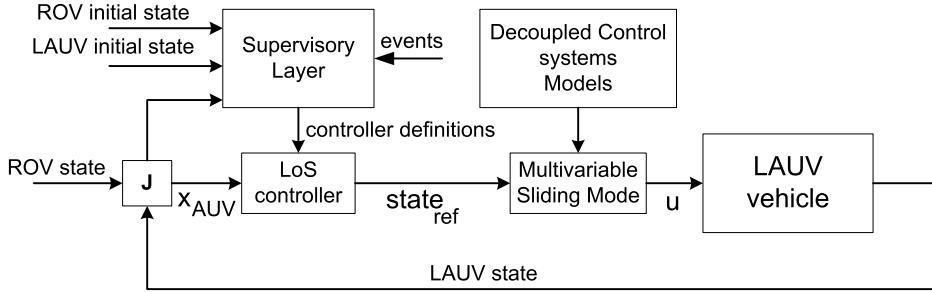


Figure 5.13: Problem 2 control block diagram

vers will be considered for the ROV vehicle. Move along the ROV body frame longitudinal axis with some constant forward speed,  $U_{\text{rov}}$ , or turn the vehicle a specific heading,  $\psi_{\text{rov}}$ , during the docking procedures.

The purpose is to verify the stability of the system when the ROV is fixed and when is in motion with constant speed. The results will be analyzed and presented in chapter 6.

Since the purpose of the ROV is to execute very simple maneuvers throughout the docking operation, there is no need to explain in great detail the controller implemented. The low level controller is a multivariable sliding mode controller (section 2.5.1.2) using the decoupled control systems (section 5.9). For simplicity, and without loss of generality, state references are given directly to the ROV controller.

## 5.12 Problem 3 – Docking with disturbances

This problem was formally introduced in section 4.8. For this problem, external disturbances are considered. The presence of external disturbances difficult the track of the desired states for the AUV.

The following sections will provide techniques to counteract the effect of the ocean currents, while still providing a motion plan that allows the LAUV to dock safely inside the dock structure. To avoid transversal external disturbances, a solution is to align the ROV with the ocean currents. Since the LAUV uses its state relative to the ROV body-fixed reference frame, no changes to the AUV control strategy are needed. The control of the ROV is easy, hence this problem complexity would by highly reduced if one considers only this solution. However, other solutions will be developed to solve this docking problem.

### 5.12.1 Follow Track maneuver

The presence of external disturbances introduce complications if the **Maneuver 1** (line of sight guidance) is used. Notice that this maneuver only points the vehicle to the goal. Therefore, if line of sight guidance is used to travel through waypoints, then it is not guaranteed that the state of the vehicle remains in the track connecting the waypoints. In the presence of external disturbances there is the risk that the state of the vehicle moves too far away from the track, even if it is headed to the next way point. Figure 5.14 illustrates this behavior. While the vehicle is correctly heading to the next waypoint, it is away from the track defined between both waypoints. The controller does not try to decrease this error ( $\varepsilon$ ) since the heading error,  $\tilde{\psi}(t)_{LoS}$  is the only variable of control (section 5.6).

This is a problem since the purpose is not only to drive the state of the vehicle to the docking position, but the orientation is a factor also. The heading of the LAUV must be aligned with the heading of the dock structure.

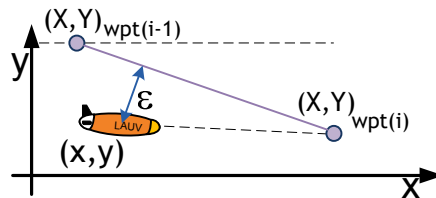


Figure 5.14: Possible error when using pure line of sight guidance

Hence, another solution must be used in addition with the line of sight controller. Section 5.7 presents the cross track error controller which is responsible to perform **Maneuver 2** (follow a line between two prescribed points with some additional constraints).

### 5.12.2 Control design using reachability results

This section summarizes the changes in the control design for this current problem. Figure 5.15 presents the high level hybrid systems controller implemented for this problem. The difference between this controller and the previous one is the addition of a new maneuver. To prevent the vehicle from moving away from the track connecting two way points near the latching moment with the ROV, the supervisory layer will switch the maneuver to the cross track error controller after reaching some position behind the ROV.

Finally, figure 5.16 presents the complete control block diagram for this problem.

### 5.12.3 Stability of the solution

Section 2.3.1.3 introduced the definition of the backward reachability problem. The computation of the reach set using differential games theory (section 2.3.2.4) is used to derive

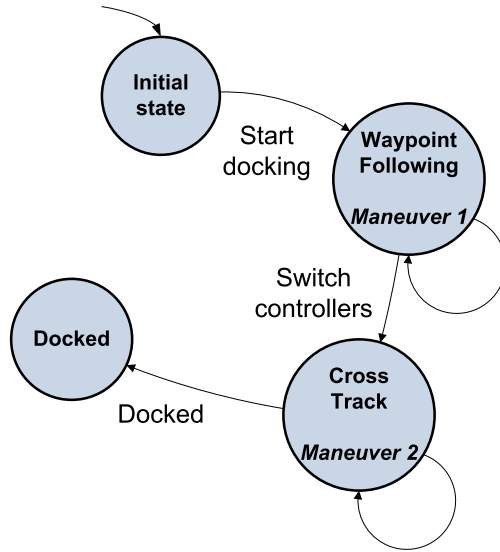


Figure 5.15: High level controller for Problem 3

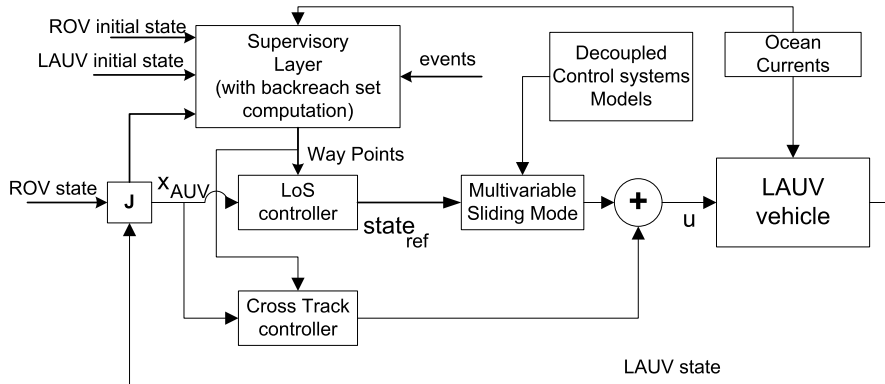


Figure 5.16: Problem 3 control block diagram

an inner approximation of the reach set for this particular problem. Hence, the following applies:

- if the vehicle is **inside** the set it is guaranteed that a feasible sequence of controls exists that drives the state of the system to the goal;
- once the vehicle is at the boundary of the set it is possible to use optimal control to drive the state of the vehicle along the boundary while still reaching the goal;
- if the vehicle reaches a position **outside** the set, then it is not guaranteed such a sequence of controls exists, and unless other information is available, it is safer to consider that the docking is not possible.

**Theorem 6 (Attainability).** The dock is attainable (section 2.3.1.4) if the vehicle is inside the backward reach set while performing the described motion plan that divides the “cone” in the longitudinal direction, and if the offset of the tracking of the low level controllers is such that

$$|\varepsilon(t)| < w_i(t) \quad i = 1, 2 \quad \forall t_0 < t < t_{dock} \quad (5.48)$$

where  $\varepsilon(t)$  is the error of the tracking, and  $w_i(t)$  are the boundaries of the set.

## 5.13 Problem 4 – Collision Avoidance in the early stages of the operation

This problem was formally introduced in section 4.9. The collision avoidance system was introduced in section 5.8.1. The collision avoidance maneuver is designated as **round-about maneuver**. The solution for this problem is to verify the zone of the initial state of the LAUV. Hence, the LAUV may be inside the safety zone, the collision avoidance zone or the line of sight zone. The gradient lines guide the vehicle to the goal, which is the beginning of the motion plan.

### 5.13.1 Initial state of the LAUV inside the Backreach Set

A special case to consider is when the vehicle initial state is inside the backward reach set. Depending of the time used to compute the backreach set under adversarial behavior, the position of the LAUV may be inside the set, but also, inside the safety zone. In such a case, it is more efficient to drive the LAUV directly to the dock structure. Hence, one of two cases may happen when the vehicle initial state is inside the safety zone.

- **Inside the Backreach Set** – To increase system efficiency, in the case where the vehicle’s initial state is inside the backward reach set, the hybrid state should drive the state to directly dock inside the ROV, without having to perform the complete motion plan.
- **Outside the Backreach Set** – If the LAUV initial state is outside the backward reach set, then it is not possible to guarantee a sequence of controls that will drive the vehicle directly to the docking position, without risk of collisions. Hence, it will be considered that the vehicle is in the safety zone position, and the gradient lines should be computed in order to move the vehicle away from the ROV to prevent mechanical malfunctions, in the case of collisions.

Figure 5.17 illustrates some possible trajectories of the vehicle when its initial state is inside the safety zone (circle of radius  $R$  around the ROV)

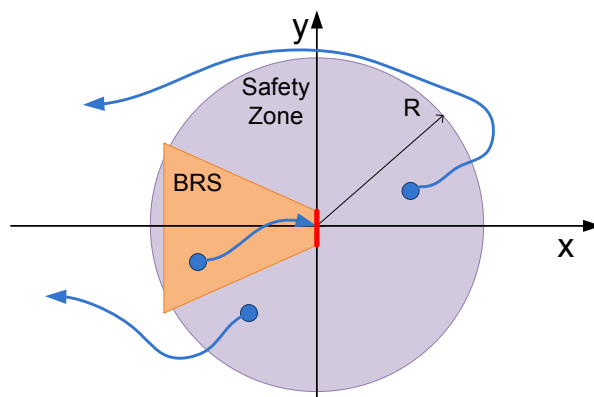


Figure 5.17: Possible trajectories when starting inside the safety zone

### 5.13.2 Complete Hybrid Systems

This section explains the new hybrid systems arrangement. Some new hybrid states were introduced to prevent possible collisions between both vehicles, and also a hybrid state was derived from the case when the LAUV is inside the backward reach set.

Figure 5.18 presents the high level hybrid systems controller implemented for this problem.

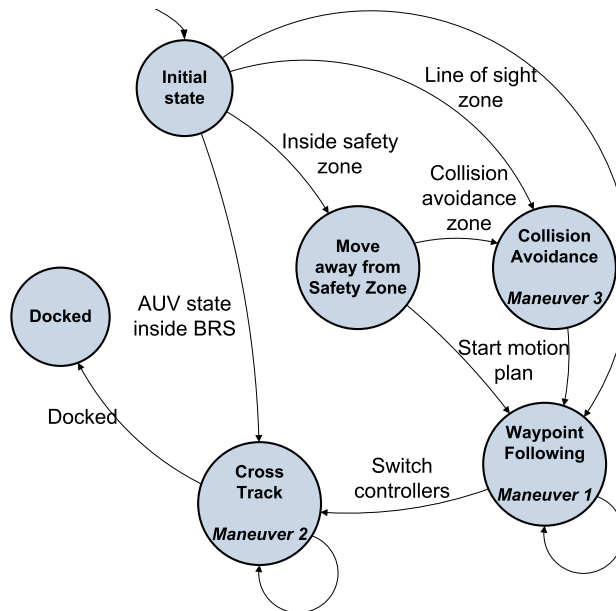


Figure 5.18: High level controller for Problem 4

At the beginning of the docking, the vehicle will inspect its initial state. One of the following four situations may be valid.

- **Inside the Backreach Set** – Then the vehicle will directly dock in the ROV.

- **Inside the Safety Zone** – The vehicle will move away from the ROV to avoid collisions. After moving away from the safety zone, the vehicle will inspect if it is inside the collision avoidance zone or inside the line of sight zone.
- **Inside the Collision Avoidance Zone** – The vehicle will start the roundabout maneuver to circle around the ROV in order to start the glide path. If the maneuver is correctly performed the vehicle enters the line of sight zone.
- **Inside the Line of Sight Zone** – The vehicle will head to the beginning of the motion plan.

## 5.14 Problem 5 – Abort sequence

This problem was formally introduced in section 4.10. This section studies the possibility of aborting the docking maneuver while it is being performed.

Two situations will be analyzed, respectively, when the LAUV receives an *abort command* and when the state of the vehicle leaves the backward reach set, during the final moments of the docking sequence.

### 5.14.1 Receiving a new mission assignment

During the docking operation, the LAUV may receive a new mission assignment. Then, the vehicle has to immediately interrupt the docking, move away from the ROV to avoid collisions and start the next mission assignment.

Nevertheless, a special case must be considered. When the LAUV is almost finishing the docking maneuver, an abort maneuver could possibly result in a collision with the ROV. In such a case, the abort command must be ignored. During simulation tests, the LAUV is able to circle around with a radius less than 2.5 meters, considering a maximum rudder deflection angle of  $\pm 20^\circ$ . To increase safety, the LAUV should ignore the abort command if it is less than 5 meters away from the dock structure.

### 5.14.2 Reaching a position outside of the backward reach set

Another situation must be considered that leads the LAUV to abort the docking maneuver even if it is less than 5 meters (section 5.14.1) away from the ROV. In the presence of strong external disturbances, there is the eventuality of the LAUV not being able to remain inside the backward reach set, independently of the controller utilized. In such a case, continuing the docking operation may lead the vehicle to collide with the ROV. Hence, if the vehicle leaves the backward reach set, it is not guaranteed the existence of a feasible sequence of control inputs that drive the vehicle to the goal, so the vehicle must

immediately terminate the docking operation and move away from the ROV. Figure 5.19 illustrates the possible trajectories during the final moments of the docking sequence.

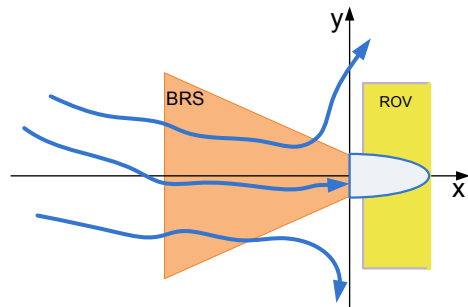


Figure 5.19: Possible trajectories during the final docking maneuver

# Chapter 6

## Simulation Results

This chapter presents the simulation results for the problems described in chapter 4. The models of the underwater vehicles are introduced and the test plan is defined.

### 6.1 Models of the vehicles

This section presents the models of the underwater vehicles used in the simulations, respectively, the LAUV and the ROV.

#### 6.1.1 LAUV

This section presents the parameters of the LAUV equations of motion (4.1). For a complete study about the LAUV parameters the reader is referred to Silva *et. al.* [7]. The body velocities relative to the fluid motion,  $v_R = [u_R, v_R, w_R, p_R, q_R, r_R]^T$  will be presented without the subscript for simplicity. Hence,  $v_R = [u, v, w, p, q, r]^T$ .

The constant inertia and added mass matrix,  $M$ , is

$$M = \begin{bmatrix} 19 & 0 & 0 & 0 & 0.27 & 0 \\ 0 & 34 & 0 & -0.27 & 0 & 0 \\ 0 & 0 & 34 & 0 & 0 & 0 \\ 0 & -0.27 & 0 & 0.04 & 0 & 0 \\ 0.27 & 0 & 0 & 0 & 2.1 & 0 \\ 0 & 0 & 0 & 0 & 0 & 2.1 \end{bmatrix} \quad (6.1)$$

The Coriolis and centripetal matrix,  $C(v_R)$

$$C(v_R) = \begin{bmatrix} 0 & 0 & 0 & 0.27r & 34w & -34v \\ 0 & 0 & 0 & -34w & 0.27r & 19u \\ 0 & 0 & 0 & -0.27p + 16v & -0.27q - u & 0 \\ -0.27r & 34w & 0.27p - 34v & 0 & 2.1r & -2.1q \\ -34w & -0.27r & 0.27q - 19u & -2.1r & 0 & 0.04p \\ 34v & -19u & 0 & 2.1q & -0.04p & 0 \end{bmatrix} - \begin{bmatrix} 0 & 0 & 0 & -18w_c & 18v_c \\ 0 & 0 & 0 & 18w_c & 0 & -18u_c \\ 0 & 0 & 0 & -18v_c & 18u_c & 0 \\ 0 & 0 & 0 & 0 & 0 & 0 \\ 0 & 0 & 0 & 0 & -0.27w_c & 0.27v_c \\ 0 & 0 & 0 & 0 & 0 & 0 \end{bmatrix} \quad (6.2)$$

The damping matrix,  $D(v_R)$ , is given by

$$D(v_R) = - \begin{bmatrix} 2.4 & 0 & 0 & 0 & 0 & 0 \\ 0 & 23 & 0 & 0 & 0 & -11.5 \\ 0 & 0 & 23 & 0 & 11.5 & 0 \\ 0 & 0 & 0 & 0.3 & 0 & 0 \\ 0 & 0 & -3.1 & 0 & 9.7 & 0 \\ 0 & 3.1 & 0 & 0 & 0 & 9.7 \end{bmatrix} - \begin{bmatrix} 2.4|u| & 0 & 0 & 0 & 0 & 0 \\ 0 & 80|v| & 0 & 0 & 0 & -0.3|r| \\ 0 & 0 & 80|w| & 0 & 0.3|q| & 0 \\ 0 & 0 & 0 & 6 \times 10^{-4}|p| & 0 & 0 \\ 0 & 0 & -1.5|w| & 0 & 9.1|q| & 0 \\ 0 & 1.5|v| & 0 & 0 & 0 & 9.1|r| \end{bmatrix} \quad (6.3)$$

The lift matrix,  $L(v_R)$  is

$$L(v_R) = \begin{bmatrix} 0 & 0 & 0 & 0 & 0 & 0 \\ 0 & -20.6 & 0 & 0 & 0 & 2.84 \\ 0 & 0 & -20.6 & 0 & -2.84 & 0 \\ 0 & 0 & 0 & 0 & 0 & 0 \\ 0 & 0 & -8.96 & 0 & -1.5360 & 0 \\ 0 & 8.96 & 0 & 0 & 0 & -1.5360 \end{bmatrix} \quad (6.4)$$

The vector of restoring forces and moments,  $g(\eta_2)$  is given by,

$$g(\eta_2) = \begin{bmatrix} -\sin \theta \\ \cos \theta \sin \phi \\ \cos \theta \cos \phi \\ 2.646(\cos \theta \sin \phi) \\ 2.646(\sin \theta) \\ 0 \end{bmatrix} \quad (6.5)$$

Finally, the vector of body-fixed forces from the actuators,  $\tau = Bu$ , where  $B$  is the control matrix and  $u$  is the control vector.

$$B = \begin{bmatrix} 1 & 0 & 0 \\ 0 & 9.6u^2 & 0 \\ 0 & 0 & -9.6u^2 \\ -0.0639 & 0 & 0 \\ 0 & 0 & -3.8400u^2 \\ 0 & -3.8400u^2 & 0 \end{bmatrix} \quad (6.6)$$

### 6.1.2 ROV

This section presents the parameters of the ROV equations of motion (4.14). Once again,  $v_R = [u, v, w, p, q, r]^T$ .

Although the purpose is to model the behavior of the ROV Luso, there is no information regarding the hydrodynamic parameters of the vehicle as to this date. However, keep in mind that only low complexity maneuvers are required for the ROV which is an over-actuated system. Hence, an approximation is required. Thus, the simulation results are achieved with the parameters of the ROV-IES ([100] and [101]) of the LSTS. Although ROV-IES is a much lighter weight ROV, it serves the purposes of the problems defined in the section 4. The thruster allocation considered is equal to the thruster allocation of the ROV-KOS [86].

Thus, the constant added mass and inertia matrix  $M$ , is

$$M = \text{diag}(131, 132, 192, 107.2, 109.2, 105.3) \quad (6.7)$$

The Coriolis and centripetal matrix  $C(v_R)$  is given by

$$C = \begin{bmatrix} 0 & 0 & 0 & 0 & mw + 90w & -mv - 30v \\ 0 & 0 & 0 & -mw - 90w & 0 & mu + 29u \\ 0 & 0 & 0 & mv + 30v & -mu - 29u & 0 \\ 0 & mw + 90w & -mv - 30v & 0 & ar + 3.3r & bq - 7.2q \\ -mw - 90u & 0 & mu + 29u & ar - 3.3r & 0 & cp + 5.2p \\ mv + 30v & -mu + 29u & 0 & br + 7.2q & cp - 5.2p & 0 \end{bmatrix} - \begin{bmatrix} 0 & 0 & 0 & -102w_c & 102v_c \\ 0 & 0 & 0 & 102w_c & 0 & -102u_c \\ 0 & 0 & 0 & -102v_c & 102u_c & 0 \\ 0 & 0 & 0 & 0 & 0 & 0 \\ 0 & 0 & 0 & 0 & -10.2w_c & 10.2v_c \\ 0 & 0 & 0 & 0 & 0 & 0 \end{bmatrix} \quad (6.8)$$

where  $m = 102$ ,  $a = -2.3$ ,  $b = -2.1$ , and finally,  $c = -1.3$ . The damping matrix,  $D(v_R)$ ,

$$D(v_R) = -\text{diag}[-72, -77, -95, -40, -30, -30] \quad (6.9)$$

The vector of restoring moments and forces,  $g(\eta_2)$  is given by

$$g(\eta_2) = [0, 0, 0, 100.164 \cos \theta \sin \phi, 100.164 \sin \theta, 0]^T \quad (6.10)$$

Finally, the control matrix  $B$  is

$$B = \begin{bmatrix} 0.7071 & 0.7071 & -0.7071 & -0.7071 & 0 \\ 0.7071 & -0.7071 & 0.7071 & -0.7071 & 0 \\ 0 & 0 & 0 & 0 & 1 \\ 0 & 0 & 0 & 0 & 0 \\ 0.085 & 0.085 & -0.085 & -0.085 & 0.13 \\ 0.4709 & -0.4709 & -0.4709 & 0.4709 & 0 \end{bmatrix} \quad (6.11)$$

## 6.2 Test Plan

This section presents the test plan defined to verify the robustness of the control strategy developed to solve the problems defined in section 4. Obviously, the plan does not test every possibility, however, it demonstrates important notions and results achieved with the control strategy developed in section 5. The cases tested for problem 1 and 2 intend to test the following scenarios: the AUV initial position is between the first waypoint and the ROV (hence, in the middle of the motion plan); the waypoint is between the vehicles, but the AUV is pointed in the opposite direction; finally, the AUV position is horizontally equal to the first waypoint but with a different depth. In problem 3 we test the docking maneuver with ocean currents acting in the horizontal plane.

Table 6.1: Test Plan for the first three problems

Test Plan						
	AUV		ROV		Ocean currents	
	initial state		surge	initial state		surge
	[x y z]	[\phi \theta \psi]	u / u <sub>f</sub>	[x y z]	[\phi \theta \psi]	u
<b>Prob 1</b>						
case 1	[-20 10 -5]	[0 0 0]	1.5 / 0.6	[0 0 0]	[0 0 0]	0
case 2	[-50 -10 5]	[0 0 \pi]	1.5 / 0.6	[0 0 0]	[0 0 0]	0
case 3	[-40 0 20]	[0 0 0]	1.5 / 0.6	[0 0 0]	[0 0 0]	0
<b>Prob 2</b>						
case 1	[-20 10 -5]	[0 0 0]	1.5 / 0.6	[0 0 0]	[0 0 0]	0.3
case 2	[-50 -10 5]	[0 0 \pi]	1.5 / 0.6	[0 0 0]	[0 0 0]	0.3
case 3	[-40 0 20]	[0 0 0]	1.5 / 1	[0 0 0]	[0 0 0]	0.3
<b>Prob 3</b>						
case 1	[-50 0 0]	[0 0 0]	1.5 / 1	[0 0 0]	[0 0 0]	0.3 $v_{cy} = 0.3$
case 2	[-50 0 0]	[0 0 0]	1.5 / 1	[0 0 0]	[0 0 0]	0.3 $v_{cy} = -0.3$
case 3	[-50 0 0]	[0 0 0]	1.5 / 1	[0 0 0]	[0 0 0]	0.3 $u_{cx} = 0.2$
case 4	[-50 0 0]	[0 0 0]	1.5 / 1	[0 0 0]	[0 0 0]	0.3 $u_{cx} = -0.2$
<b>Prob 4</b>						
case 1	[-2 0 0]	[0 0 0]	1.5 / 1	[0 0 0]	[0 0 0]	0.3 $v_{cy} = 0.3$
case 2	[-2 1 0]	[0 0 0]	1.5 / 1	[0 0 0]	[0 0 0]	0.3 $v_{cy} = 0.3$
case 3	[2 0 0 0]	[0 0 0]	1.5 / 1	[0 0 0]	[0 0 0]	0.3 [0 0 0]
case 4	[10 10 0]	[0 0 \pi]	1.5 / 1	[0 0 0]	[0 0 0]	0.3 [0 0 0]
<b>Prob 5</b>						
case 1	[-50 -30 0]	[0 0 0]	1.5 / 1	[0 0 0]	[0 0 0]	0.3 [-0.4 0.7 0]
case 2	[-50 -30 0]	[0 0 0]	1.5 / 1	[0 0 0]	[0 0 0]	0.3 [0 0.7 0]

To test the **Problem 4**, the four different scenarios in the collision avoidance system, presented in section 5.13, will be tested. Hence,

- **Case 1: Inside the Backreach Set** – Then the vehicle will directly dock in the ROV.

- **Case 2: Inside the Safety Zone** – The vehicle will move away from the ROV to avoid collisions. After moving away from the safety zone, the vehicle will inspect if it is inside the collision avoidance zone or inside the line of sight zone.
- **Case 3: Inside the Collision Avoidance Zone** – The vehicle will start the round-about maneuver to circle around the ROV in order to start the glide path. If the maneuver is correctly performed the vehicle enters the line of sight zone.
- **Case 4: Inside the Line of Sight Zone** – The vehicle will head to the beginning of the motion plan.

To test the **Problem 5**, strong external disturbances will be used to force the state of the LAUV to leave the backward reach set. Keep in mind, that although the backward reach set is computed using the bounded ocean currents, the controllers may not be able to efficiently track the motion plan.

The results are presented in the following sections.

## 6.3 Problem 1 – Docking without disturbances with the ROV fixed

### 6.3.1 Case 1

This section demonstrates the results achieved when there are no external disturbances to the system, and the ROV is performing dynamic positioning. Moreover, the initial state of the LAUV is  $\mathbf{x} = [-20, 10, -5, 0, 0, 0]^T$  considering  $\mathbf{x} = [x, y, z, \phi, \theta, \psi]^T$ . The desired surge during the docking sequence is  $u = 1.5$  m/s, and the final desired surge (*i.e.*, the surge during the latching moment with the dock structure) is  $u_f = 0.6$  m/s.

In this case the vehicle was able to dock in  $t_d = 49.34$  seconds. When the vehicle latched with the dock structure its position is  $y = -0.026$  and  $z = -0.0593$  meters relative to the center of the dock. Hence, the final distance is  $d = 0.0648$  meters. The docking is considered successful if the distance between the vehicles is less than 0.50 meters when the AUV reaches  $x = 0$ .

Figure 6.1 demonstrates the trajectory of the LAUV in the horizontal and vertical planes, respectively. The blue line is the trajectory of the LAUV and the dashed green line is the motion plan constituted by the waypoints. The waypoints are represented in the figure in green squares (with black colored edges). The red cone is just for illustrative purposes, and can be viewed as a possible set of states that drive the LAUV to the dock structure. The cyan colored square represents the ROV frame. The docking position is located at the origin of the frame.

Figure 6.2 demonstrates the position of the vehicle along time and the distance between the LAUV and the ROV. In the left hand side of the figure, blue lines are the position of the AUV in  $x$ ,  $y$  and  $z$ , respectively, across time, while the green points are the

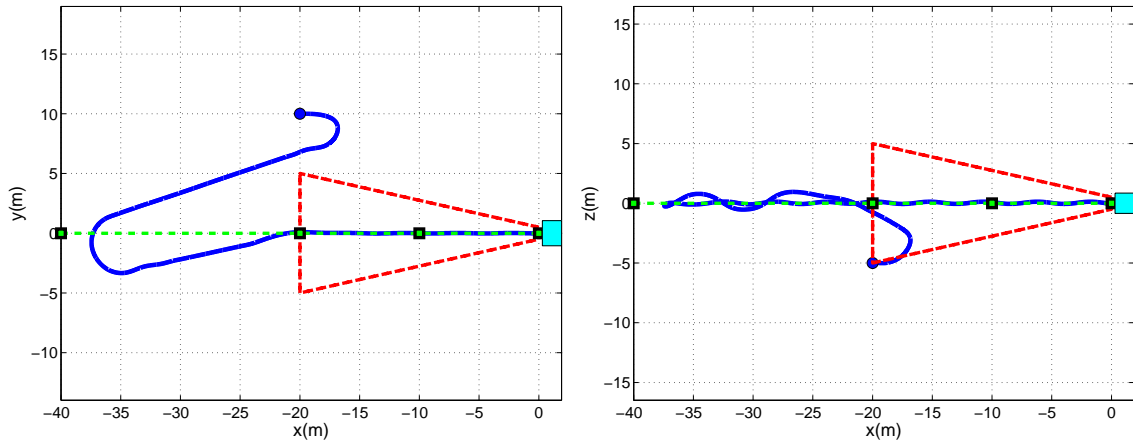


Figure 6.1: Problem 1 - case 1: Position of the vehicle in the XY and XZ planes, respectively

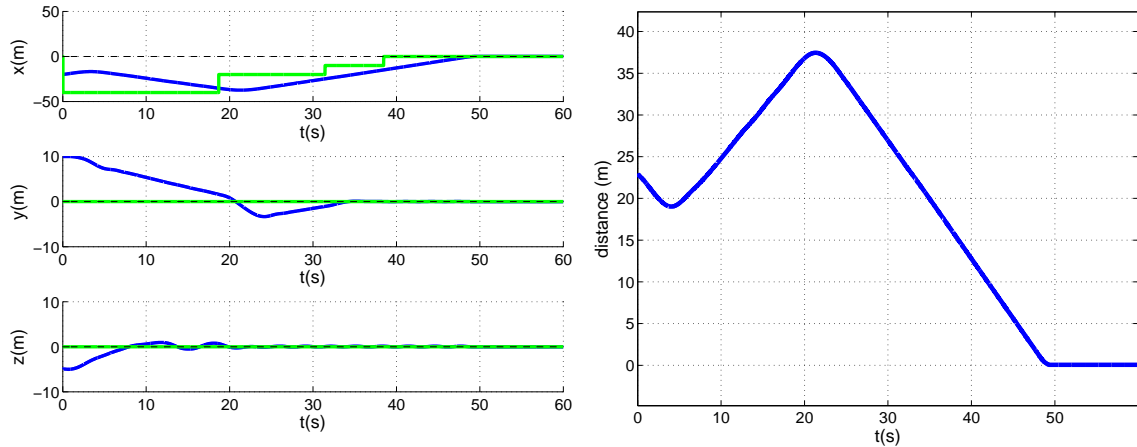


Figure 6.2: Problem 1 - case 1: The position of the vehicle along time and the euclidean distance between both vehicles

coordinates of the active waypoints. In the right hand side of the figure, the blue line is the distance between both vehicles. It can be seen that the docking moment occurs near the  $t_d = 49.34$  seconds mark as stated. The final distance is  $d = 0.0648$ .

Finally, figure 6.3 shows the velocity ( $u$ ,  $v$  and  $w$ ) of the vehicle expressed in its body-fixed reference, and the actuator inputs to the system across time. The actuator inputs are the thruster force acting in the longitudinal axis and the rudder (R) and stern (S) angles of deflection in degrees, respectively.

### 6.3.2 Case 2

The initial state of the LAUV is  $\mathbf{x} = [-50, -10, 5, 0, 0, \pi]^T$ . The desired surge during the docking sequence is  $u = 1.5$  m/s, and the final desired surge is  $u_f = 0.6$  m/s.

The vehicle was able to dock in  $t_d = 43.03$  seconds. When the vehicle latches with the dock structure its position is  $y = -0.0154$  and  $z = -0.0131$  meters relative to the center

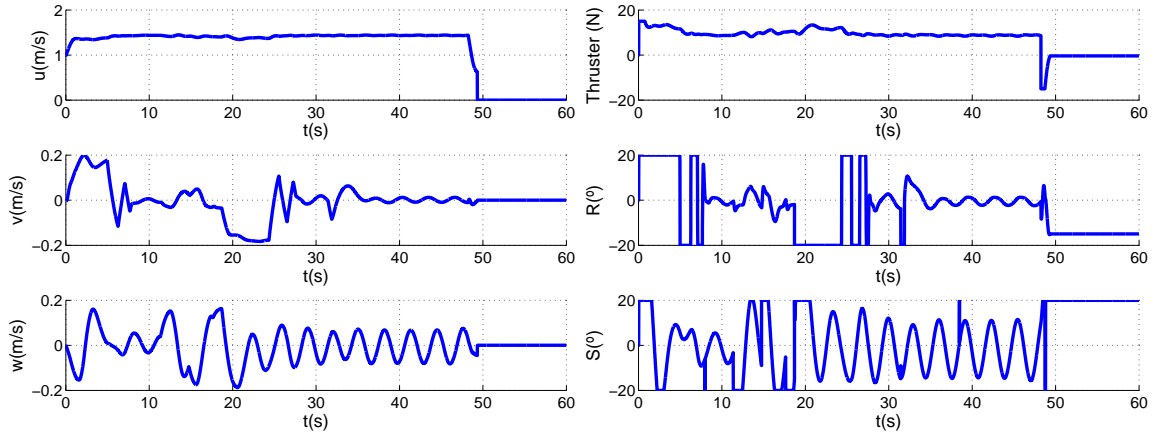


Figure 6.3: Problem 1 - case 1: The velocity of the vehicle expressed in its body-fixed reference frame and the necessary actuation across time

of the dock. Hence, the final distance is  $d = 0.0202$  meters. The tracking achieved in this case is better than the first case.

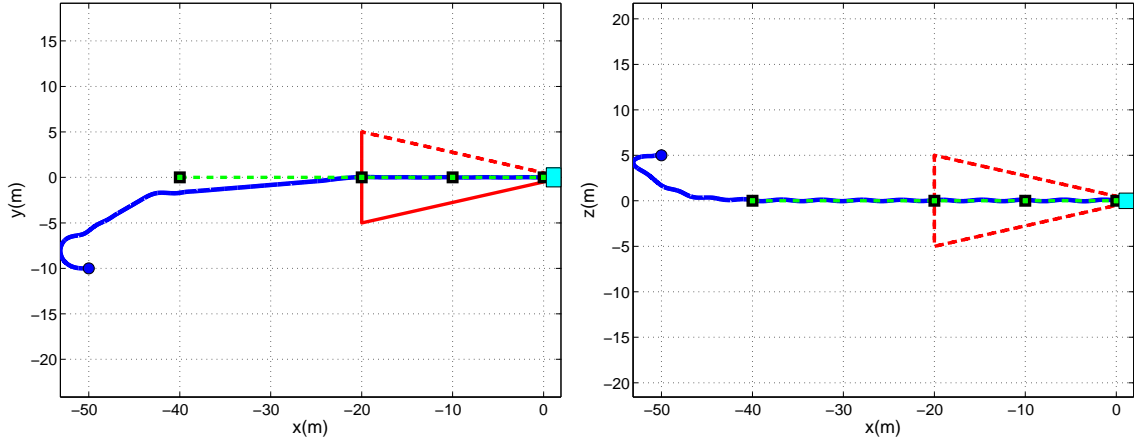


Figure 6.4: Problem 1 - case 2: Position of the vehicle in the XY and XZ planes, respectively

Once again, figure 6.4 demonstrates the trajectory of the LAUV in the horizontal and vertical planes, respectively. The figure demonstrates that the vehicle performed a smoother trajectory when compared with the first case (figure 6.1).

Figure 6.5 demonstrates the position of the vehicle over time and the distance between the LAUV and the ROV.

Finally, figure 6.6 shows the velocity ( $u$ ,  $v$  and  $w$ ) of the vehicle expressed in its body-fixed reference, and the actuator inputs to the system across time. The vehicle surge is kept constant near the 1.5 m/s, and at the final moments of docking decreases to 0.6 m/s until the latching happens and the vehicle stops.

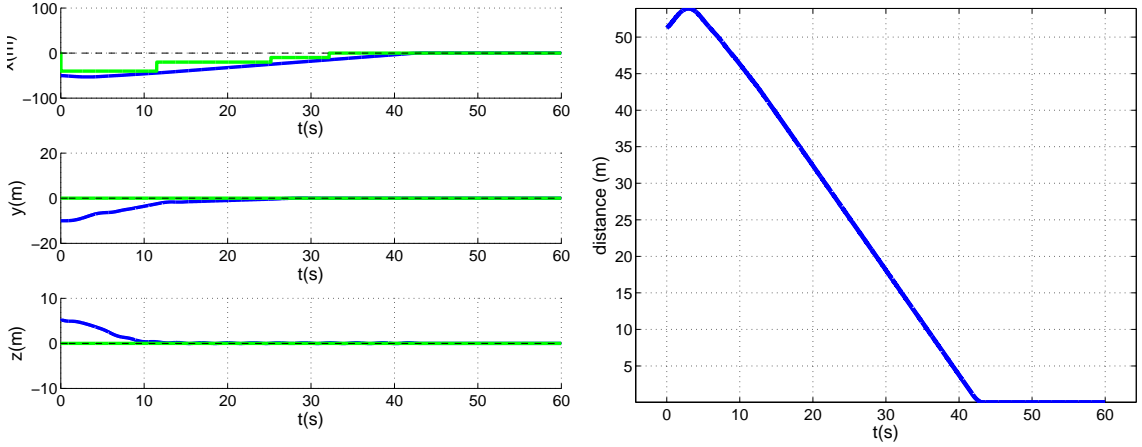


Figure 6.5: Problem 1 - case 2: The position of the vehicle along time and the euclidean distance between both vehicles

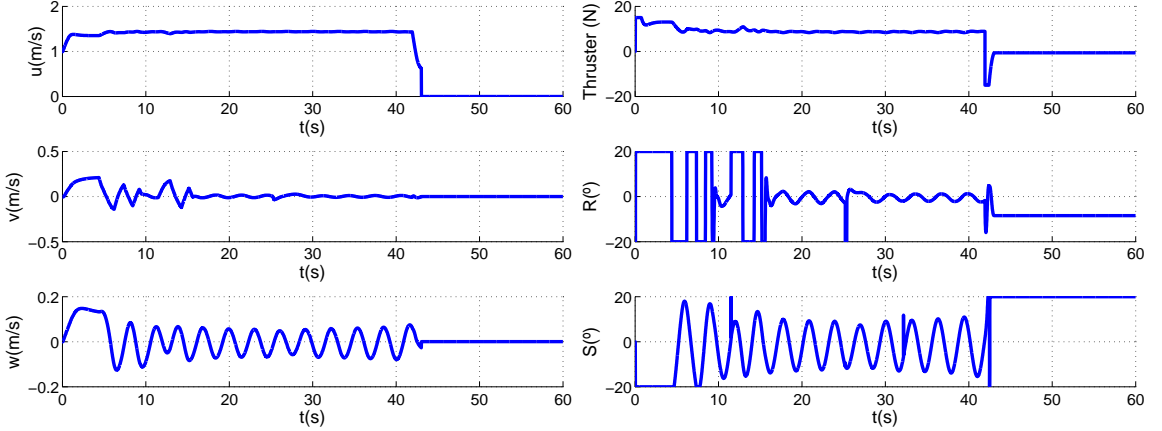


Figure 6.6: Problem 1 - case 2: The velocity of the vehicle expressed in its body-fixed reference frame and the necessary actuation across time

### 6.3.3 Case 3

The initial state of the LAUV is  $\mathbf{x} = [-40, 0, 20, 0, 0, 0]^T$ . The purpose is to test the depth controllers since the first waypoint ( $x_{wp} = -40$ ,  $y_{wp} = 0$ ) is located exactly with the same horizontal position, but with a different depth.

The vehicle was able to dock in  $t_d = 54.14$  seconds. When the vehicle latches with the dock structure its position is  $y = 0.0056$  and  $z = 0.0175$  meters relative to the center of the dock. Hence, the final distance is  $d = 0.0144$  meters. The lowest of the three cases compared. This results prove the robustness of the low level sliding mode controllers.

Once again, figure 6.7 demonstrates the trajectory of the LAUV in the horizontal and vertical planes, respectively. The figure demonstrates that the vehicle needed to circle around (considering the horizontal plane) while correcting the depth necessary to perform the glide path to dock inside the ROV.

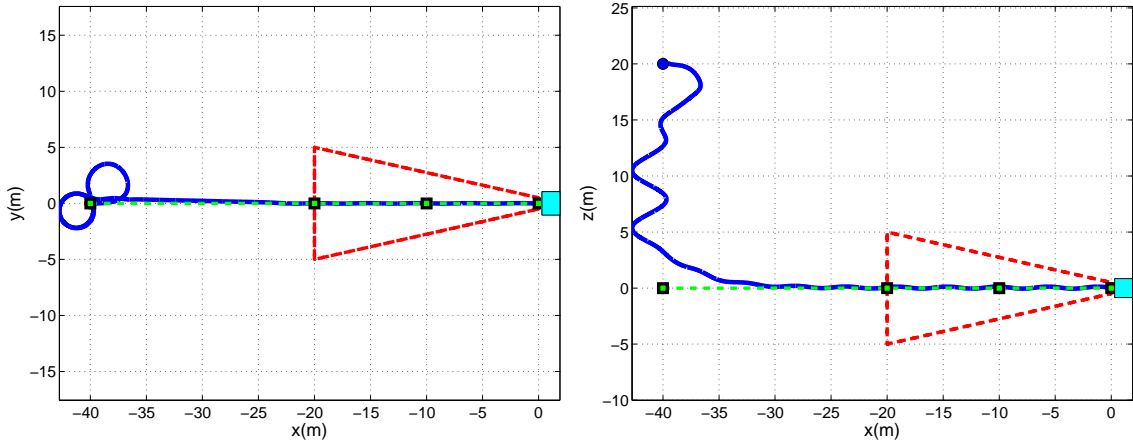


Figure 6.7: Problem 1 - case 3: Position of the vehicle in the XY and XZ planes, respectively

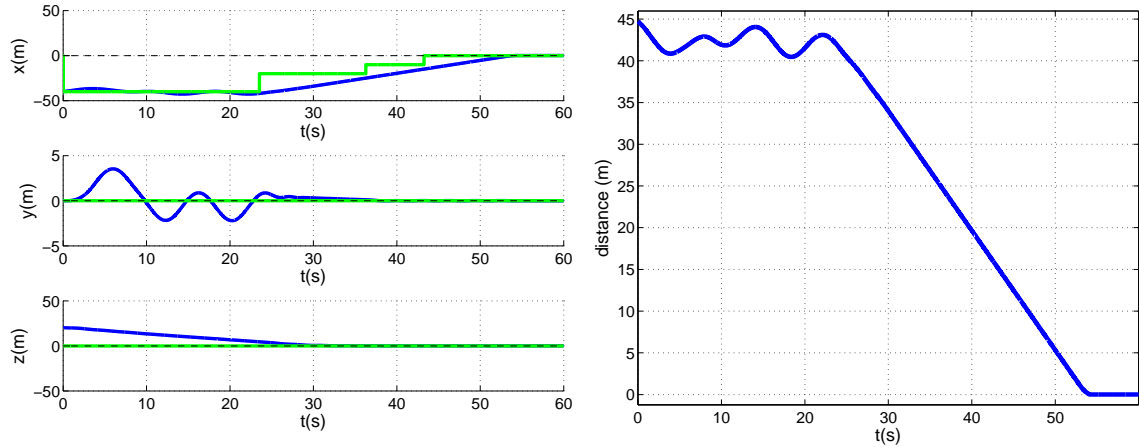


Figure 6.8: Problem 1 - case 3: The position of the vehicle along time and the euclidean distance between both vehicles

Figure 6.8 demonstrates the position of the vehicle along time and the distance between the LAUV and the ROV. Firstly, the vehicle corrects the depth and only then moves in the horizontal plane to perform the docking maneuver.

Finally, figure 6.9 shows the velocity ( $u$ ,  $v$  and  $w$ ) of the vehicle expressed in its body-fixed reference frame, and the actuator inputs to the system across time. The vehicle surge is kept constant near the 1.5 m/s, and at the final moments of docking decreases to 0.6 m/s until the latching happens and the vehicle stops. Furthermore, it is possible to verify that the stern input is kept constant at  $\delta_s = -20^\circ$ , which is responsible for the heave motion ( $w$ ) that changes the depth of the vehicle.

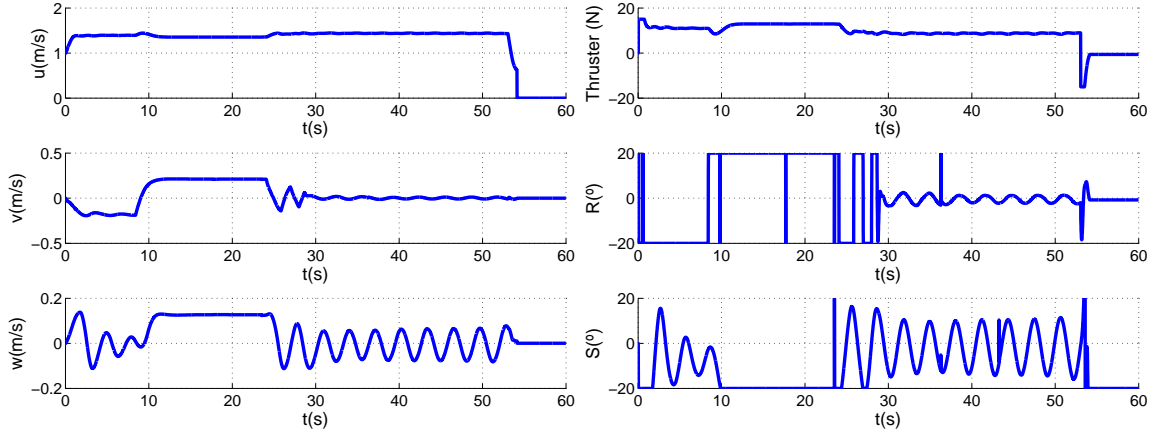


Figure 6.9: Problem 1 - case 3: The velocity of the vehicle expressed in its body-fixed reference frame and the necessary actuation across time

## 6.4 Problem 2 – Docking without disturbances with the ROV in motion

### 6.4.1 Case 1

This section demonstrates the results achieved when there are no external disturbances to the system, but the ROV is moving in constant forward motion (along the inertial  $x$ -axis with heading  $\psi = 0$ ). Moreover, the initial state of the LAUV is  $\mathbf{x} = [-20, 10, -5, 0, 0, 0]^T$  considering  $\mathbf{x} = [x, y, z, \phi, \theta, \psi]^T$ . The initial ROV state is  $\mathbf{x} = [0, 0, 0, 0, 0, 0]^T$ . The ROV is moving with constant surge  $u_{\text{rov}} = 0.3$  m/s. The desired surge during the docking sequence is  $u = 1.5$  m/s, and the final desired surge is  $u_f = 0.6$  m/s. Thus, the relative reference surge for the AUV is  $u = 1.2$  m/s and  $u_f = 0.3$ .

In this case the vehicle was able to dock in  $t_d = 56.67$  seconds. Although the initial position of both vehicles is the same as the case 1 of problem 1 in section 6.3.1, the constant surge of the ROV results in a delay in the docking sequence. When the vehicle latched with the dock structure its position is  $y = -0.0335$  and  $z = 0.0178$  meters relative to the center of the dock. Hence, the distance is  $d = 0.0380$  meters. The results are better than when the ROV is not in motion (remember, the distance when the ROV is performing dynamic positioning is  $d = 0.0648$  m).

Figure 6.10 demonstrates the trajectory of the LAUV in the horizontal and vertical planes, respectively. However, we have now a moving reference frame since the ROV is moving with  $u_{\text{rov}} = 0.3$  m/s.

Figure 6.11 demonstrates the evolution of the states of both vehicles in the earth-fixed reference frame. The blue line is the AUV trajectory and the green line is the ROV trajectory. The black cone illustrates a possible entry for the AUV in the beginning of the docking sequence, however, since the state of the ROV evolves in time, the red cone

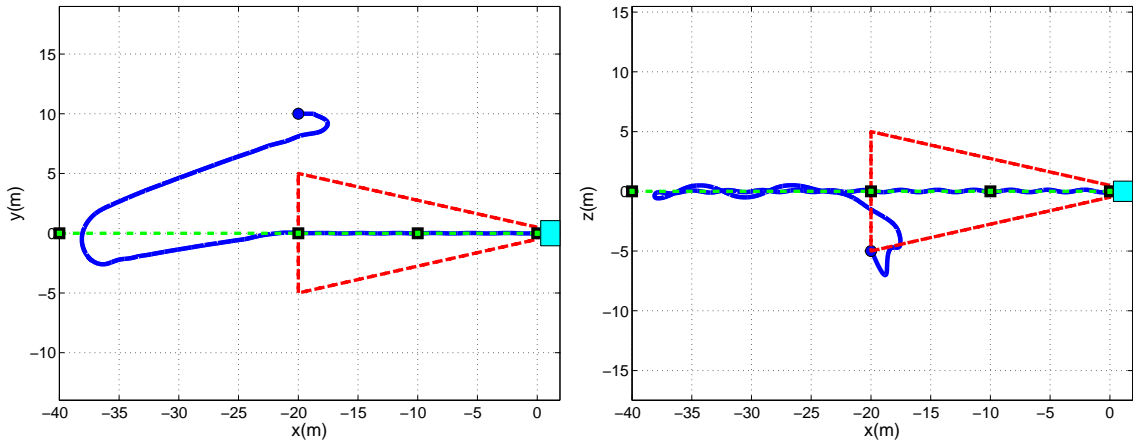


Figure 6.10: Problem 2 - case 1: Position of the vehicle expressed in the ROV body frame in the XY and XZ planes, respectively

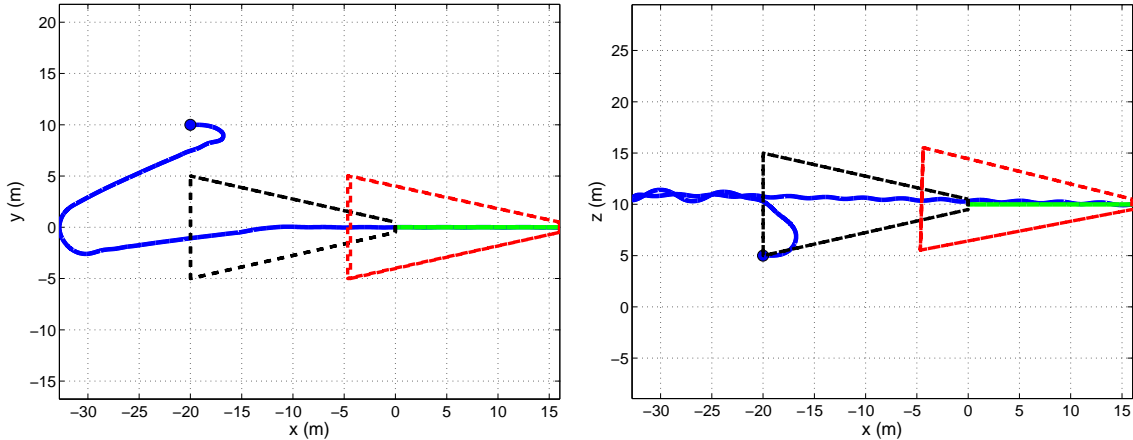


Figure 6.11: Problem 2 - case 1: Position of the vehicles in the inertial frame

indicates the final ROV state when the LAUV latches on. The final ROV state is  $\mathbf{x}_{\text{rov}} = [16.0353, 0, 0]^T$ .

Figure 6.12 demonstrates the position of the vehicle in the ROV body frame along time and the distance between the LAUV and the ROV. It can be seen that the latching moment occurs near the  $t_d = 56.67$  seconds mark as stated. The final distance is  $d = 0.0380$ .

Finally, figure 6.13 shows the velocity ( $u$ ,  $v$  and  $w$ ) of the vehicle expressed in its body-fixed reference, and the actuator inputs to the system across time.

#### 6.4.2 Case 2

The initial state of the LAUV is  $\mathbf{x} = [-50, -10, 5, 0, 0, 0]^T$ . The initial ROV state is  $\mathbf{x} = [0, 0, 0, 0, 0, 0]^T$  and is moving with constant surge  $u_{\text{rov}} = 0.3$  m/s.

The LAUV was able to dock in  $t_d = 57.5$  seconds. When the vehicle latches with the dock structure its position is  $y = 0.0311$  and  $z = 0.0056$  meters relative to the center of

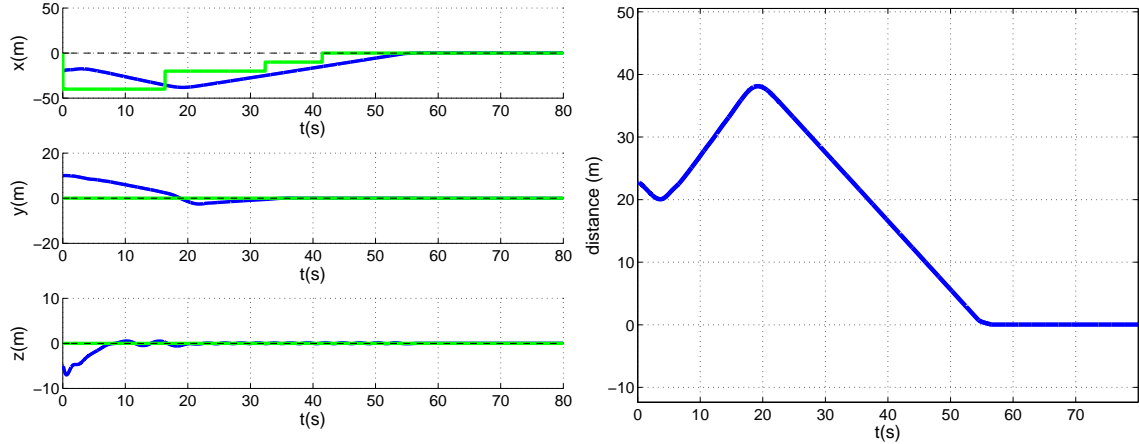


Figure 6.12: Problem 2 - case 1: The position of the vehicle in the ROV body frame along time and the euclidean distance between both vehicles

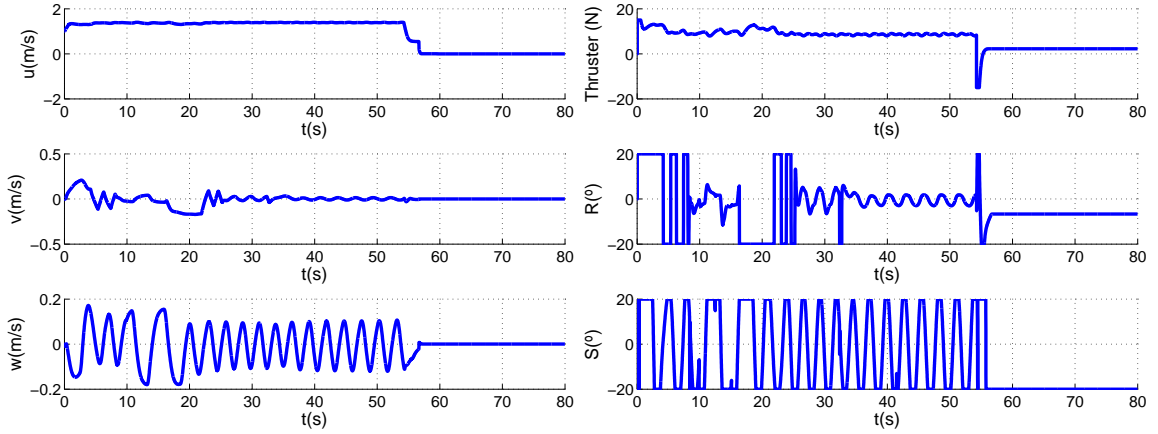


Figure 6.13: Problem 2 - case 1: The velocity of the vehicle expressed in its body-fixed reference frame and the necessary actuation across time

the dock. Hence, the distance is  $d = 0.0317$  meters, which is higher than when the ROV is performing DP ( $d = 0.0202$  m).

Figure 6.14 demonstrates the trajectory of the LAUV, expressed in the ROV body frame, in the horizontal and vertical planes, respectively. The final ROV state is  $\mathbf{x}_{\text{rov}} = [16.2703, 0, 0]^T$ . It is possible to see that the vehicle circling around in the beginning of the docking affects the depth of the LAUV.

Figure 6.15 demonstrates the position of the vehicle in the ROV body frame along time and the distance between the LAUV and the ROV.

#### 6.4.3 Case 3

The initial state of the LAUV is  $\mathbf{x} = [-40, 0, 20, 0, 0, 0]^T$ . The initial ROV state is  $\mathbf{x} = [0, 0, 0, 0, 0, 0]^T$  and is moving with constant surge  $u_{\text{rov}} = 0.3$  m/s. The desired final surge

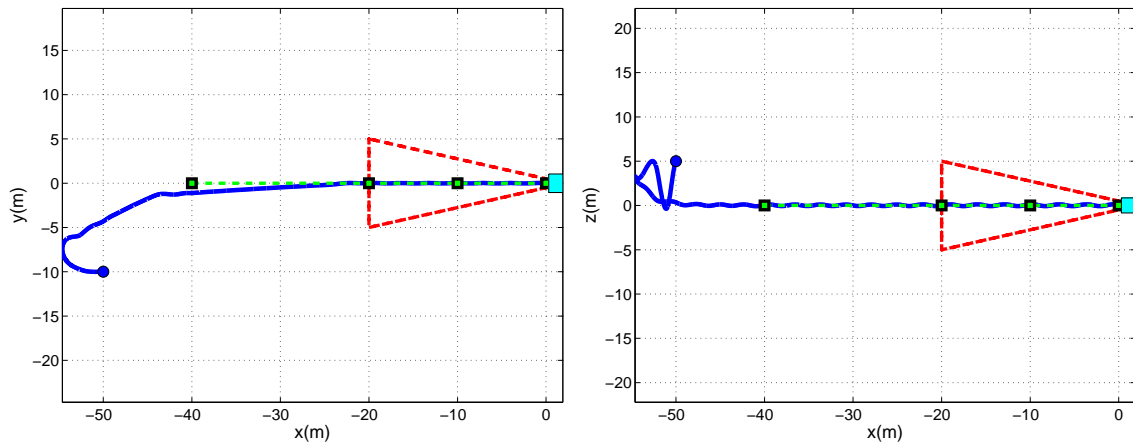


Figure 6.14: Problem 2 - case 2: Position of the vehicle expressed in the ROV body frame in the XY and XZ planes, respectively

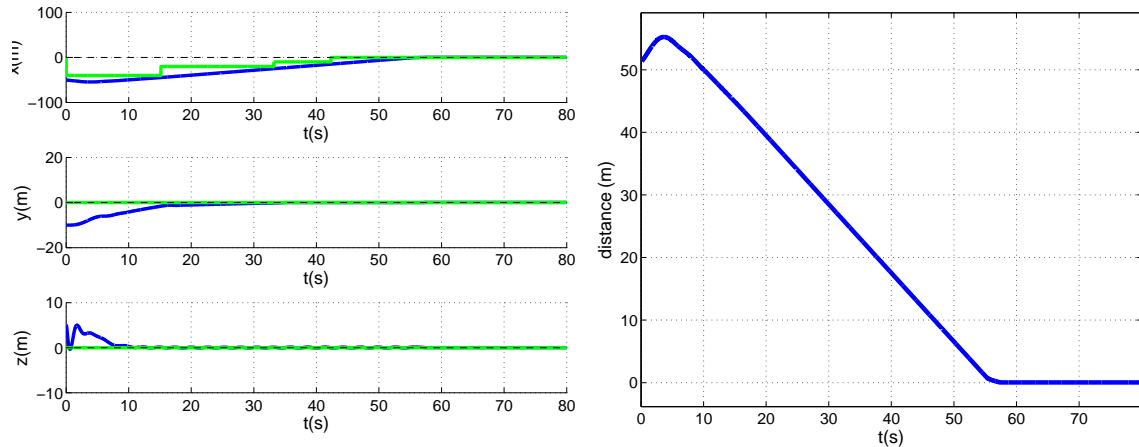


Figure 6.15: Problem 2 - case 2: The position of the vehicle in the ROV body frame along time and the euclidean distance between both vehicles

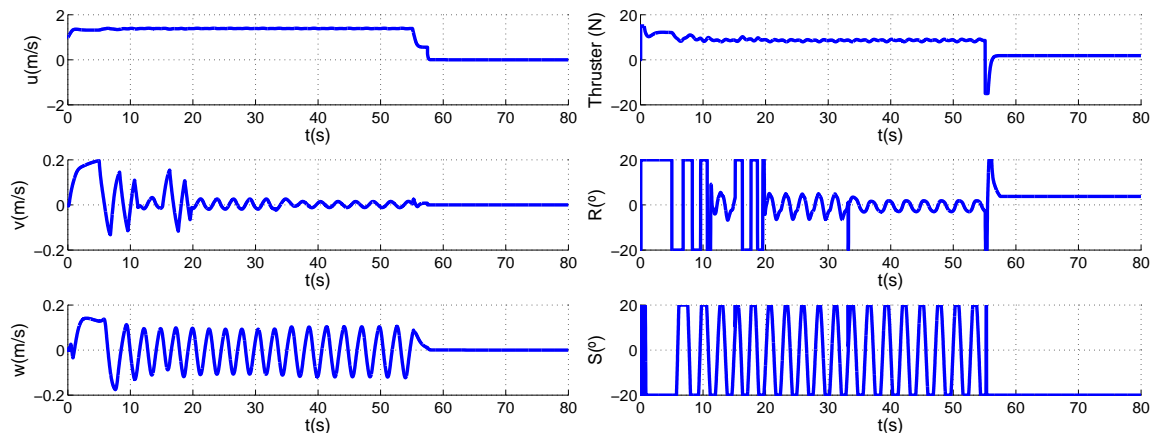


Figure 6.16: Problem 2 - case 2: The velocity of the vehicle expressed in its body-fixed reference frame and the necessary actuation across time

for the LAUV is 1 m/s, hence the reference for the controllers will be  $u_f = 0.7$  m/s.

The LAUV was able to dock in  $t_d = 58.49$  seconds. When the vehicle latches with the dock structure its position is  $y = 0.0017$  and  $z = 0.0726$  meters relative to the center of the dock. Hence, the distance is  $d = 0.0728$  meters, which is higher than when the ROV is performing DP ( $d = 0.0144$  m).

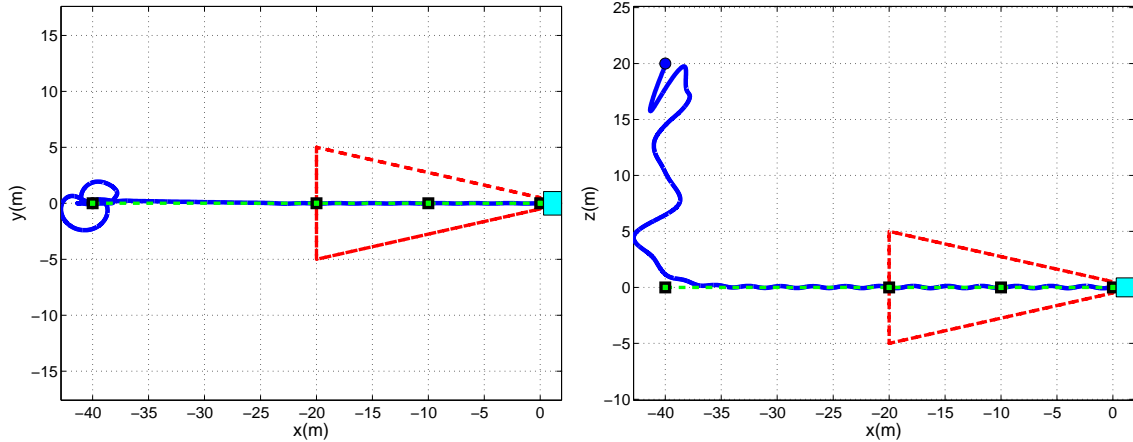


Figure 6.17: Problem 2 - case 3: Position of the vehicle expressed in the ROV body frame in the XY and XZ planes, respectively

Figure 6.17 demonstrates the trajectory of the LAUV, expressed in the ROV body frame, in the horizontal and vertical planes, respectively. Once again, it can be seen that the horizontal and vertical motions are coupled, because when the AUV is circling around, the depth control is affected. The final ROV state is  $\mathbf{x}_{\text{rov}} = [16.5506, 0, 0]^T$ .

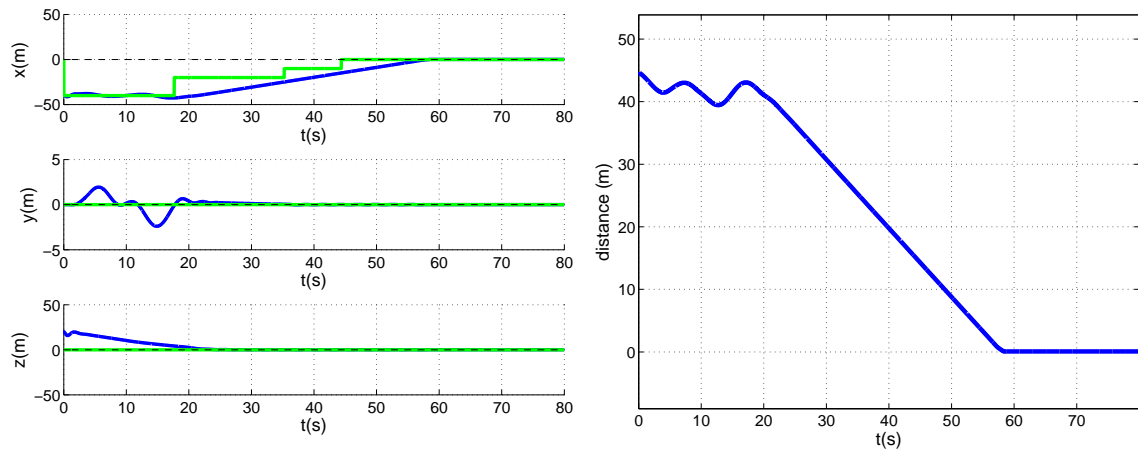


Figure 6.18: Problem 2 - case 3: The position of the vehicle in the ROV body frame along time and the euclidean distance between both vehicles

Figure 6.18 demonstrates the position of the vehicle in the ROV body frame along time and the distance between the LAUV and the ROV.

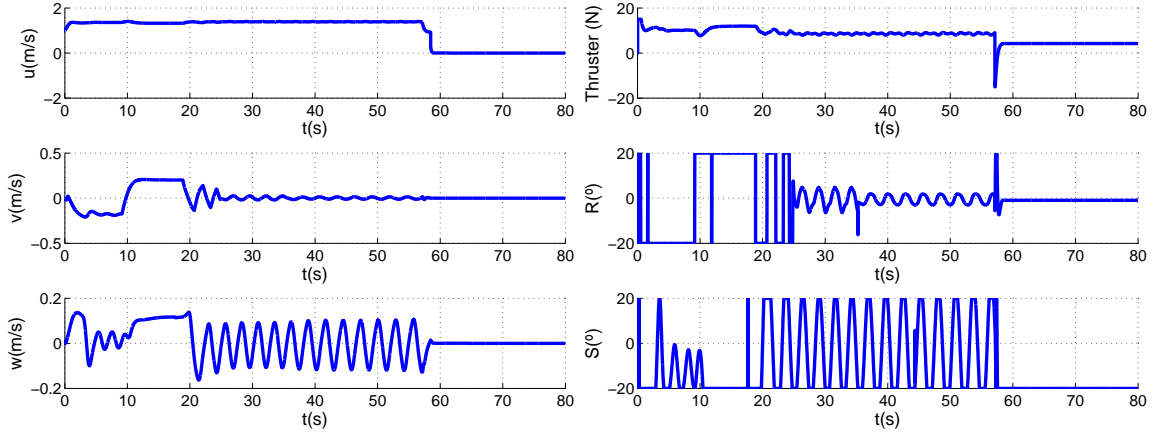


Figure 6.19: Problem 2 - case 3: The velocity of the vehicle expressed in its body-fixed reference frame and the necessary actuation across time

In conclusion, the final distances are small (compared with the size of the dock structure considered, 50cm radius) which is a good result. Nonetheless, no external disturbances were considered. Adding external disturbances will make it harder for the controllers to track the motion plan.

## 6.5 Problem 3 – Docking with disturbances

In what follows, for all the cases, this conditions holds:

The initial state of the LAUV is  $\mathbf{x} = [-50, 0, 0, 0, 0, 0]^T$ . The initial ROV state is  $\mathbf{x} = [0, 0, 0, 0, 0, 0]^T$  and is moving with constant surge  $u_{\text{rov}} = 0.3$  m/s. The vehicle will perform the docking maneuver with a nominal speed  $u = 1.5$  m/s. The desired final surge for the LAUV is 1 m/s, hence the reference for the controllers will be  $u_f = 0.7$  m/s.

Ocean currents will be added to the system along the  $x$ -axis and  $y$ -axis to test the system robustness.

### 6.5.1 Case 1

With ocean currents acting on the transversal axis, with  $v_{cy} = 0.3$  m/s, the LAUV was able to dock in  $t_d = 55.02$  seconds. When the vehicle latches with the dock structure its position is  $y = 0.0469$  and  $z = -0.0048$  meters relative to the center of the dock. Hence, the distance is  $d = 0.0473$  meters, which is much less than the maximum considered  $d_{\max} = 0.5$  m.

The error in the  $y$ -axis is very reduced, even in the presence of lateral external disturbances. The reason is the cross-track error controller combined with the dynamical allocation of the waypoints using backward reach set under adversarial behavior information.

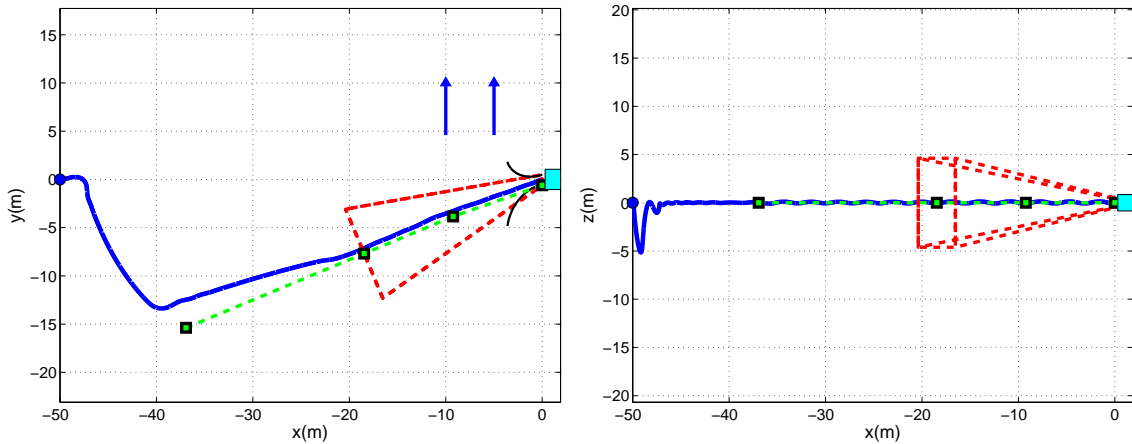


Figure 6.20: Problem 3 - case 1: Position of the vehicle expressed in the ROV body frame in the XY and XZ planes, respectively

Figure 6.20 introduces some changes when compared with previous figures. In addition two blue arrows are plotted to illustrate the direction of the ocean currents. Near the docking point, two thin black lines are the boundary of the backreach set under adversarial behavior. The backreach set information helps the controller to derive the motion plan for the LAUV. Figure 6.21 presents the final moments of the docking sequence in the horizontal plane only.

Notice the location of the final waypoint. The presence of such strong external disturbances makes it harder for the low level controllers to track the desired path. However, the offset information was studied and compensated in the motion planning (section 5.5).

Hence, the final waypoint is defined in the  $y$ -axis as follows

$$y_{wp} = -2v_{cy} \quad (6.12)$$

Equation (6.12) is used to allocate the final waypoint of the motion plan, and holds for the rest of the simulation results.

Figure 6.22 shows once again the position of the LAUV expressed in the ROV body-fixed reference frame (left hand side of the figure). The blue line is the vehicle state, while the green line is the motion plan.

Figure 6.23 presents the velocity of the LAUV as also the actuation during the docking procedures.

### 6.5.2 Case 2

With ocean currents acting on the transversal axis,  $v_{cy} = -0.3$  m/s, the LAUV was able to dock in  $t_d = 54.96$  seconds. When the vehicle latches with the dock structure its position is  $y = -0.0309$  and  $z = 0.0294$  meters relative to the center of the dock. Hence, the distance is  $d = 0.0427$  meters.

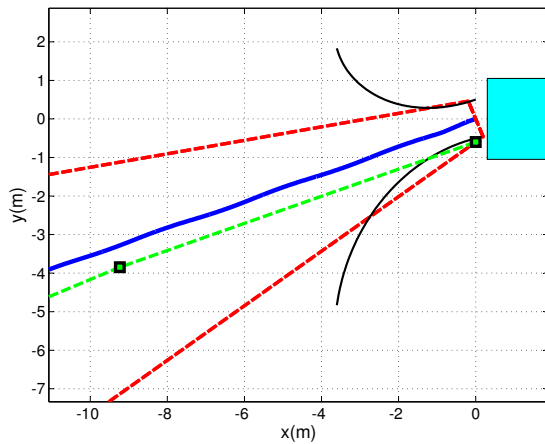


Figure 6.21: Problem 3 - case 1: Final moments of docking in the horizontal plane

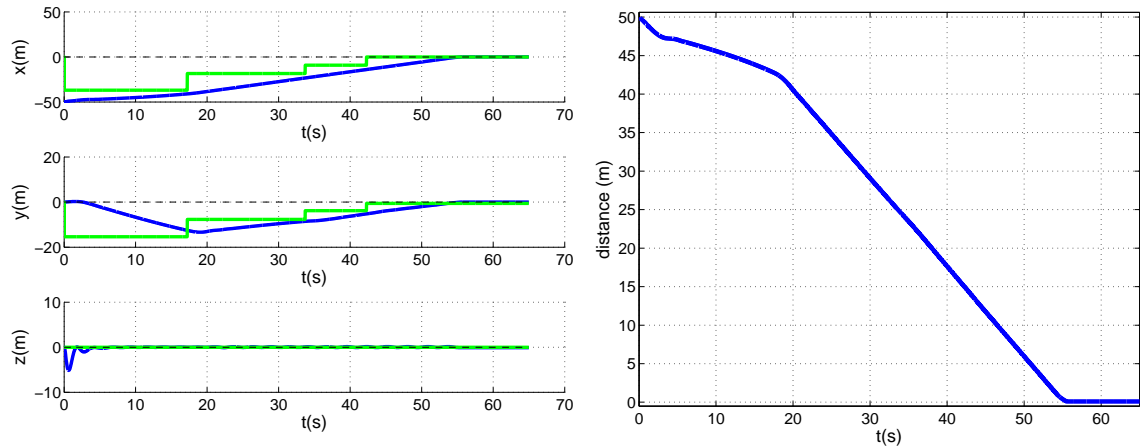


Figure 6.22: Problem 3 - case 1: The position of the vehicle in the ROV body frame along time and the euclidean distance between both vehicles

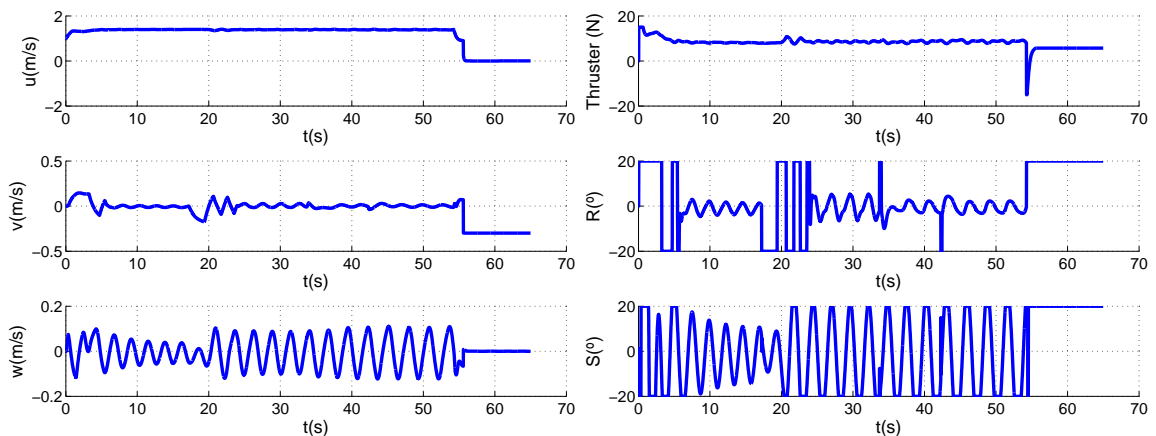


Figure 6.23: Problem 3 - case 1: The velocity of the vehicle expressed in its body-fixed reference frame and the necessary actuation across time

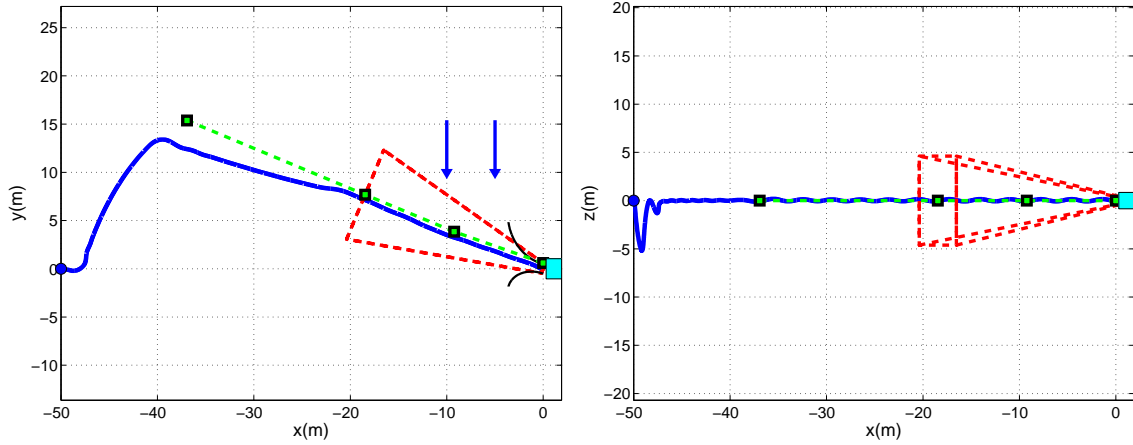


Figure 6.24: Problem 3 - case 2: Position of the vehicle expressed in the ROV body frame in the XY and XZ planes, respectively

Figure 6.24 presents the path performed by the AUV. Since the currents are pointed in the opposite direction compared with the first case, the heading of the motion plan is opposite too, in order for the vehicle to null the effect of the ocean currents. Figure 6.25 presents the final moments of the docking sequence in the horizontal plane only, as also the position of the LAUV relative to the ROV during the docking procedure. The final waypoint is not in the origin of the frame, but with a offset in the y-axis, dependent of the direction and amplitude of the ocean currents.

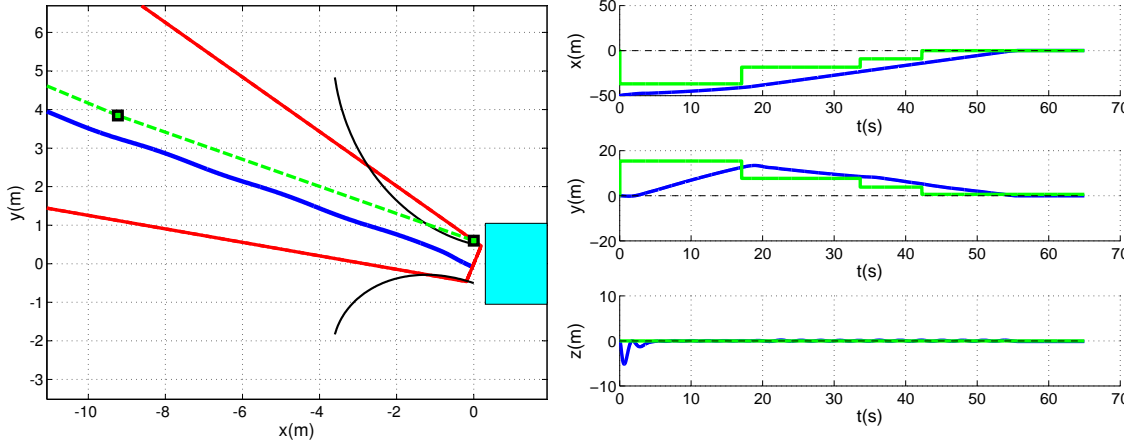


Figure 6.25: Problem 3 - case 2: Final moments of docking in the horizontal plane, and the position of the vehicle in the ROV body frame along time

### 6.5.3 Case 3

Considering ocean currents acting on the longitudinal axis, with  $u_{cx} = 0.3$  m/s, the LAUV was able to dock in  $t_d = 45.98$  seconds, which is faster than for the previous cases. This is due to the ocean currents helping the docking maneuver. When the vehicle latches with

the dock structure its position is  $y = 0.0060$  and  $z = 0.0740$  meters relative to the center of the dock. Hence, the distance is  $d = 0.0744$ .

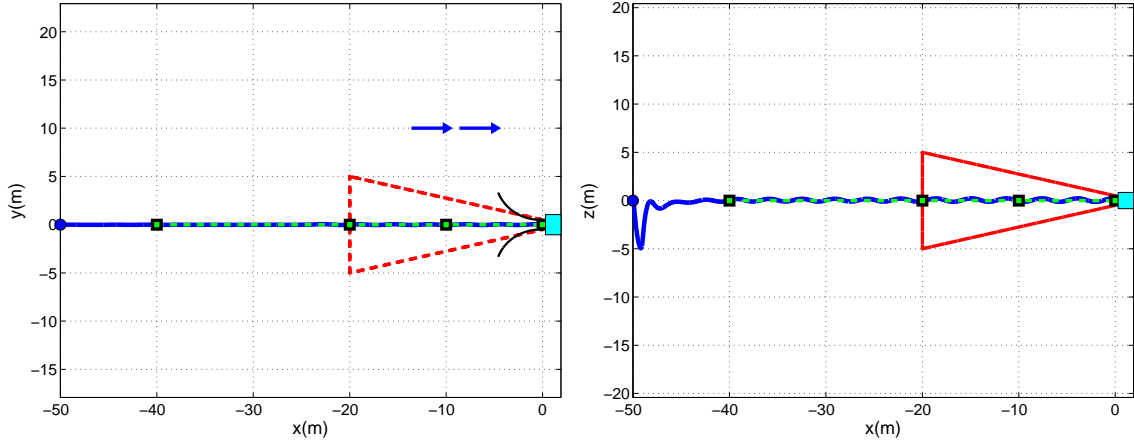


Figure 6.26: Problem 3 - case 3: Position of the vehicle expressed in the ROV body frame in the XY and XZ planes, respectively

Figure 6.27 shows that the docking is achieved with a very few offset ( $y = 0.0356$ ), in the horizontal plane.

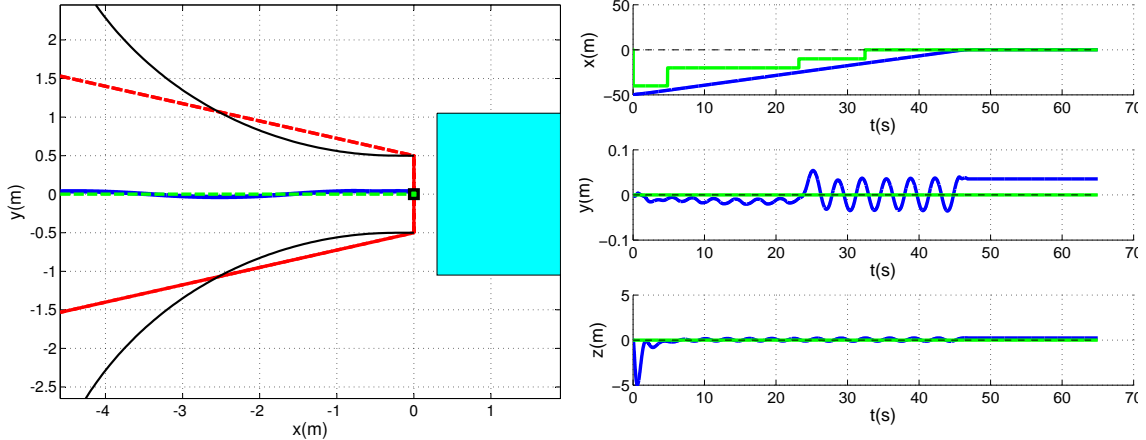


Figure 6.27: Problem 3 - case 3: Final moments of docking in the horizontal plane, and the position of the vehicle in the ROV body frame along time

#### 6.5.4 Case 4

With ocean currents acting in the longitudinal direction in the opposite direction,  $u_{cx} = -0.3$  m/s, the AUV was able to dock in  $t_d = 45.86$  seconds. This is shorter than for case 3 ( $t_d = 45.98$ ) because of the presence of the external disturbances acting against the vehicles. Keep in mind that the frame of the ROV has a bigger surface than the LAUV, hence the LAUV feels less drag from the ocean currents. When the vehicle latches with

the dock structure its position is  $y = 0.0167$  and  $z = 0.0656$  meters relative to the center of the dock. Hence, the distance is  $d = 0.0678$  meters, which is a very good result.

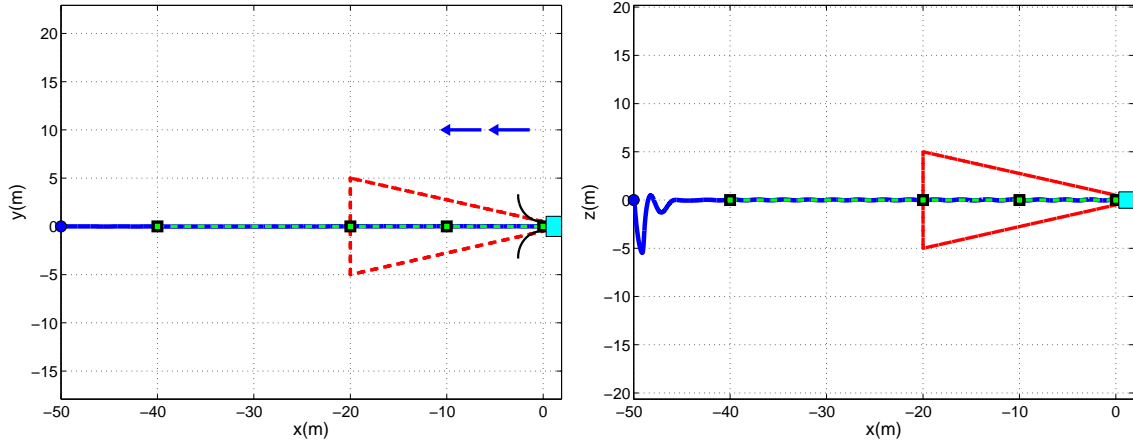


Figure 6.28: Problem 3 - case 4: Position of the vehicle expressed in the ROV body frame in the XY and XZ planes, respectively

Figure 6.29 presents the good horizontal tracking during the final moments of the docking sequence.

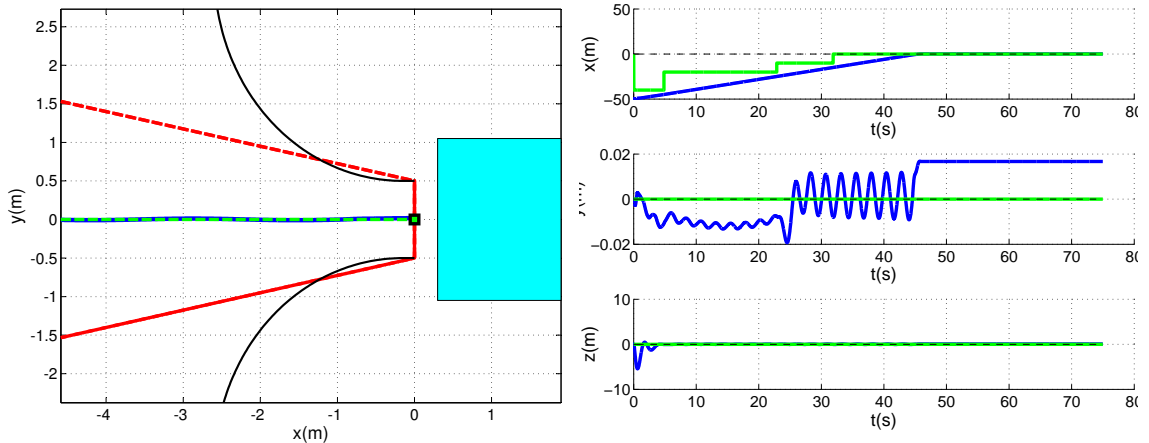


Figure 6.29: Problem 3 - case 4: Final moments of docking in the horizontal plane, and the position of the vehicle in the ROV body frame along time

## 6.6 Problem 4 – Collision Avoidance in the early stages of the operation

### 6.6.1 Case 1

This case presents the behavior of the system when the LAUV initial state is inside the backward reach set under adversarial behavior. For this case the LAUV initial state is

$\mathbf{x} = [-2, 0, 0, 0, 0, 0]$ . The ROV is in constant forward motion with  $u_{\text{rov}} = 0.3$  and external disturbances are present acting on the  $y$ -axis,  $v_{cy} = 0.3$ .

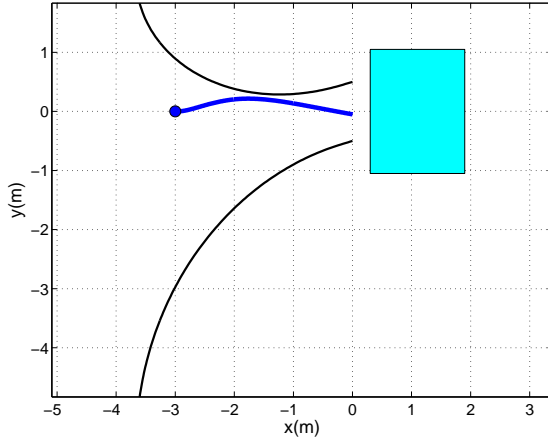


Figure 6.30: Problem 4 - case 1: Position of the vehicle expressed in the ROV body frame in the XY and XZ planes, respectively

Figure 6.30 presents the path performed by the LAUV when the initial state is inside the backward reach set. The final distance is  $d = 0.1506$  which is a small offset comparing with the dock structure considered.

## 6.6.2 Case 2

This case presents the behavior of the system when the LAUV initial state is inside the safety zone but outside of the backward reach set. For this case the LAUV initial state is  $\mathbf{x} = [-2, 1, 0, 0, 0, 0]$ . The ROV is in constant forward motion with  $u_{\text{rov}} = 0.3$  and external disturbances are present acting on the  $y$ -axis,  $v_{cy} = 0.3$ .

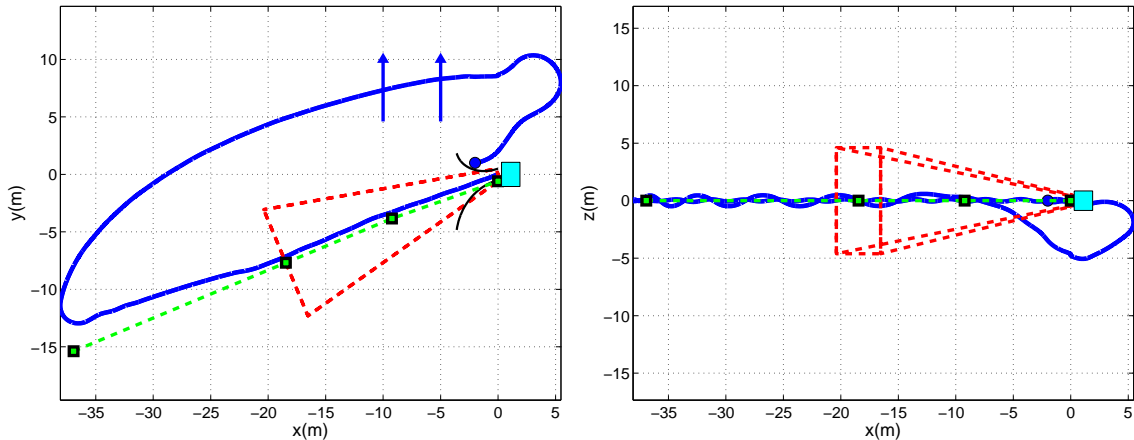


Figure 6.31: Problem 4 - case 2: Position of the vehicle expressed in the ROV body frame in the XY and XZ planes, respectively

The final distance for this case is  $d = 0.0861$  m which is a small offset with  $y = -0.0147$  and  $z = -0.0848$ . The docking is achieved in  $t_d = 87.06$  s.

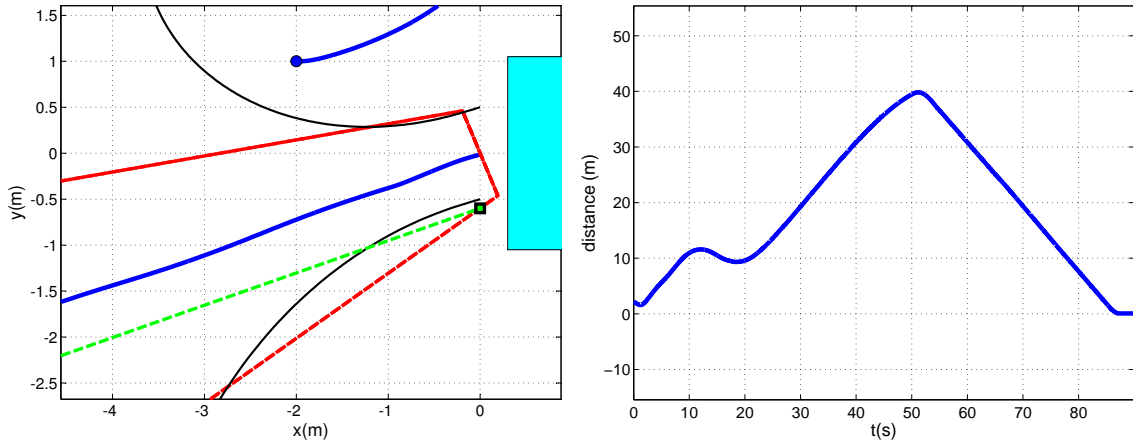


Figure 6.32: Problem 4 - case 2: Final moments of docking in the horizontal plane, and the distance between vehicles during docking

### 6.6.3 Case 3

This case presents the behavior of the system when the LAUV initial state is inside the collision avoidance zone. For this case the LAUV initial state is  $\mathbf{x} = [20, 0, 0, 0, 0, 0]$ . The ROV is in constant forward motion with  $u_{\text{rov}} = 0.3$  without external disturbances considered to the system.

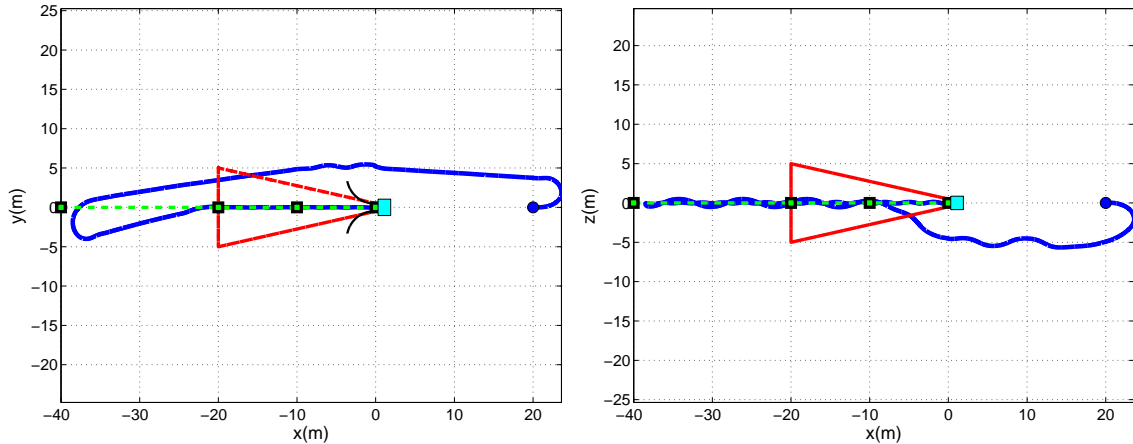


Figure 6.33: Problem 4 - case 3: Position of the vehicle expressed in the ROV body frame in the XY and XZ planes, respectively

The docking happens in  $t_d = 91.04$  s. The final distance is  $d = 0.0802$  due to the offset during latching,  $y = -0.0279$  and  $z = -0.0751$ . Notice that the LAUV avoids the ROV performing a roundabout maneuver. The safety zone is defined within 5m around

the ROV state. When the vehicle is performing the roundabout maneuver the distance between both vehicles is never less than 5m.

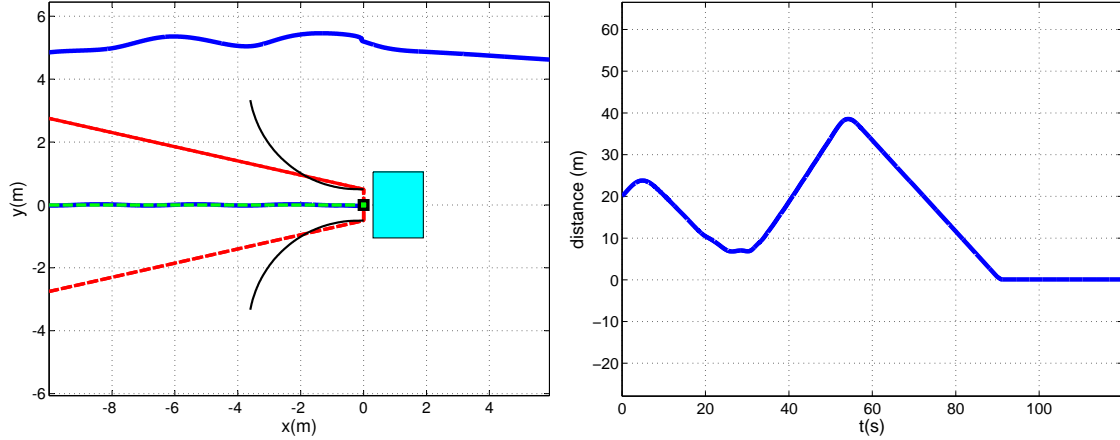


Figure 6.34: Problem 4 - case 3: Final moments of docking in the horizontal plane, and the distance between vehicles during docking

#### 6.6.4 Case 4

This case presents the behavior of the system when the LAUV initial state is in the Line of Sight zone. Although similar to the previous problems, keep in mind, that the hybrid system implemented is the one suggested in section 5.13.2. For this case the LAUV initial state is  $\mathbf{x} = [10, 10, 0, 0, 0, \pi]$ . The ROV is in constant forward motion with  $u_{\text{rov}} = 0.3$  without external disturbances considered to the system.

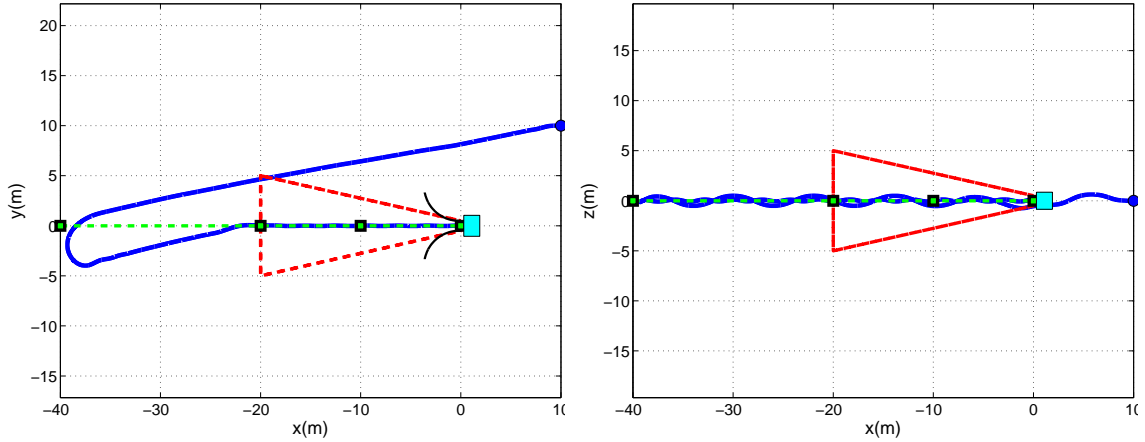


Figure 6.35: Problem 4 - case 4: Position of the vehicle expressed in the ROV body frame in the XY and XZ planes, respectively

The docking operation lasted  $t_d = 73.4$  s. The final distance is  $d = 0.1376$  due to the offset  $y = 0.0265$  and  $z = 0.1350$ . It can be seen in figure 6.35 that since the vehicle initial state is outside the collision avoidance zone (to compute the boundary of the collision

avoidance we use equations (5.33) in section 5.8.1), the vehicle heads directly to the first waypoint defined in the motion plan.

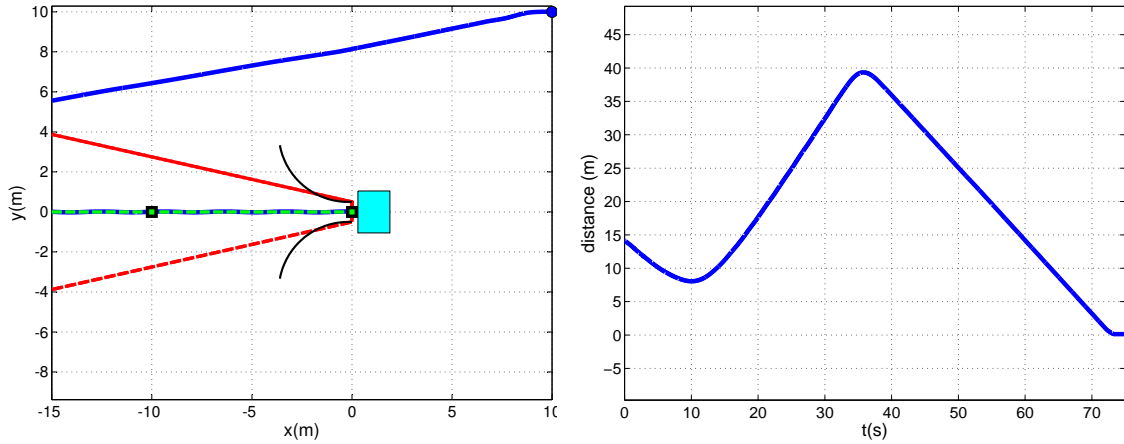


Figure 6.36: Problem 4 - case 4: Final moments of docking in the horizontal plane, and the distance between vehicles during docking

However, there is the possibility of the vehicle entering either the safety zone or the collision avoidance zone. The high level control system addresses this situation changing the discrete state of the system. Hence, if we define the initial state of the LAUV as  $\mathbf{x} = [10, 10, 0, 0, 0, 0]$ , the vehicle will enter the collision avoidance zone, and perform the roundabout maneuver (figure 6.37).

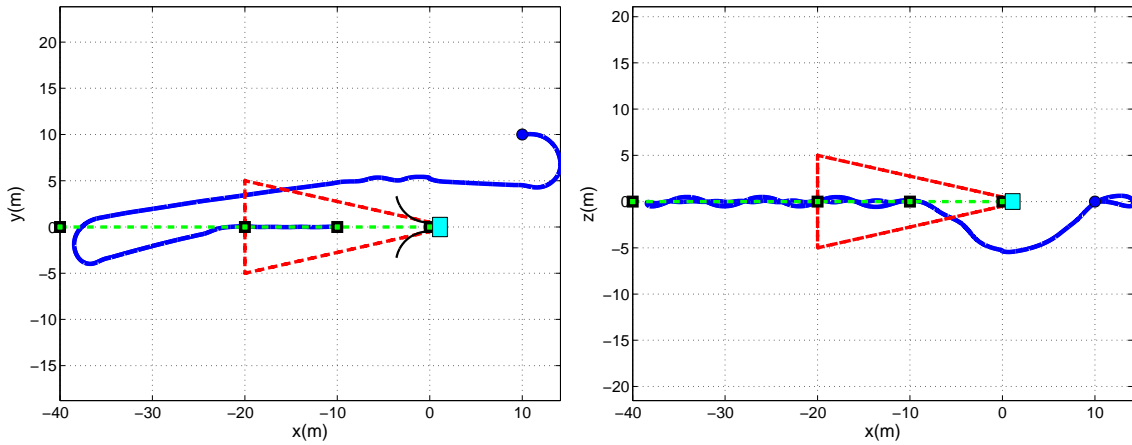


Figure 6.37: Problem 4 - case 4: Position of the vehicle expressed in the ROV body frame in the XY and XZ planes, respectively

## 6.7 Problem 5 – Abort sequence

For the abort sequence problem cases, the initial state for both vehicles holds. Thus  $\mathbf{x}_{\text{auv}} = [-50, -30, 0, 0, 0, 0]^T$  and  $\mathbf{x}_{\text{rov}} = [0, 0, 0, 0, 0, 0]^T$ . The ROV is in constant forward motion

with  $u_{\text{rov}} = 0.3$ . The difference between the two cases concerns the external disturbances.

### 6.7.1 Case 1

For this case the external disturbance is  $u_{cx} = -0.4$  and  $v_{cy} = 0.7$  m/s.

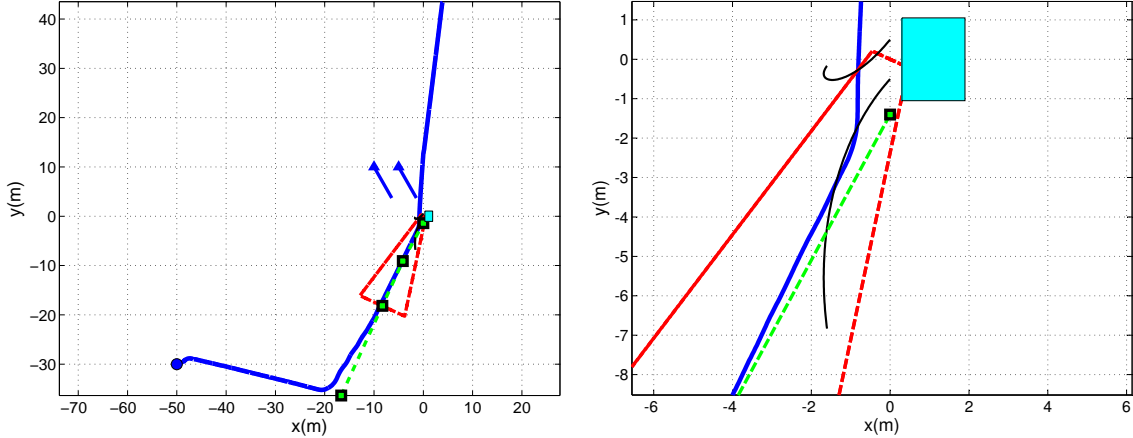


Figure 6.38: Problem 5 - case 1: Position of the vehicle in the horizontal plane during an abort situation

It can be seen in figure 6.38 that the LAUV is unable to dock. Once the vehicle reaches a position outside of the backward reach set there are no guarantees of the existence of a feasible sequence of controls that lead the state of the vehicle to a position inside the dock station with the same heading and elevation. Hence the supervisory layer of control aborts the docking sequence. The vehicle uses the ocean currents to drive the state of the LAUV away from the ROV to avoid collisions.

### 6.7.2 Case 2

For this case the external disturbance is  $v_{cy} = 0.7$  m/s.

Despite the presence of strong external disturbances in the  $y$ -axis the vehicle is able to find a feasible path that drives its state to the desired docking state inside the ROV (figure 6.39).

In this case the docking is achieved in  $t_d = 49.16$  s, and the final distance is  $d = 0.0923$  m (with  $y = 0.0684$  m and  $z = -0.0615$  m), which is a low offset compared with the dock size considered along the simulations (0.50 m).

In figure 6.39 it is evident that the motion plan accounts with the offset observed when the low level controllers track some reference in the presence of external disturbances.

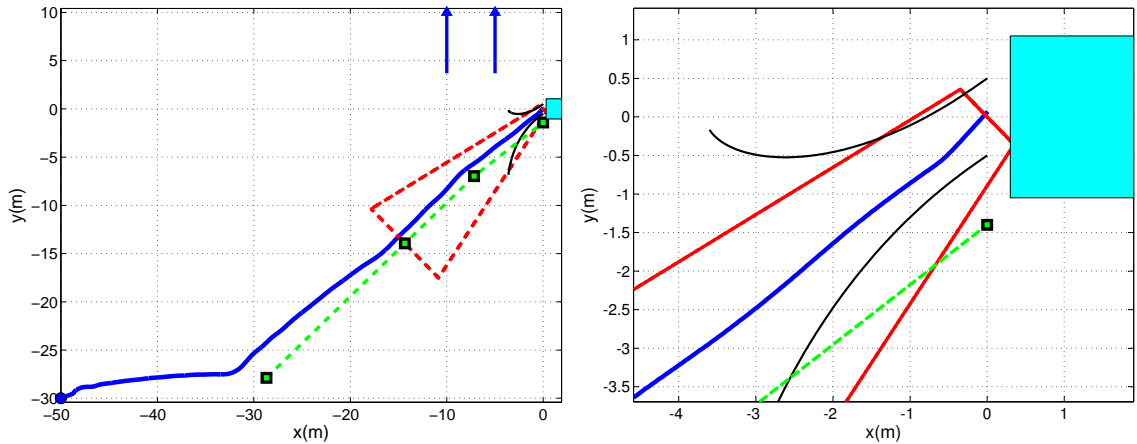


Figure 6.39: Problem 5 - case 2: Position of the vehicle in the presence of strong external disturbances

## 6.8 Final results

This section presents all the results achieved in the simulation for the Test Plan defined in section 6.2.

Table 6.2: Final results for problem 1

Problem 1: Final results					
	Dock ?	Docking Time (s)	Distance (m)	Offset in y (m)	Offset in z (m)
Case 1	Yes	49.34	0.0648	-0.026	-0.0593
Case 2	Yes	43.03	0.0202	-0.0154	-0.0131
Case 3	Yes	54.14	0.0144	0.0056	0.0175

Without disturbances the final distance is under 10 cm, which shows a good tracking of the system, considering the nonlinear dynamical behavior of the underwater vehicles. This holds for when the ROV inertial position is fixed (table 6.2), and when the ROV is in constant forward motion (table 6.3).

Table 6.3: Final results for problem 2

Problem 2: Final results					
	Dock ?	Docking Time (s)	Distance (m)	Offset in y (m)	Offset in z (m)
Case 1	Yes	56.67	0.0380	-0.0335	0.0178
Case 2	Yes	57.5	0.0317	0.0311	0.0056
Case 3	Yes	58.49	0.0728	0.0017	0.0726

Table 6.4 shows that the presence of external disturbances increases the complexity of the task of the controllers. Nevertheless, the final distance to the center of the dock structure remains small due to the cross track controller and the waypoint allocation. Notice that the main source of errors is with the depth control. This makes sense since the

Table 6.4: Final results for problem 3

Problem 3: Final results					
	Dock ?	Docking Time (s)	Distance (m)	Offset in y (m)	Offset in z (m)
Case 1	Yes	55.02	0.0473	0.0469	-0.0048
Case 2	Yes	54.96	0.0427	-0.0309	0.0294
Case 3	Yes	45.98	0.0744	0.0060	0.0740
Case 4	Yes	45.86	0.0678	0.0167	0.0656

cross-track controller (section 5.7) was developed for the control of the horizontal plane of motion only.

Table 6.5: Final results for problem 4

Problem 4: Final results					
	Dock ?	Docking Time (s)	Distance (m)	Offset in y (m)	Offset in z (m)
Case 1	Yes	2.05	0.1506	0.1234	-0.0863
Case 2	Yes	87.06	0.0861	-0.0147	-0.0848
Case 3	Yes	91.04	0.0802	-0.0279	-0.0751
Case 4	Yes	73.4	0.1376	0.0265	0.1350

The collision avoidance techniques were shown to be efficient since they were able to avoid collisions with the ROV and still dock (table 6.5).

Table 6.6: Final results for problem 5

Problem 5: Final results					
	Dock ?	Docking Time (s)	Distance (m)	Offset in y (m)	Offset in z (m)
Case 1	No	-	-	-	-
Case 2	Yes	49.16	0.0923	0.0684	0.0615

The maneuver was aborted (table 6.6) when we introduced an ocean current with amplitude  $U_c = 0.8$  m/s. Since the LAUV nominal speed is 1.5 m/s it is understandable that the controllers are unable to successfully dock the LAUV. Notice that we considered a current with longitudinal ( $u_{cx} = -0.4$ ) and transversal ( $v_{cy} = 0.7$ ) components, which increases the difficulty of the docking operation.

To achieve a better tracking the sliding mode controllers can be tuned to improve efficiency.

# **Chapter 7**

## **Conclusions**

### **7.1 Autonomous docking systems**

This report presents a control strategy to drive the Light Autonomous Underwater Vehicle (LAUV) to a dock structure placed inside the ROV Luso. The problems were formulated considering possible scenarios while in underwater operation.

The solution is a hierarchical control architecture divided in three levels of automation. The first level of automation is the supervisor layer, which is responsible to supervise and control the whole docking operation, and uses hybrid systems theory to interact discrete events and continuous states evolving in time described by nonlinear ordinary differential equations. To achieve a better performance the docking operation is divided into basic maneuvers. Each one of the basic maneuvers has a dedicated controller. The supervisor layer is responsible for switching the maneuvers. The maneuvers are controlled in the next level of automation. This maneuver layer uses the maneuver controllers to derive the necessary state references. The lower level of automation is the regulation layer which receives the state feedback and uses the models of the underwater vehicles to compute the necessary inputs (thruster force allocation and/or fins angle of deflection) for the hardware. Each one of the layers can be changed or expanded without affecting the other layers.

This work presents a set of basic maneuvers and respective controllers that can be used to control the underwater vehicles. Sliding mode controllers using decoupled linearized systems were implemented to derive the input references to the system.

Three other scenarios were considered. First, docking while in the presence of external disturbances. Second, the possibility of collisions between the LAUV and the ROV Luso. And finally, the scenario where the vehicle is unable to keep the correct path and risks to

fail the dock structure and collide with the ROV. All these scenarios were considered, and respective solutions were derived and tested.

Reachability theory is applied to dynamically allocate motion plans using known bounds for the external disturbances. This way the vehicle is able to compensate for the effects of those disturbances. The backreach set under adversarial behavior is also used to prevent the risk of failing the dock and collide with the ROV during the final moments of the procedure. Potential theory is applied to solve the collision avoidance problem, using gradient lines to avoid the obstacle and drive the vehicle to the goal.

One of the main difficulties concerns the tuning of the low level sliding mode controllers. This is due mainly to two reasons. First, the LAUV is an underactuated system, which makes it harder for the low level controllers to track the desired reference in the presence of external disturbances. Second, the vehicle state is described not only by its position but also by its orientation, which leads to the necessity of controllability in 6 degrees of freedom. Furthermore, the dynamical behavior of underwater vehicles is highly nonlinear. Therefore, it is typical to have an offset when the vehicle is trying to perform the prescribed motion plan, in the presence of transversal currents. A solution discussed in section 5.5 involves the development of the motion plan taking into account the estimated offset of the controllers. This solution was implemented and tested for problems 3, 4 and 5, with very successful results.

A solution is discussed where the vehicles align themselves with the currents to counteract any transversal disturbances. This solution was not tested because the controllability of the ROV is higher than for the AUV. Hence, it is very easy for the ROV to align with the ocean currents. For the LAUV the difference is none, since its state is always referred to the ROV body-fixed reference frame. Adopting and testing this solution, would result in discarding the transversal currents, for the final moments of docking, hence simplifying the controllability problem. Nevertheless, if the LAUV is docking, the ROV can still change its heading to align to the ocean currents, and the LAUV is still able to perform the correct motion plan to dock inside the dock structure.

Hence, I consider that all the initial objectives are satisfied.

## 7.2 Future work

This thesis assumed the full knowledge of the state of both vehicles. However, in practice, the current navigational techniques are unable to provide that information. Hence, further work has to take into account estimation state errors for both vehicles, as well as possible delays in the state information. Some sensing techniques were presented in the state of the art section 3.

Another suggestion for further work is to test the control strategy in real environment. To overcome the uncertainty related to the estimation of the states of the vehicles, a fixed dock structure can be used.

The backreach set under adversarial behavior computation can be extended to three dimensions, in order to compute the backward state of the system related to the position coordinates  $x$ ,  $y$  and  $z$ , the heading  $\psi$  and elevation  $\theta$ . An approximation can be used if one considers the decoupled control systems. This thesis has already developed the model to compute the backward reach set in the horizontal plane. The vertical plane backreach set computation follows the exact same guidelines. Notice that the vertical plane would have to consider the state  $\mathbf{x} = [x, z, \theta]^T$ .

Optimal controllers, as discussed in section 5.4.3, to control the LAUV while at the boundary of the backreach set, can be studied to address the stability and convergence of the system. With bounded disturbances the LAUV must be able to compute the backreach set under adversarial behavior, and once the state reaches the boundary of the set, the optimal control drives the state of the vehicle along one of the boundaries of the set, until it reaches the dock structure.

Another suggestion is to build a control strategy for the docking system using a multiple vehicle network. Consider, for instance, that we have several AUVs in operation and that there is the need for them to dock to transfer data with new mission assignments. The control strategy would have to prioritize the AUVs to increase efficiency, reduce time costs and still providing safety and robustness, much like an Air Traffic Management system.



# References

- [1] T. Fossen. *Guidance and Control of Ocean Vehicles*. Wiley, New York, NY, 1995.
- [2] J. Borges de Sousa, S. Fraga, Alfredo Martins, and Fernando Lobo Pereira. A control framework for a remotely operated vehicle. *Proceedings of the International Conference on Engineering for Ocean and Offshore Structures*, 12/2001 2001.
- [3] T. Podder, M. Sibenac, and J. Bellingham. Auv docking system for sustainable science missions. *Robotics and Automation, 2004. Proceedings. ICRA '04. 2004 IEEE International Conference on*, 5:4478 – 4484 Vol.5, april-1 may 2004.
- [4] J. Borges de Sousa and Fernando Lobo Pereira. Coordinated control of networked vehicles: an autonomous underwater system. *IFAC Workshop Modelling and Analysis of Logic Controlled Dynamic Systems*, 2003.
- [5] M. Gertler and G. R. Hagen. Standard equations of motion for submarine simulation. *David W. Taylor Naval Ship Research and Development Center*, jun 1967.
- [6] A. J. Healey. ME4823 class notes: Dynamics and control of mobile robotic vehicles. *Naval Postgraduate School, Monterey, California*, 2009.
- [7] Jorge Estrela da Silva, Bruno Terra, Ricardo Martins, and J. Borges de Sousa. Modeling and simulation of the lauv autonomous underwater vehicle. *MMAR*, 2007 2007.
- [8] O.E. Fjellstad and T.I. Fossen. Position and attitude tracking of auv's: a quaternion feedback approach. *Oceanic Engineering, IEEE Journal of*, 19(4):512 –518, oct 1994.
- [9] V. Arnold. *Mathematical Methods of Classical Mechanics*. Springer, 1997.
- [10] O. M. Faltinsen. *Sea loads on ships and offshore structures / O.M. Faltinsen*. Cambridge University Press, Cambridge ; New York :, 1990.
- [11] Edward V. Lewis, editor. *Principles of naval architecture*. The Society of naval architects and marine engineers, Jersey City, 1989.
- [12] J. Garus. Optimization of thrust allocation in the propulsion system of an underwater vehicle. *International Journal of Applied Mathematics and Computer Science*, 14(4):461 – 7, 2004//. unconstrained control;propulsion system;thrust allocation;optimization;thrust distribution;unmanned underwater vehicle;configuration matrix;

- [13] William C. Webster and J. Borges de Sousa. Optimum allocation for multiple thrusters. *Proceedings of the International Offshore and Polar Engineering Conference*, 1:83 – 89, 1999. Mobile offshore bases (MOB);Multiple thrusters;.
- [14] P. Varaiya. Smart cars on smart roads: problems of control. *Automatic Control, IEEE Transactions on*, 38(2):195 –207, feb 1993.
- [15] D.N. Godbole, J. Lygeros, and S. Sastry. Hierarchical hybrid control: an ivhs case study. In *Decision and Control, 1994., Proceedings of the 33rd IEEE Conference on*, volume 2, pages 1592 –1597 vol.2, dec 1994.
- [16] S. Sastry, G. Meyer, C. Tomlin, J. Lygeros, D. Godbole, and G. Pappas. Hybrid control in air traffic management systems. In *Decision and Control, 1995., Proceedings of the 34th IEEE Conference on*, volume 2, pages 1478 –1483 vol.2, dec 1995.
- [17] Thomas A. Henzinger, Peter W. Kopke, Anuj Puri, and Pravin Varaiya. What's decidable about hybrid automata? *J. Comput. Syst. Sci.*, 57(1):94–124, 1998.
- [18] A. Deshpande and P. Varaiya. Information structures for control and verification of hybrid systems. In *American Control Conference, 1995. Proceedings of the*, volume 4, pages 2642 –2647 vol.4, jun 1995.
- [19] Anuj Puri and Pravin Varaiya. Decidable hybrid systems. In *In Hybrid Systems III, LNCS 1066*, pages 413–423. Springer, 1996.
- [20] João Hespanha. ECE229 class notes: Hybrid and switched systems, 2005. Available in <http://www.ece.ucsb.edu/~hespanha/ece229/>, Last time visited: April 22nd 2010.
- [21] A. Deshpande and P. Varaiya. Viable control of hybrid systems. In *Decision and Control, 1996., Proceedings of the 35th IEEE*, volume 2, pages 1196 –1201 vol.2, dec 1996.
- [22] Rajeev Alur, Costas Courcoubetis, Thomas A. Henzinger, and Pei-Hsin Ho. Hybrid automata: An algorithmic approach to the specification and verification of hybrid systems. In *Lecture notes in Computer Science 736*, pages 209–229. Springer-Verlag, 1993.
- [23] Anuj Puri and Pravin Varaiya. Decidability of hybrid systems with rectangular differential inclusion. In *CAV '94: Proceedings of the 6th International Conference on Computer Aided Verification*, pages 95–104, London, UK, 1994. Springer-Verlag.
- [24] C.J. Tomlin, J. Lygeros, and S. Shankar Sastry. A game theoretic approach to controller design for hybrid systems. *Proceedings of the IEEE*, 88(7):949 –970, jul 2000.
- [25] J. Lygeros, D.N. Godbole, and S. Sastry. Verified hybrid controllers for automated vehicles. *Automatic Control, IEEE Transactions on*, 43(4):522 –539, apr 1998.
- [26] J. Lygeros, C. Tomlin, and S. Sastry. On controller synthesis for nonlinear hybrid systems. In *Decision and Control, 1998. Proceedings of the 37th IEEE Conference on*, volume 2, pages 2101 –2106 vol.2, dec 1998.

- [27] C. Livadas, J. Lygeros, and N.A. Lynch. High-level modeling and analysis of the traffic alert and collision avoidance system (tcas). *Proceedings of the IEEE*, 88(7):926 –948, jul 2000.
- [28] C. Tomlin, I. Mitchell, and R. Ghosh. Safety verification of conflict resolution manoeuvres. *Intelligent Transportation Systems, IEEE Transactions on*, 2(2):110 –120, jun 2001.
- [29] I. Kitsios and J. Lygeros. Final glide-back envelope computation for reusable launch vehicle using reachability. In *Decision and Control, 2005 and 2005 European Control Conference. CDC-ECC '05. 44th IEEE Conference on*, pages 4059 – 4064, dec. 2005.
- [30] J. Sprinkle, J.M. Eklund, and S.S. Sastry. Deciding to land a uav safely in real time. *American Control Conference, 2005. Proceedings of the 2005*, pages 3506 – 3511 vol. 5, june 2005.
- [31] J. Borges de Sousa. Notes on concepts and interpretation of control systems (draft). *DEEC, Faculty of Engineering of University of Porto*, 2008.
- [32] J. Borges de Sousa. Reachability and control for continuous-time systems. *DEEC, Faculty of Engineering of University of Porto*, 2010.
- [33] G. Leitmann. Optimality and reachability with feedback controls. In *Dynamic Systems and Microphysics*, Blaquier A., Leitmann G., eds., 2001.
- [34] A.B. Kurzhanski and P. Varaiya. Optimization methods for target problems of control. In *Proceedings of Mathematical Theory of Networks and Systems*, Notre Dame, IL, USA, 2002.
- [35] A. B. Kurzhanski and P. Varaiya. Dynamic optimization for reachability problems. *Journal of Optimization Theory & Applications*, 108(2):227–251, 2001.
- [36] N. N. Krasovskii, A. I. Subbotin, and Samuel Kotz. *Game-theoretical control problems*. Springer-Verlag, New York, NY, USA, 1987.
- [37] Martino Bardi and Italo Capuzzo-Dolcetta. *Optimal Control and Viscosity Solutions of Hamilton-Jacobi-Bellman equations*. Birkhauser, Berlin, Germany, 1997.
- [38] J. A. Sethian. Level set methods and fast marching methods - evolving interfaces in computational geometry, fluid mechanics, computer vision, and materials science. In *Interfaces in Computational Geometry, Fluid Mechanics, Computer Vision, and Materials Science*. Cambridge University Press, 1998.
- [39] I.M. Mitchell, A.M. Bayen, and C.J. Tomlin. A time dependent hamilton jacobi formulation of reachable sets for continuous dynamic games. *Automatic Control, IEEE Transactions on*, 50(7):947 – 957, july 2005.
- [40] E.A. Cross and I.M. Mitchell. Level set methods for computing reachable sets of systems with differential algebraic equation dynamics. In *American Control Conference, 2008*, pages 2260 – 2265, june 2008.

- [41] A. B. Kurzhanski and P. Varaiya. Ellipsoidal techniques for reachability under state constraints. *SIAM J. Control Optim.*, 45(4):1369–1394, 2006.
- [42] Jean-Jacques E Slotine and Weiping Li. *Applied nonlinear control*. Pearson, Upper Saddle River, NJ, 1991.
- [43] M. Vidyasagar. *Nonlinear Systems Analysis*. Prentice-Hall Inc., Englewood Cliffs, NJ, 1993.
- [44] Hassan K. Khalil. *Nonlinear Systems*. MacMillan, New York, NY, USA, 1992.
- [45] Shankar Sastry and Marc Bodson. *Adaptive control: stability, convergence, and robustness*. Prentice-Hall, Inc., Upper Saddle River, NJ, USA, 1989.
- [46] A. Girard. ME237 class notes: Control of nonlinear dynamic systems. *The University of California at Berkeley*, 2002.
- [47] Jean-Jacques E. Slotine. Sliding controller design for nonlinear systems. *International Journal of Control*, 40(2):421 – 434, 1984. SLIDING CONTROLLER;.
- [48] Vadim I. Utkin. Variable structure systems with sliding modes. *IEEE Transactions on Automatic Control*, AC-22(2):212 – 222, 1977.
- [49] S.M. Swei and M. Corless. On the necessity of the matching condition in robust stabilization. In *Decision and Control, 1991., Proceedings of the 30th IEEE Conference on*, pages 2611 –2614 vol.3, 11-13 1991.
- [50] Y.H. Chen. A new matching condition for robust control design. In *American Control Conference, 1993*, pages 122 –126, 2-4 1993.
- [51] Martin J. Corless and George Leitmann. Continuous state feedback guaranteeing uniform ultimate boundedness for uncertain dynamical systems. *IEEE Transactions on Automatic Control*, AC-26(5):1139 – 1144, 1981.
- [52] Miroslav Krstic, Petar V. Kokotovic, and Ioannis Kanellakopoulos. *Nonlinear and Adaptive Control Design*. John Wiley & Sons, Inc., New York, NY, USA, 1995.
- [53] J. H. Green and J. K. Hedrick. Nonlinear speed control for automotive engines. In *American Control Conference, 1990*, pages 2891 –2897, 23-25 1990.
- [54] M. Won and J. K. Hedrick. Multiple surface sliding control of a class of uncertain nonlinear systems. *International Journal of Control*, 64(4):693–706, 1996.
- [55] J. K. Hedrick and P. P. Yip. Multiple sliding surface control: Theory and application. *Journal of Dynamic Systems, Measurement, and Control*, 122(4):586–593, 2000.
- [56] J. C. Gerdes and J. K. Hedrick. Vehicle speed and spacing control via coordinated throttle and brake actuation. *Control Engineering Practice*, 5(11):1607 – 1614, 1997.
- [57] D. Swaroop, J.C. Gerdes, P.P. Yip, and J.K. Hedrick. Dynamic surface control of nonlinear systems. In *American Control Conference, 1997. Proceedings of the 1997*, volume 5, pages 3028 –3034 vol.5, jun 1997.

- [58] D. Swaroop, J.K. Hedrick, P.P. Yip, and J.C. Gerdes. Dynamic surface control for a class of nonlinear systems. *Automatic Control, IEEE Transactions on*, 45(10):1893 – 1899, oct. 2000.
- [59] D. Yoerger and J. Slotine. Robust trajectory control of underwater vehicles. *Oceanic Engineering, IEEE Journal of*, 10(4):462 – 470, oct 1985.
- [60] A.J. Healey and D. Lienard. Multivariable sliding mode control for autonomous diving and steering of unmanned underwater vehicles. *Oceanic Engineering, IEEE Journal of*, 18(3):327 –339, jul 1993.
- [61] Anouck R. Girard and J. Borges de Sousa. Autopilots for underwater vehicles: Dynamics, configurations and control. In *OCEANS 2007*, Aberdeen, Scotland, 05/2007 2007.
- [62] W. Levine, editor. *The Control Handbook*. CRC Press, Boca Raton, FL, 1996.
- [63] J.K. Hedrick. Nonlinear controller design for automated vehicle applications. In *Control '98. UKACC International Conference on (Conf. Publ. No. 455)*, volume 1, pages 23 –32 vol.1, 1-4 1998.
- [64] J. C. Gerdes. *Decoupled design of robust controllers for nonlinear systems: as motivated by and applied to coordinated throttle and brake control for automated highways*. PhD thesis, Berkeley, CA, USA, 1996.
- [65] R. Stokey, M. Purcell, N. Forrester, T. Austin, R. Goldsborough, B. Allen, and C. von Alt. A docking system for remus, an autonomous underwater vehicle. *OCEANS '97. MTS/IEEE Conference Proceedings*, 2:1132 –1136 vol.2, oct 1997.
- [66] R. Stokey, B. Allen, T. Austin, R. Goldsborough, N. Forrester, M. Purcell, and C. von Alt. Enabling technologies for remus docking: an integral component of an autonomous ocean-sampling network. *Oceanic Engineering, IEEE Journal of*, 26(4):487 –497, oct 2001.
- [67] B. Allen, T. Austin, N. Forrester, R. Goldsborough, A. Kukulya, G. Packard, M. Purcell, and R. Stokey. Autonomous docking demonstrations with enhanced remus technology. *OCEANS 2006*, pages 1 –6, sept. 2006.
- [68] M.D. Feezor, P.R. Blankinship, J.G. Bellingham, and F.Y. Sorrell. Autonomous underwater vehicle homing docking via electromagnetic guidance. *OCEANS '97. MTS/IEEE Conference Proceedings*, 2:1137 –1142 vol.2, oct 1997.
- [69] S. Cowen, S. Briest, and J. Dombrowski. Underwater docking of autonomous undersea vehicles using optical terminal guidance. *OCEANS '97. MTS/IEEE Conference Proceedings*, 2:1143 –1147 vol.2, oct 1997.
- [70] H. Singh, J.G. Bellingham, F. Hover, S. Lemer, B.A. Moran, K. von der Heydt, and D. Yoerger. Docking for an autonomous ocean sampling network. *Oceanic Engineering, IEEE Journal of*, 26(4):498 –514, oct 2001.
- [71] Pan-Mook Lee, Bong-Hwan Jeon, and Chong-Moo Lee. A docking and control system for an autonomous underwater vehicle. *OCEANS '02 MTS/IEEE*, 3:1609 –1614 vol.3, oct. 2002.

- [72] J.C. Evans, K.M. Keller, J.S. Smith, P. Marty, and O.V. Rigaud. Docking techniques and evaluation trials of the swimmer auv: an autonomous deployment auv for work-class rovs. *OCEANS, 2001. MTS/IEEE Conference and Exhibition*, 1:520 –528 vol.1, 2001.
- [73] J. Evans, P. Redmond, C. Plakas, K. Hamilton, and D. Lane. Autonomous docking for intervention-auvs using sonar and video-based real-time 3d pose estimation. *OCEANS 2003. Proceedings*, 4:2201 – 2210 Vol.4, sept. 2003.
- [74] T. Fukasawa, T. Noguchi, T. Kawasaki, and M. Baino. "marine bird", a new experimental auv with underwater docking and recharging system. *OCEANS 2003. Proceedings*, 4:2195 – 2200 Vol.4, sept. 2003.
- [75] L. Brignone, M. Perrier, and C. Viala. A fully autonomous docking strategy for intervention auvs. *OCEANS 2007 - Europe*, pages 1 –6, june 2007.
- [76] Pakpong Jantapremjit and Philip A. Wilson. Optimal control and guidance for homing and docking tasks using an autonomous underwater vehicle. *Mechatronics and Automation, 2007. ICMA 2007. International Conference on*, pages 243 –248, aug. 2007.
- [77] R.S. McEwen, B.W. Hobson, L. McBride, and J.G. Bellingham. Docking control system for a 54-cm-diameter (21-in) auv. *Oceanic Engineering, IEEE Journal of*, 33(4):550 –562, oct. 2008.
- [78] P. Sotiropoulos, D. Grossset, G. Giannopoulos, and F. Casadei. Auv docking system for existing underwater control panel. *OCEANS 2009-EUROPE, 2009. OCEANS '09.*, pages 1 –5, may 2009.
- [79] T. Palmer, D. Ribas, P. Ridao, and A. Mallios. Vision based localization system for auv docking on subsea intervention panels. *OCEANS 2009-EUROPE, 2009. OCEANS '09.*, pages 1 –10, may 2009.
- [80] Jin-Yeong Park, Bong huan Jun, Pan mook Lee, and Junho Oh. Experiments on vision guided docking of an autonomous underwater vehicle using one camera. *Ocean Engineering*, 36(1):48 – 61, 2009. Autonomous Underwater Vehicles.
- [81] Jin-Yeong Park, Bong-Huan Jun, Kihun Kim, Pan-Mook Lee, Jun-Ho Oh, and Yong-Kon Lim. Improvement of vision guided underwater docking for small auv isimi. *OCEANS 2009, MTS/IEEE Biloxi - Marine Technology for Our Future: Global and Local Challenges*, pages 1 –5, oct. 2009.
- [82] G. Remmers, R. Taylor, P. Palo, and R. Brackett. Mobile offshore base: a seabasing option. *Proceedings of Third International Workshop on Very Large Floating Structures*, 1-7, 1999.
- [83] Anouck Girard, J. Karl Hedrick, and J. Borges de Sousa. A hierarchical control architecture for mobile offshore bases. *Marine Structures*, 13(4-5):459 – 476, 2000.
- [84] A. Girard, J. Borges de Sousa, and K. Hedrick. Coordinated control of agent formations in uncertain, dynamic environments. In *Proceedings of the European Control Conference*, Porto, Portugal, 9 2001.

- [85] J. Borges de Sousa, J. Karl Hedrick, Anouck Girard, and William Webster. A ship maneuvering control framework. In *Proceedings of the International Conference on Offshore Mechanics and Arctic Engineering - OMAE*, volume 5, pages 111 – 119, Rio de Janeiro, Brazil, 2001. Control architecture;Hybrid systems;.
- [86] R.M.F. Gomes, A. Martins, A. Sousa, J. Borges de Sousa, S.L. Fraga, and F.L. Pereira. A new rov design: issues on low drag and mechanical symmetry. In *Oceans 2005 - Europe*, volume 2, pages 957 – 962 Vol. 2, 20-23 2005.
- [87] J. Almeida, F.L. Pereira, and J. Borges de Sousa. A hybrid feedback control system for a nonholonomic car-like vehicle. In *Robotics and Automation, 1997. Proceedings., 1997 IEEE International Conference on*, volume 3, pages 2614 –2619 vol.3, 20-25 1997.
- [88] C.J. Tomlin, G.J. Pappas, J. Kosecka, J. Lygeros, and S.S. Sastry. Advanced air traffic automation: a case study in distributed decentralized control. pages 261 – 95, Berlin, Germany, 1998.
- [89] J Carbaugh, DN Godbole, and R Sengupta. Safety and capacity analysis of automated and manual highway systems. *Transportation Research Part C-Emerging Technologies*, 6(1-2):69–99, FEB-APR 1998.
- [90] A. A. Kurzhanskiy and P. Varaiya. Ellipsoidal toolbox. Technical Report UCB/EECS-2006-46, EECS Department, University of California, Berkeley, May 2006.
- [91] Ian M. Mitchell. The flexible, extensible and efficient toolbox of level set methods. *J. Sci. Comput.*, 35(2-3):300–329, 2008.
- [92] R. Schiavi, A. Bicchi, and F. Flacco. Integration of active and passive compliance control for safe human-robot coexistence. In *Robotics and Automation, 2009. ICRA '09. IEEE International Conference on*, pages 259 –264, 12-17 2009.
- [93] M. Eichhorn. A new concept for an obstacle avoidance system for the auv "slocum glider" operation under ice. In *OCEANS 2009-EUROPE, 2009. OCEANS '09.*, pages 1–8, May 2009.
- [94] L. Pallottino, V.G. Scordio, A. Bicchi, and E. Frazzoli. Decentralized cooperative policy for conflict resolution in multivehicle systems. *Robotics, IEEE Transactions on*, 23(6):1170 –1183, dec. 2007.
- [95] Ge Yang, Rubo Zhang, and Dong Xu. A fuzzy-q method to improve the adaptability of auv in variable ocean current environment. In *Intelligent Systems, 2009. GCIS '09. WRI Global Congress on*, volume 3, pages 78 –82, May 2009.
- [96] M. Eichhorn. An obstacle avoidance system for an autonomous underwater vehicle. In *Underwater Technology, 2004. UT '04. 2004 International Symposium on*, pages 75 – 82, 20-23 2004.
- [97] M. Eichhorn. A reactive obstacle avoidance system for an autonomous underwater vehicle. In *16th IFAC World Congress, IFAC*, Prague, Czech Republic, July 2005.

- [98] A.J. Healey and D.B. Marco. Slow speed flight control of autonomous underwater vehicles. experimental results with nps auv ii. *Proceedings of the 2nd International Offshore and polar Engineering Conference*, pages 523 – 532, 1992. Swimmer Delivery Vehicles;Underwater Vehicles;.
- [99] Bruno Siciliano and Oussama Khatib, editors. *Springer Handbook of Robotics*. Springer, Berlin, Heidelberg, 2008.
- [100] R. Gomes, J. Borges de Sousa, and F. L. Pereira. Integrated maneuver and control design for rov operations. In *OCEANS 2003. Proceedings*, volume 2, pages 703 – 710 Vol.2, 22-26 2003.
- [101] Rui M. F. Gomes, J. Borges de Sousa, and Fernando Lobo Pereira. Modeling and control of the ies project rov. In *European Control Conference*, Cambridge, UK, 2003.